# Dietary supplementation of haskap berry (*Lonicera caerulea L.*) anthocyanin-rich fraction and probiotics attenuates the severity of dextran sulfate sodium-induced acute colitis in Balb/C mice

by

Kananke Vithanage Surangi Priyangika Dharmawansa

Submitted in partial fulfilment of the requirements
for the degree of Masters of Science

at

Dalhousie University
Halifax, Nova Scotia
March 2023

Dalhousie University is located in Mi'kma'ki, the
ancestral and unceded territory of the Mi'kmaq.
We are all Treaty people.

*Life is all about choices…*

*I dedicate this thesis to my parents and to my sister for supporting me in every significant decision I have made in my life and to those who are going through a rough patch in life, this is for you!*

## TABLE OF CONTENTS

# LIST OF TABLES

# LIST OF FIGURES

# ABSTRACT

Haskap (*Lonicera caerulea* L.) berry is a rich dietary source of anthocyanins with anti-inflammatory properties. This study aimed at investigating the supplementation of haskap anthocyanin-rich fraction alone or with probiotics on the severity reduction of dextran sulfate sodium (DSS)-induced acute colitis in Balb/c mice. Mice were divided into seven dietary groups (n=5) to receive anthocyanin (free or encapsulated) with or without probiotics. As observed by clinical data, anthocyanin + probiotics supplementation significantly reduced the severity of colitis. The supplementary diets suppressed the DSS-induced elevation of serum inflammatory (Interleukin (IL)-6, and Tumor necrosis factor - α) and apoptosis markers (B cell lymphoma-2, Bcl-2-associated X protein) in mice colon tissues. The free anthocyanin + probiotics significantly reduced the serum IL-6 levels. Dietary supplementation of haskap berry anthocyanin + probiotics protects against DSS-induced colitis possibly through attenuating the epithelial inflammation and can be utilized in developing health-promoting dietary supplements and nutraceuticals.



Key words: inflammation, colitis, haskap anthocyanin, probiotics, dextran sulfate sodium

# LIST OF ABBREVIATIONS USED

| | |
|---|---|
| AHF | Anthocyanin-rich haskap berry fraction |
| ALT | Alanine aminotransferase |
| AST | Aspartate aminotransferase |
| BAX | bcl-2-like protein |
| BCL-2 | B-cell lymphoma |
| BSA | Bovine serum albumin |
| C3G | Cyanidine-*3*-*O*-glucoside |
| CAC | Colitis-associated colon cancer |
| cAMP | Cyclic adenosine mono phosphate |
| CCL2 | Chemokine ligand |
| CCL5 | Chemokine ligand |
| cGMP | Cyclic-guanosine monophosphate |
| CO | Carbon monoxide |
| COX | Cyclooxygenase |
| DAI | Disease activity index |
| DAMPs | Danger-associated molecular patterns |
| DCs | Dendritic cells |
| DEL-1 | Developmental endothelial locus-1 |
| DNA | Deoxyribose nucleic acid |
| DSS | Dextran sulfate sodium |
| ECL | Enhanced chemiluminescence |
| ECM | Extracellular matrix |
| EDTA | Ethylenediaminetetraacetic acid |
| EE | Encapsulation efficiency |
| ELISA | Enzyme-linked immunosorbent assays |
| eNOS | Endothelial NOS |
| ER | Encapsulation recovery |
| ERK | Extracellular signal-regulated kinase |
| ERK1 | Extracellular-signal-related kinase |

| | |
|---|---|
| ERK2 | Extracellular-signal-related kinase |
| ERT | Encapsulation retention |
| ESI | Electrospray ionization |
| EY | Encapsulation yield |
| FFAR | Free fatty acid receptor |
| FTIR | Fourier transform infrared spectroscopy |
| GIT | Gastrointestinal tract |
| GLP | Glucagon-like peptide |
| GM-CSFs | Granulocyte-monocyte colony-stimulating factors |
| GTP | Guanosine triphosphate |
| $H_2S$ | Hydrogen sulfide |
| HRP | Horseradish peroxidase |
| IBD | Inflammatory bowel disease |
| IFN-γ | Interferon-gamma |
| IL | Interleukin |
| IN | Inulin |
| iNOS | Inducible NOS |
| LAB | Lactic acid bacteria |
| LB4 | Leukotriene B4 |
| LPS | Lipopolysaccharide |
| LXs | Lipoxins |
| MCP | Monocyte chemoattractant protein |
| MD | Maltodextrin |
| MD-IN | Maltodextrin and inulin |
| ME | Microencapsulation |
| MMP | Matrix metalloproteinases |
| MS | Mass spectrometry |
| NaCl | Sodium chloride |
| NaF | Sodium fluoride |
| NETs | Neutrophil extracellular traps |
| NF-κB | Nuclear factor-kappa B |

| | |
|---|---|
| NK cells | Natural killer cells |
| nNOS | Neuronal NOS |
| NO | Nitric oxide |
| NOS | Nitric oxide synthase |
| NSAIDS | Non-steroidal anti-inflammatory drugs |
| PAMPs | Pathogen-associated molecular patterns |
| PCA | Protocatechuic acid |
| PET | Probiotic encapsulation technology |
| PGA | Phloroglucinaldehyde |
| PGD | Prostaglandin-D |
| PGl2 | Prostacyclin |
| PI3K | Phosphoinositide 3-kinase |
| PVDF | Polyvinylidene difluoride |
| RDA | Recommended dietary allowance |
| RIPA | Radio-immunoprecipitation assay |
| RNS | Reactive nitrogen species |
| ROS | Reactive oxygen species |
| SAC | Surface anthocyanin content |
| SCFAs | Short chain fatty acids |
| SEM | Scanning electron microscope |
| STAT3 | Signal transducer and activator of transcription |
| TAC | Total anthocyanin content |
| TEM | Trans-endothelial migration |
| Th cells | T-helper cells |
| TIM-4 | T cell/transmembrane immunoglobulin mucin |
| TJ | Tight junctions |
| TLR | Toll-like receptors |
| TNBS | 2,4,6,-trinitrobenzene sulfonic acid |
| TNF-α | Tumor necrosis factor-alpha |
| UAE | Ultrasound-assisted extraction |
| UC | Ulcerative colitis |

| | |
|---|---|
| UCLA | University Committee on Laboratory Animals |
| UPLC | Ultra-pressure liquid chromatography |
| VE cadherin | Vascular endothelial cadherin |
| WM | Wall materials |
| WSI | Water solubility index |

# ACKNOWLEDGEMENT

First and foremost, I would like to express my deepest gratitude to my supervisor, Dr. Vasantha Rupasinghe, for giving me this valuable opportunity to join his research team and to work on this interesting project related to human health. Succeeding in graduate school while facing and overcoming challenges in the scientific research environment and in my personal life has not been easy for me. I had to go through some major life-changing events over the past few years and I have no words to say how grateful I am to Dr. Rupasinghe for his excellent understanding, patience and most importantly, his exceptional humanity. I would like to take this moment to express my deepest gratitude to my supervisor for his inspiring guidance, encouraging supervision and for having confidence in me throughout my study period. I can't thank Dr. Rupasinghe enough for providing me with financial support and motivating me through out the time. I would like to express my sincere thanks to my committee members, Dr. Gefu Wang-Pruski and Dr. Sophia He for their valuable comments, suggestions and also for supporting me in producing data; thank you for understanding my personal challenges and for being there with open hands.

I gratefully acknowledge the help I received from Dr. Andrew Stadnyk, especially for my animal experiment. Thank you for providing me with your laboratory facilities, clear and helpful explanations and, the invaluable time you spent teaching me the practicalities of mouse dissection and histopathological analysis. Additionally, I would like to express my gratitude to Dr. Jodi Nettleton, for sharing her expertise in animal tissue and blood harvesting procedures and for facilitating in-person training. I owe my gratitude to

Dr. Jenifer Davit for guiding me through animal care training, and Dr. Suzanne Pearse and Ms. Belinda Dunn for helping me in every way possible to make my animal study a success.

I would also like to share credit with a few people who have helped me in many ways; many thanks to Dr. Wasundara Fernando for guiding me, inspiring me, providing valuable ideas, and never making me feel alone during my stay at Dalhousie main campus. I cannot begin to express my thanks to Mr. Wasitha Praveen De Wass, my lab mate and who is purely a brother to me for helping me to troubleshoot many of my experiments, making me familiarized with different laboratory protocols and being there for me whenever I needed clarifications and advice. Also, I owe him a big thank you for being a very good listener and for guiding me toward the correct path. Special thanks to Dr. Niluni Wijesundara for spending late nights with me in the lab, motivating me and giving me valuable advice; Mrs. Madumani Amararathna for her practical suggestions, constructive criticism and the help she offered me during my animal experimentation. I also greatly appreciate the cheerful and continuous support I received from my lab colleague, Mr. Tharindu Suraweeraarchchilage. Thank you for always watching over me, taking care of me in difficult times, and being an understanding friend. I am happy to thank Mrs. Gayani Gamage for helping me to get myself familiarize with the Carlton Animal Care Facility and for her invaluable support during animal sacrifices. I am so indebted to all my lab colleagues for sharing my smiles and tears and for their incredible teamwork. This study could not have been a possibility without the financial support including the scholarships I received from Killam Chair funds of Dr. Rupasinghe, the Faculty of Agriculture, Dalhousie University and Lab2Market-Atlantic Canada-2021 and as well as the Mitacs accelerated scholarships, thank you for your support. Also, I am very grateful to the following

personnel Ms. Beverly Zinck, Mr. Paul McNeil, Mr. Ryan Snitynsky, Ms. Kalyani Prithiviraj, Ms. Sherry Matheson, Mr. Fred Manley, and Mr. Jonathan Wang for giving me opportunities to work with them which indeed was a tremendous support in diluting my financial burden.

Last but not least, my beloved amma… thank you so much for enlightening my academic life, thank you for believing in me even when I am unsure of my abilities, though you are miles away from me, your daily phone calls and long hours of talking gave me the tons of strength I really needed to accomplish this task; my dear thaththa…thank you so much for getting me into the habit of reading, for moulding me and for love me so dearly, I miss you so much, I'm sure you're watching me from the stars above and still protecting and guiding me; my sister-Nirosha…thank you for leading me on the right path and keeping me close to your heart until I see the light; my ex husband, Sethiya… I definitely couldn't have achieved a lot of my dreams without you, thank you for being by my side for a long time, protecting me, and providing me with every possible help. I am thankful to you especially for the patience and the calm you have had and for all the sacrifices you have made.

Our lives are changing every moment. Looking back at the time, it was actually not a smooth journey. However, with all these wonderful people around me, I was able to achieve my goal and I'm really proud of it. To all the people who supported me with even a single word, sacrificing their time, caring for me genuinely, laughing with me and being there for me, I am indebted to you all, THANK YOU!

# CHAPTER 01: INTRODUCTION

Inflammation can be identified as the body's protective mechanism against bacteria, viruses, toxins and infections which ultimately promotes tissue repair and recovery (Kotas & Medzhitov, 2015). Inflammation is divided into two main categories as acute and chronic inflammation. The acute inflammation is usually of short duration, lasting from minutes to days depending on the severity of the injury. If the body experiences prolong acute inflammation without resolution, it leads to chronic inflammation (H. Zhao et al., 2021). Worldwide, three of five people die due to chronic inflammatory diseases such as stroke, chronic respiratory diseases, heart disorders, cancer, obesity, and diabetes (Tsai et al., 2019). Inflammation of the mucosal lining of the colon or colitis results from the interaction between genetic and environmental factors which influence the immune responses (Seyedian et al., 2019). Ischemic colitis is an acute form of inflammation in the colon that results in inadequate blood flow to the colonic tissues. Infectious colitis that cause by bacterial, viral, or parasitic pathogens and colitis arises by prolonged and/or misuse of high local concentrations of drugs such as non-steroidal anti-inflammatory drugs, are the major types of colonic inflammations. Also, it may occur secondary to immune deficiency disorders or secondary to exposure to radiation (Kelly, 2003). Colitis-associated colon cancer (CAC) is the colon cancer subtype that is associated with inflammatory bowel disease (IBD), is difficult to treat, and has high mortality. More than 20% of IBD patients develop CAC within 30 years of disease onset, and >50% of these will die from CAC (Terzić et al., 2010). Therefore, attenuation of colitis can be figured as one of the essential and possible processes to reduce the prevalence of CAC.

There is a strong link between diet and inflammation. The westernized diets rich in red meat, processed foods, refined sugar, and saturated fat tend to promote the "imbalance" in the gut microbial community i.e., gut microbial dysbiosis, and impaired intestinal permeability leading to the onset and progression of inflammation. On the other hand, diets rich in fruits and vegetables, whole grains and sea foods are associated with protecting the natural gut microbial diversity and preserving intestinal integrity (Keshteli et al., 2019). Based on the scientific evidence gathered, the consumption of colorful fruits and vegetables rich in plant flavonoids called anthocyanins has been intensively studied for its anti-cancer and anti-inflammatory properties. There are six main anthocyanins found in nature; however, cyanidin-*3*-*O*-glucoside (C3G) exhibits significantly strong antioxidant, anti-inflammatory and anti-cancer properties. The metabolism of C3G in the gastrointestinal tract could produce bioactive phenolic metabolites, such as protocatechuic acid (PCA), phloroglucinaldehyde (PGA), vanillic acid, and ferulic acid, which enhance C3G bioavailability and contribute to both the mucosal barrier and microbiota (Tan et al., 2019). It is noteworthy that anthocyanins improve the intestinal tight junctions (TJ) barrier integrity by promoting the expression of crucial barrier-forming TJ proteins such as occludin, claudin-5 and, zonnula occuldin-1 (Nunes et al., 2019). Besides, anthocyanin has the potential in down-regulating the major pro-inflammatory cytokines such as tumor necrosis factor-alpha (TNF-α), interleukin (IL)-6 (IL-6), IL-1beta (IL-1β) and interferon-gamma (IFN-γ) potentially by suppressing the activation of nuclear factor-kappa B (NF-κB) and extracellular signal-regulated kinase (ERK) (Ferrari et al., 2016). Anthocyanin is readily available in fruits such as berries. However, emerging evidence suggests that haskap berry *(Lonicera caerulea)*, which is fairly new to Canada, outstand all the other

types of berries for its significantly higher content of anthocyanins primarily consist of C3G, cyanidin-3,5-*O*-diglucoside, and cyanidin-3-*O*-rutinoside (Celli et al., 2014).

Human gut bacteria can use C3G as substrates to form fermentable metabolites which can exert bioactive functions similar to parent anthocyanins thus, gut microbiota plays an important role in the metabolism of anthocyanins (Keppler & Humpf, 2005). The probiotics such as *Lactobacillus* and *Bifidobacterium* have the maximum ability to produce the β-glucosidase so that anthocyanins can be transformed to PCA (Braga et al., 2018). On the other hand, anthocyanins and their metabolites are capable of modulating the growth of gut microbiota and improving the relative abundance of probiotics such as *Bifidobacterium* and *Akkermansia*, which are believed to be closely related to anti-inflammatory effects (Morais et al., 2016). Therefore, combining anthocyanin with probiotics might be one of the best solutions to attenuate colonic inflammation. However, due to the low bioavailability of anthocyanin and poor stability of probiotics in the gastrointestinal tract, the pronounced health benefits of these compounds are minimized. To overcome that, anthocyanins can be microencapsulated. Microencapsulated anthocyanin particles are in the micrometer range and are resistant to harsh gastric conditions; can be directed to the colon where it is then subjected to biotransformation by gut microbiota. Among many dehydration technologies, freeze drying produces microencapsulated bioactive compounds with the least process-induced damage with higher physicochemical activity (Wilkowska et al., 2016). Hence, the first phase of this study is focused on microencapsulation of haskap berry anthocyanin-rich fraction and during the second phase, the anti-inflammatory potential of haskap berry anthocyanin-rich

fraction with/without probiotics is evaluated using experimental animal model on which the colitis was induced by the chemical dextran sulfate sodium (DSS).

## 1.1 Hypothesis

A combination of haskap berry anthocyanin-rich fraction (free or microencapsulated forms) and probiotics are potent in significant attenuation of the severity of DSS-induced acute colitis in vivo.

## 1.2 Research objectives.

*Overall objective*

To produce microencapsulated haskap berry anthocyanin-rich fraction using maltodextrin and inulin and to evaluate the anti-inflammatory potential of free and microencapsulated forms of anthocyanin along with probiotics in DSS-induced acute colitis in male Balb/c mice.

*Specific objectives*

I. To optimize the use of maltodextrin and inulin in microencapsulation of haskap berry anthocyanin-rich fraction.
II. To characterize the physical and chemical properties of anthocyanin-rich microparticles.
III. To investigate the reduction of DSS-induced colitis severity in male Balb/c mice by a combination of microencapsulated haskap berry anthocyanin-rich fraction and probiotics in comparison to control and free anthocyanin and probiotics alone.

# CHAPTER 02: LITERATURE REVIEW

## 2.1 The inflammatory response

Inflammation is the body's response to a wide variety of physiological and pathological processes which includes events such as infection, exposure to toxins, and tissue injury. Inflammation can be defined as the reaction of vascularized living tissue to local injury (J.J Li & Zreiqat, 2019). However, there is a complex regulatory process underlying the classic inflammatory responses which consist of redness, swelling, healing, and pain (L. Silva & Silva, 2015). These processes are responsible for inducing inflammation and triggering leukocytes (neutrophils, monocytes, and eosinophils) and plasma protein recruitment to the site of tissue damage (Medzhitov, 2008). When the body is incapable of controlling the inflammation, it can lead to excessive tissue injury and can cause physiological decompensation, organ dysfunction and even death (Sherwood & Toliver-Kinsky, 2004). Inflammatory responses result in repairing the damaged tissue and inducing cell proliferation consistent with the changes that occur in cellular and immune responses (N. Singh et al., 2019).

The inflammatory pathway consists of four major contributors: inducers, sensors, mediators, and effectors (Figure 1). Stimuli for an inflammatory response such as infections, tissue necrosis, trauma, physical and chemical agents, immune reactions such as autoimmune disorders, and, foreign bodies are examples of inducers (Hannoodee & Nasuruddin, 2020). Sensors such as toll-like receptors (TLRs) are specialized molecules present on epithelial cells and capable of recognizing inflammatory stimuli. The TLRs are membrane-spinning proteins and are present on the surface of macrophages and dendritic cells. They possess the capability in recognizing the pathogen-associated molecular

patterns (PAMPs) and danger-associated molecular patterns (DAMPs) on which the former represents the pathogen-specific carbohydrate, lipoproteins or nucleic acids and the latter represents the host-specific molecules released upon cellular stress or tissue injury (Brennan & Gilmore, 2018; L. Chen et al., 2018). Once the stimuli are recognized by sensors then they trigger the production of mediators such as inflammasomes, and arachidonic acid mediators (Varela et al., 2018).

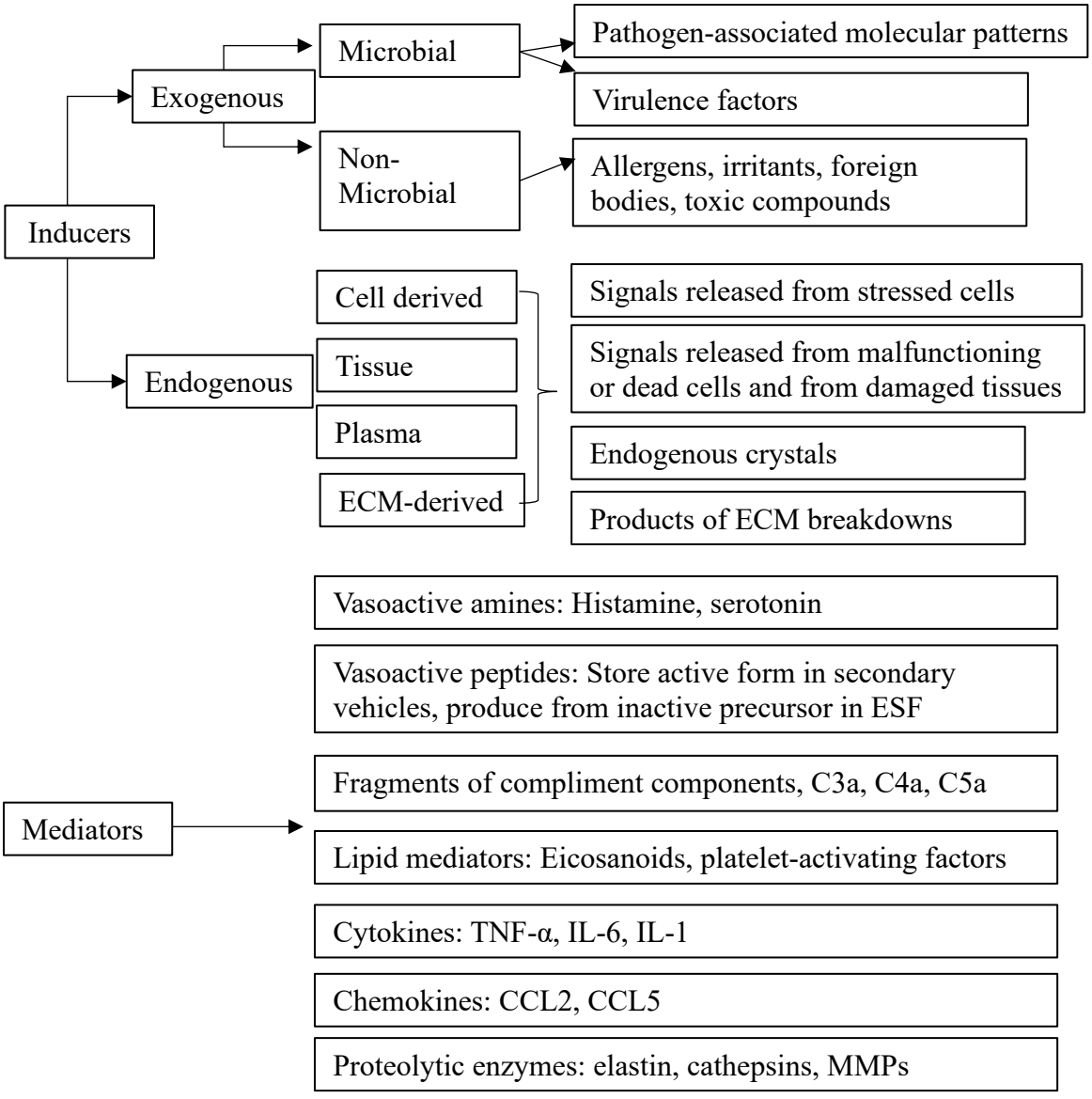

**Figure 1: The major classes of inflammatory contributors**. A generic inflammatory pathway consists of several types of inducers and mediators. a) Inducers of inflammation can be classified as exogenous and endogenous, and these two groups are further classifieds as shown. b) There are seven types of inflammatory mediators that have been identified. ECM, extracellular matrix; TNF-α, tumor necrosis factor; IL-6, interleukin 6; IL-1, interleukin 1; CCL2, chemokine ligand 2; CCL5, chemokine ligand 5; MMPs, matrix metalloproteinases (Medzhitov, 2008).

Being endogenous chemicals, mediators act as either anti-inflammatory or pro-inflammatory facilitators. The inflammasomes are multiprotein cytoplasmic complexes, and they are activated by the innate immune system. Inflammasomes regulate the activation of caspase-1 and interleukin (IL)-1 where the latter is a mediator of leukocyte recruitment (Guo et al., 2015). While being a phospholipid, arachidonic acid mediators are activated by infections and tissue damage. They are metabolized into two main components, namely prostaglandins and other prostanoids and leukotrienes following cyclooxygenase and lipoxygenase pathways aiding the inflammatory response in both the ways, such as aiding the vasodilation as well as vasoconstriction, promoting and inhibiting the platelet aggregation, facilitate, and disaffiliate the chemotaxis (B. Wang et al., 2021). The effectors of the inflammatory response are the target tissue and cells such as endothelial cells, hepatocytes, leukocytes, and hypothalamus.

## 2.2 Types of inflammation

Based on the time duration of the inflammation, it can be divided into two main types, namely acute inflammation and chronic inflammation which former occurs immediately after stimulation and lasts for a few days whereas the latter initiates because of the failure of resolution of the former one and lasts for months to years (H. Zhao et al.,

2021). Persistent unresolved inflammation is evident in promoting the onset of diseases such as cancer (Coussens & Werb, 2002), atherosclerosis (Hansson et al., 2006), obesity (Ellulu et al., 2017), diabetes (Tsalamandris et al., 2019), cardiovascular disease (Golia et al., 2014), and auto-immune disease (Duan et al., 2019).

### 2.2.1 Acute inflammation

Considering the characteristics of acute inflammation, it can be identified as the body's first defensive response to a specific injury. Pathologically acute inflammation involves predetermined events consisting of two main alterations: vascular changes and cellular changes (Figure 2). The former phase is characterized by momentary vasoconstriction in which small blood vessels in the damaged area are constricted immediately due to the external or internal stimuli which lasts for a few seconds while having no or minimum effect on inflammation, vasodilation, where the arteriole and venule dilation resulting increase in blood flow, and finally increase in capillary permeability which aids in releasing protein-rich fluid to extracellular matrix (H. Zhao et al., 2021).

#### Vascular changes

From a clinical point of view, vasodilation is characterized by the redness and heat associated with the hyperemia condition. Dilation of newly generated capillary vessels and larger arterioles facilitates the supply of inflammatory proteins and soluble mediators to the site of injury (Arulselvan et al., 2016). Inflammation-induced vasodilation is facilitated by nitric oxide (NO), histamine (pre-formed mediators), bradykinin, and various prostaglandins (newly synthesized) (Williams & Peck, 1977). The major route of NO production is from *l*-arginine and, is regulated by three main nitric oxide synthase (NOS) isoforms; endothelial NOS (eNOS), neuronal NOS (nNOS), and inducible NOS (iNOS).

The first two enzymatic isoforms are controlled by the intracellular $Ca^{2+}$/calmodulin availability whereas, iNOS activation is Ca independent, and stimulation depends on the presence of cytokines and interleukins aid in vasodilation via promoting smooth muscle relaxation by activating guanylate cyclase which is found in vascular smooth muscle cells and most other cells of the body (K. Chen et al., 2008). Guanylate cyclase is responsible for catalyzing the dephosphorylation of guanosine triphosphate (GTP) to cyclic-guanosine monophosphate (cGMP) which in turn facilitates smooth muscle relaxation followed by vasodilation (Karabucak et al., 2005). Considering the activity of histamine in the process of inflammation, it is found that histamine plays a key role in acute inflammation through its involvement in vasodilation, smooth muscle contraction, and increased vascular permeability (Benly, 2015). Histamine is released by mast cells. The main factors that determine vascular permeability are blood flow and endothelial barrier function. According to a study done by Wessel et al., 2014, histamine increased vascular permeability by phosphorylating vascular endothelial (VE) cadherin which is a principle contributor to maintaining the endothelial barrier by being a constitute of intercellular adherens junctions. Because of dilating submucosal arterioles, histamine directly activates vascular H1 and H2 receptors resulting in the release of NO from the endothelium and further involved in activating the H3 receptors on sympathetic nerve terminals which in turn result in presynaptic inhibition of vasoconstrictor tone (Beyak & Vanner, 1995). Prostaglandins, lipid mediators derived from arachidonic acid, play a vital role in contributing to the cardinal signals of acute inflammation. The production of prostaglandins is usually elevated in inflammatory tissues. Once pro-inflammatory macrophages are activated, they contribute to the exacerbation of inflammation by producing and releasing more than 100

substances, including pro-inflammatory cytokines such as IL-1β and prostaglandins (Scott et al., 2004). Among the several other types, prostacyclin ($PGl_2$), prostaglandin-$D_2$ ($PGD_2$), prostaglandin-$E_2$ ($PGE_2$), and prostaglandin-$F_{2\alpha}$ ($PGF_{2\alpha}$) are primarily involved in vasodilator effects (Ricciotti & Fitzgerald, 2011). The chemotactic activity of prostaglandins facilitates the attraction of leukocytes to the locally inflamed area and $PGE_2$ has demonstrated synergized effects with other mediators such as bradykinin in enhancing vascular permeability (J. Li & Kirsner, 2005). As vasodilation increases the local blood floor, it accounts for the clinically visible redness and warmth associated with acute inflammation.

**Fluid exudation and leukocyte migration**

Once the adherent junctions are disassembled and barrier functions are altered during the vasodilation, fluid exudation followed by immune cell and inflammatory protein migration to extravascular space take place. Immune recruitment is not limited to plasma proteins, antimicrobials, immunoglobulins, and complement factors. This causes localized edema in the inflammatory site. The sequence of adhesive interactions of leukocytes with endothelial cells is termed the leukocyte extravasation cascade and involves a series of adhesive interactions (Schnoor et al., 2015). These steps are mediated by multiple molecules and consist of steps including the rolling of leukocytes which assists via selectins; a family of glycoprotein surface molecules that are expressed on leukocytes (L-selectin), endothelial cells (E-selectin), and platelets (P-selectin) that bind sialylated carbohydrate determinants on adjacent cells, chemokine and leukocyte activation, firm adhesion of integrin, glycosylated transmembrane proteins to endothelial cells, and trans-endothelial migration

(TEM) of leukocytes due to morphological and polarization of adhesion molecules (Garrood et al., 2006).

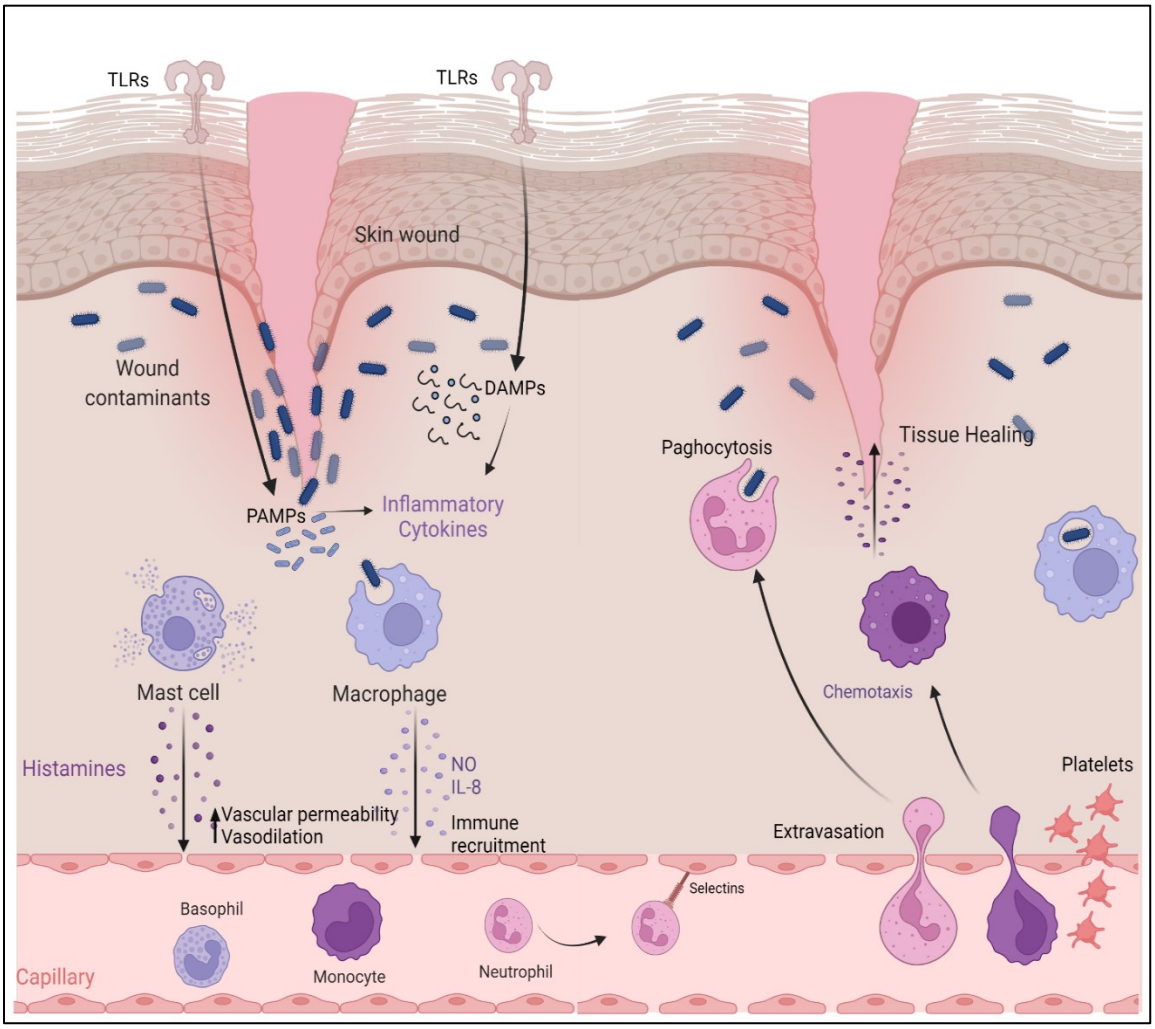


**Figure 2: Acute inflammatory response of the skin.** Upon an external inflammatory stimulus, damage and dead cells facilitate the release of DAMPs and PAMPs (caused by infectious agents) and are usually recognized by TLRs. DAMPs initiate the release of pro-inflammatory cytokines from macrophages and PAMPs facilitate the mast cell degranulation and thereby secretion of histamine which improves vasodilation and vascular permeability. Following the initiation of vascular changes, a variety of leukocytes bind to involved blood vessels and exit into the parenchyma. Since vasodilation slows the flow of blood, immune cells tend to move towards the vascular wall and build low affinity interactions with endothelial cells mediated by selectins. Once bound to the vascular wall, immune cells extravasate into the parenchyma by squeezing between endothelial cells and

moving towards the site of injury via chemotaxis and eliminating the injurious matter by phagocytosis. To facilitate sealing the inflammatory area, platelets also escape from the capillary area. PAMPs, Pathogen-associated molecular patterns; DAMPs, Danger-associated molecular patterns; TLRS, Toll-like receptors. Created with BioRender.com.

Neutrophils are the first and most abundant leukocytes to undergo extravasation within 24 h of injury. Neutrophils are designed in a way to eliminate the inflammatory stimuli via phagocytosis, degranulation, and neutrophil extracellular traps (NETs) using their specialized cytoplasmic granules which contain acid hydrolases and antimicrobial peptides that are produced in three different stages of neutrophil maturation (Rosales, 2018). Neutrophils and other leukocytes also require chemoattractants; soluble molecules such as bacterial by-products, chemoattractant cytokines, and chemokines. to facilitate their migration to sites of injury or infection. In response to primary chemoattractants such as formyl peptides, released from bacteria or cells undergoing necrosis, immune cells such as macrophages release secondary chemoattractants including pro-inflammatory mediators to enhance the leukocyte extravasation (Afonso et al., 2012). Escaped neutrophils migrate to the site of injury via chemoattractant gradient given the name “chemotaxis; one of the initial steps in innate immune response” which consists of three different processes: gradient sensing, polarization, and cell motility. As reported by Petri & Sanz. (2018), neutrophils migrate more efficiently towards single interleukine-8 (IL-8) gradients one of the alpha chemokines than leukotriene B4 (LB4) gradients, which is identified as the first secondary chemoattractant released at a site of inflammation. Likewise, neutrophil migration is largely determined by the presence, concentration, and composition of the respective chemoattractant (Li Jeon et al., 2002). Upon arrival at the injured site, immune cells begin to phagocytose and eliminate the cellular debris. Phagocytosis is defined as a

cellular process aiding in ingesting and eliminating pathogens, dead cells, and tissue debris which usually are greater than 0.5 μm in diameter (Uribe-Querol & Rosales, 2020). In addition to neutrophils, activated macrophages also engage in phagocytosis.

### 2.2.2 Inflammatory cytokines

In regulating the inflammatory response, two main interconnected branches of the immune system; the innate and adaptive immune systems play a vital role by recruiting the inflammatory cytokines. With regards to innate immune response, the cellular components which are not limited to circulating dendritic cells (DCs), neutrophils, natural killer (NK) cells, monocytes, basophils mast cells, and macrophages act as the base and serve as the frontline of the host defensive mechanism. Moreover, it consists of anatomical barriers (mucous layer, epithelial barrier functions, antimicrobial peptides) and receptors that can detect conserved structural motifs of microorganisms (Choy et al., 2017). As previously elaborated, the innate immune system is responsible for the initial phases of the inflammatory response, such as vasodilation, increased vascular permeability, and cellular infiltration and its cellular components are responsible for releasing and synchronizing the cytokines and thereby orchestrating the immune response (Lacy & Stow, 2011). Cytokines are hormone-like major signaling glycoproteins that have a wide variety of molecular weights ranging from approximately 6 to 70 kDa, and regulate the development and expression of the broad array of immune responses that are mounted against a variety of pathogens (Holdsworth & Can, 2015). Cytokines are secreted by many of the immune cell systems including neutrophils, activated lymphocytes, macrophages, B-cells, T-cells, and dendritic cells. Widely spread cytokines are classified as interleukins, lymphokines, monokines, chemokines, interferons, and colony-stimulating factors (Tasneem et al.,

2019). Considering the role of cytokines in inflammation, two major types of cytokines have been identified namely proinflammatory cytokines and anti-inflammatory cytokines. The pro-inflammatory cytokines which are mainly produced by activated macrophages are predominantly involved in the upregulation of inflammation. The IL-1β, IL-6, and TNF-α are classified as pro-inflammatory cytokines (J. M. Zhang & An, 2007). On the other hand, anti-inflammatory cytokines are identified as the regulators of pro-inflammatory cytokines and hence are defined as the cytokines involved in suppressing the inflammatory response (Opal & DePalo, 2000). The family of interleukins harbours most of the anti-inflammatory cytokines which are not limited to IL-4, IL-10, IL-11, and IL-13. As cytokines play a key role in inflammation, managing and controlling the stimulation and production of cytokines has become one of the targeted therapeutic approaches in many inflammatory diseases such as IBD (Mitsuyama et al., 2000), meningitis (Leonardis et al., 2018), and gastritis (Zavros & Merchant, 2005). Among the identified cytokines, IL-1, IL-6, IL-8, IL-11, TNF-α, and granulocyte-monocyte colony-stimulating factors (GM-CSFs) are predominantly engaged in acute phase inflammation (Feghali & Wright, 1997). Of these, IL-1 (α and β), IL-6, and TNF-α are extremely potent cytokines and identifies as key pro-inflammatory cytokines in mediating the acute inflammatory response (Turner et al., 2014).

IL-1 is expressed mainly by multiple cell types including monocytes, macrophages, neutrophils, hepatocytes, and tissue macrophages throughout the body (Arend et al., 2008). Typically, IL-1 expression is triggered by microbial invasion. Specifically, IL-1β is identified as a basic stimulator of $CD4^+$ T-lymphocytes and differentiates them towards T-helper (Th) cells particularly Th1 and Th17 cells where the former is found to be involved

in activating the macrophages and the latter is involved in recruiting the neutrophils and monocytes during an inflammatory response (Turner et al., 2014).

TNF-α, one of the members of a family of type II transmembrane proteins, which consists of 30 receptors and 19 associated ligands, has been spotted as a prototypical pro-inflammatory cytokine (Lobito et al., 2011). It is primarily secreted from activated macrophages within min of local or systematic injury. In addition to that, other cellular components such as mast cells, NK cells, monocytes, fibroblasts, and endothelial cells are also responsible for secreting transmembrane precursor protein of TNF-α. With regards to the target destinations of TNF-α, neutrophils, endothelial cells, hypothalamus, liver, heart, macrophages, and T-lymphocytes have been recognized. Moreover, the primary effects of TNF-α, include the activation of the inflammatory cascade, release of vasodilators, release of other cytokines, myocardial suppression, catabolism of fat, and increased body heat or inducing fever conditions which is one of the main clinical features of the acute phase of inflammation (Sherwood & Toliver-Kinsky, 2004).

IL-6 is another cytokine secreted during inflammation that has a pleiotropic effect. It is expressed and released by a wide variety of cells including macrophages, fibroblasts, endothelial cells, T cells, B cells, keratinocytes, hepatocytes, bone marrow cells, and some epithelial cells (Jucker et al., 1991). Physiological effects of IL-6 are broadened up to elevating the systemic responses primarily focusing on producing the acute phase proteins from the liver, inducing B cells to differentiate into antibody-producing plasma cells, T cell activation, differentiation, and regulation of Th2 and Treg phenotypes (Moens & Tangye, 2014). In this context, it is well understood that the inflammatory process is regulated by cytokines, and ensuring the recruitment of appropriate cytokines is also a concern.

### 2.2.3 Resolution of inflammation

Resolution of inflammation is a highly coordinated process that consists of tissue repair and healing mechanisms to prevent the progression of acute inflammation and restore tissue homeostasis by actively addressing the deficiencies which lead to chronic inflammation (Headland & Norling, 2015). The onset of resolution occurs shortly after the beginning of the inflammatory response. The inflammatory resolution process includes cessation of tissue infiltration of neutrophils, shut down of polymorphonuclear leukocyte recruitment, induction of apoptosis (or programmed cell death) and efferocytosis to remove the dead cells and pro-inflammatory immune cells, re-program macrophages from classically activated cells to alternatively activated cells, and initiation of the healing process (Neurath, 2019). Regarding the cellular components involved in the resolution process, the primary mediators of the resolution are comprised of lipid, protein, peptide, and gaseous mediators. During the resolution period, pro-inflammatory lipid mediators such as PGs are switched to lipoxins (LXs) which have prevailing effects in anti-inflammatory and pro-resolving activities. Lipoxins are generated from endogenous fatty acid, arachidonic acid. LXs were long known to play an essential role in resolution by controlling the entry of neutrophils to sites of inflammation, reducing the vascular permeability and extravasation of cellular components. It has also been found that LXs are potent chemoattractants of monocytes (Schwab & Serhan, 2006). Other than LXs, resolvins, protectins, and maresins are also actively engaged mediators in resolving inflammation. In an attempt to understand the role and actions of latter mediators in resolving inflammation, much evidence has been stored. Resolution actions of these mediators are not limited to the inhibition of neutrophil infiltration (Serhan et al., 2000),

modulation of the chemokine and cytokine synthesis (Bannenberg et al., 2005), promotion of the healing of inflamed tissues, and enhancement of phagocytosis (Schwab et al., 2007). In addition to the lipid mediators, protein mediators such as Annexin A1, chemokine binding protein (D6), T cell/transmembrane immunoglobulin mucin (TIM-4), and developmental endothelial locus-1 (DEL-1) are also playing a crucial role in the resolution phase of the acute inflammation (Feehan & Gilroy, 2019). The main functions of protein mediators in resolution are cytokine scavenging, anti-inflammatory macrophage polarization, and efferocytosis. Once the apoptotic neutrophils are formed during the resolution phase, appropriate clearance of them is carried out via phagocytes through the process called efferocytosis. Besides the D6 mediator, Annexin A1, TIM-4, and DEL-1 involvement in efferocytosis are well documented (L. Chen et al., 2014; Kobayashi et al., 2007; Kourtzelis et al., 2018). Referring to the gaseous mediators in the resolution of inflammation, the best characterized are NO, hydrogen sulfide ($H_2S$), and carbon monoxide (CO). During apoptosis, activated inflammatory cells generate reactive oxygen species (ROS) and reactive nitrogen species (RNS) including NO which has both pro-apoptotic and anti-apoptotic properties (Quinn et al., 1995). However, as the evidence supports, a lower concentration of NO produced by eNOS and nNOS promotes cell protection whereas, excessive levels produced by iNOS promote cell death (J. L. Wallace et al., 2015). Besides NO, $H_2S$ is also found in facilitating neutrophil apoptosis which is identified as a crucial step toward the resolution of inflammation (Mariggiò et al., 2008). In addition to these mediators, changes in intracellular signaling pathways such as NF-κB, phosphoinositide 3-kinase (PI3K), extracellular-signal-related kinase 1 and 2 (ERK1 and ERK2), and cyclic adenosine monophosphate (cAMP) also play a vital role in initiating the

resolution phase of inflammation via functioning the anti-inflammatory response mainly by facilitating the process of apoptosis. Despite the well-established regulatory processes, inadequate/insufficient resolution or failures in resolution triggers chronic inflammation.

### 2.2.4 Chronic inflammation

Chronic inflammation is characterized by slow, long-term inflammation lasting for a prolonged period. In contrast to neutrophil infiltration in acute inflammation, during chronic inflammation, leukocytes including monocytes which differentiate into macrophages and T-lymphocytes are continuously recruited and accumulated (Headland & Norling, 2015). Moreover, research findings prove that chronic inflammation has an association with the proliferation of fibroblasts which results in subsequent organ failure. Thus, chronic inflammation leads to relentless disease conditions in the categories of autoimmune diseases, granulomatous diseases, metabolic disorders, and cancers (King, 2007). Characteristically, chronic inflammation is continued when the causative agent of the inflammation (bacteria, viruses, fungi, parasites) survive for a long period without complete elimination. As an example, evidence showed the relationship between the microbiota not being limited to *Mycobacterium avium* subspecies *paratuberculosis*, *Clostridium difficile*, *Escherichia coli*, *Listeria monocytogenes*, *Campylobacter concisus,* and IBD (Azimi et al., 2018). Moreover, the evidence of a direct role of the gut microbiota in the development of autoimmune arthritis arises from experimental studies on germ-free mice in which a reduced severity and/or incidence of arthritis has been demonstrated (Costello et al., 2015).

## 2.3 Inflammation associated with the gastrointestinal tract

The human gastrointestinal tract (GIT) is a continuous channel through the body that extends from the mouth to the anus. There is no specific area that can be inflamed rather, inflammation can occur at any site of the GIT demonstrating a variety of aetiologies thus, characterized as a complex biological response to different injurious stimuli including pathogens, damaged cells, and irritants (Figure 3). For instance, glossitis; inflammation of the tongue, stomatitis; inflammation of the larger parts of the oral mucosa, gingivitis; inflammation of the gums, cheilitis; inflammation of the lips, chronic inflammatory conditions such as oral lichen planus, and periodontitis in which the inflammation extends to the supporting tissues including alveolar bone has been recognized as the major oral inflammatory diseases (Hasturk et al., 2012; Kösling, 2008). In contrast to oral inflammatory conditions, inflammatory disorders of the esophagus are commonly encountered in clinical practice and are usually treatable. Lymphocytic esophagitis which has a characteristic clinical feature of isolated elevation of peripapillary lymphocytes and eosinophilic esophagitis a chronic condition of a complete dysfunction of the esophagus are two distinctive types of esophageal inflammation (Lisovsky, 2020). Gastritis is the most common inflammatory condition associated with the stomach. *Helicobacter pylori* associated with gastritis is the most common cause of gastritis worldwide. However, *H. Pylori* negative gastritis has also been spread widely which is caused by gastrointestinal reflux, tobacco smoking, alcohol consumption and/or use of long-term medications (Blasco et al., 2022). Similarly, inflammation can occur in the pancreas giving rise to acute or chronic pancreatitis. Intra-pancreatic activation of pancreases is a distinctive feature in

acute pancreatitis, whereas chronic pancreatitis is characterized by progressive fibrotic destruction of the pancreatic secretory parenchyma (Brock et al., 2013; Elfar et al., 2007).

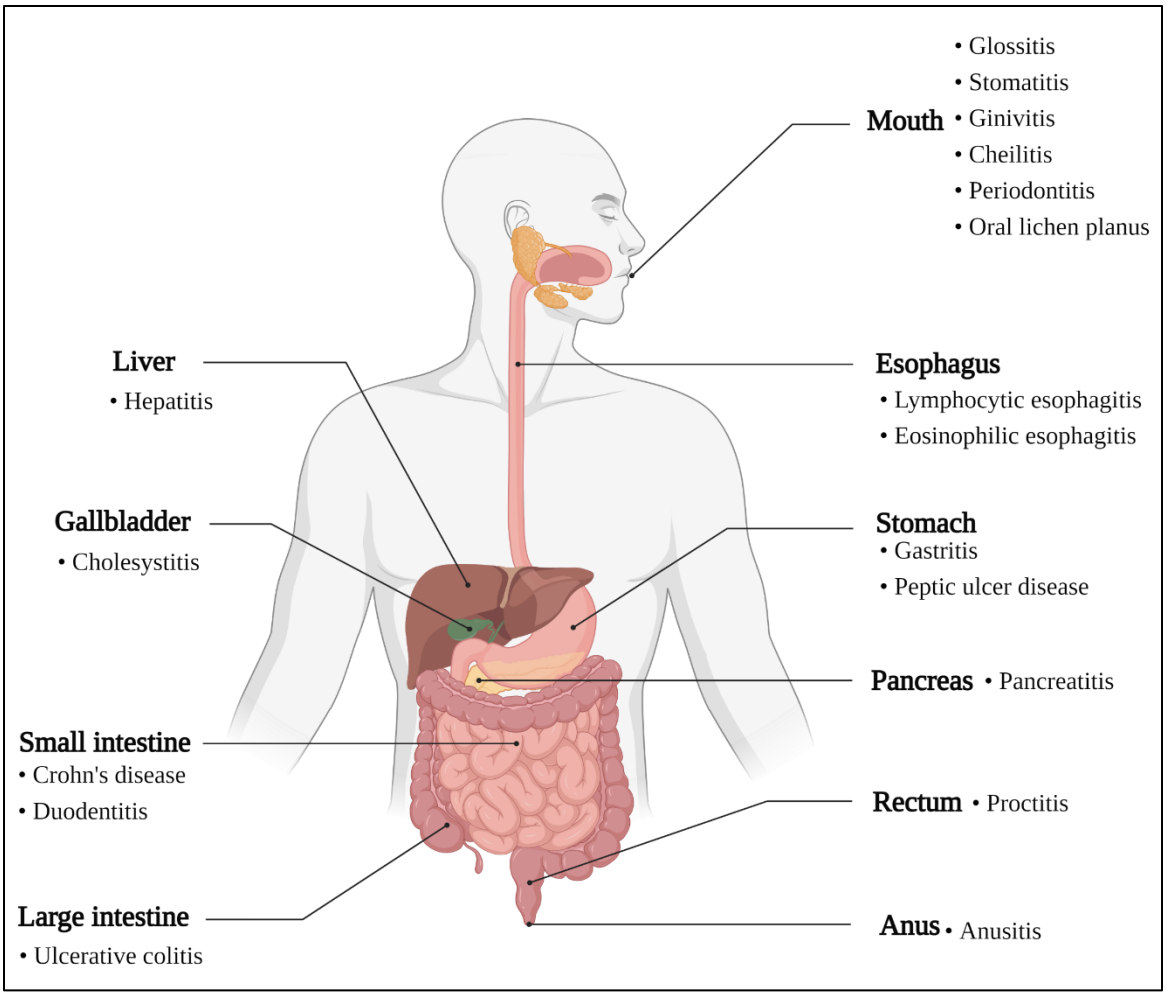


**Figure 3: Inflammatory diseases associated with GIT**. Inflammation is common in organs of GIT showing evidence of inflammatory conditions associated with every site. Starting from the mouth to the anus inflammatory disorders are prominent in GIT which includes oral inflammatory conditions, esophageal, liver, gallbladder, stomach, small intestine, pancreas, large intestine, rectum, and anus. Created with BioRender.com.

Inflammation occurs in the liver, or hepatitis can result from heavy alcohol use, harmful drugs, toxins, and viral infections. Among them, viral hepatitis has been spotted as the most common type of hepatitis which is accounted for by hepatitis viruses A, B, C, D, and E (Castaneda et al., 2021). Cholecystitis is known for the inflammation initiated in

the gallbladder which happened usually due to the blockage of the cystic duct by the gallstones (Adachi et al., 2022). Proctitis; inflammation of the lining of the rectum and anusitis; inflammation of the anal canal are also commonly occurring disorders that are more often misdiagnosed as hemorrhoids (Meseeha & Attia, 2021). Enteritis is the common name given for inflammation in the small intestine whereas regional enteritis or Crohn's disease is one of the major two types of IBD. Crohn's disease is a form of chronic inflammation which prominently affects the entire layers of the small intestine. However, it can be initiated at any site of the GIT (Gyires et al., 2014). Colitis is the common term given for colonic inflammation. Colitis has different types and results from several mechanisms including infection, autoimmunity, ischemia, and drugs. Also, it may occur secondary to immune deficiency disorders or secondary to exposure to radiation (Kelly, 2003). Ischemic colitis is an acute form of inflammation in the colon which results in inadequate blood flow to the colonic tissues (Theodoropoulou & Koutroubakis, 2008). In addition to that, intracolic pressure caused by the impacted feces is also linked with colonic ischemia. Infectious colitis is caused by bacterial (*Salmonella entarica*, *Salmonella typhimurium, Shigella dysenteriae, Campylobacter jejuni,* Enterohemorrhagic *Escherichia coli),* viral, and parasitic pathogens is one of the major public health problems in today's world. Although many other infectious agents can also contribute to infectious colitis, the above-mentioned causative agents are the most common (Navaneethan & Giannella, 2011). Colitis can also be initiated by the prolonged and/or misuse of high local concentrations of drugs such as non-steroidal anti-inflammatory drugs (NSAIDS-induced colitis). Regardless of the acute forms of colitis, ulcerative colitis (UC), the second type of

IBD affects the mucosal layers of the colon featured with recurrent inflammation with a chronic pathological atmosphere (Meier & Sturm, 2011).

## 2.4 Experimental colitis

As colonic inflammation has an immense relationship with colon cancer initiation understanding the etiology and pathophysiology of colitis has become a critical preventive factor for CAC. Thus, to fulfill the need of learning underlying mechanisms, and preventive and/or therapeutic approaches to CAC, several experimental animal models are being used primarily in the scope of colonic inflammation. Further, the induction of diseases in animals could enable us to better understand the progression of diseases from normal physiological states to inflammation and then malignant changes in particular organs (Wu & Yu, 2012).

### 2.4.1 Classification of experimental colitis models

Murine models of colitis can be classified into several different categories including administration of specific chemical substances-chemically induced colitis, spontaneous models, gene-knockout and transgenic models, and, reconstitution of immunodeficient mice with $CD4^+$ cells, and bacterial-induced models (Boismenu & Chen, 2000). For chemically induced colitis, a few types of chemical agents have been widely used. For example, DSS (Eichele & Kharbanda, 2017) and 2,4,6,-trinitrobenzene sulfonic acid (TNBS) (Antoniou et al., 2016) are the most common. TNBS-induced colitis model (0 .5-4.0 mg/ 45-50% ethanol) gained wider attention since a single rectal administration of the chemical in rats, mice, guinea pigs, dogs, and rabbits were able to produce rapid, reliable, reproducible, and efficient results (Brenna et al., 2013; Luo et al., 2020; Scheiffele & Fuss, 2002). TNBS basically facilitates colitis development via inducing acute Th1 inflammation

exemplified by infiltration of $CD4^+$ lymphocytes which mimics the features of human UC (I. Silva et al., 2019). Both DSS and TNBS models are primarily focused on epithelial barrier dysfunction and allowing bacteria and immunogenic molecules into the mucosa in colonic inflammation (Oh et al., 2014). Similarly, oxazolone is another hapten molecule when used triggers inflammation by applying 1% (v/v) the chemical which histologically resembles UC limited to the distal part of the colon. A rapid increase in IL-13 cytokine in lamina propria with the immersive appearance of NK-T cells are prominent immunological feature of oxazolone-induced colitis (Goyal et al., 2014). An acetic acid solution in a concentration of 4% v/v has been also used to provoke mucosal and submucosal inflammation in the colon mimicking the features of UC including extensive hemorrhage, occasional ulceration, and bowel wall thickening (Sotnikova et al., 2013). In addition to the above chemical inducers carrageenan, a high molecular weight sulfated polygalactan (Martino et al., 2017), iodoacetamide, blocker of sulfhydryl compounds in the colon (Satoh et al., 1997) have been used as colitis inducers less frequently.

Spontaneous models of colitis provide the advantages of being more effective, efficient, and carrying more similar clinical features to human disease. C3H/HejBir mice model in which the mice are produced by selective breeding of C3H/Hej mice with colitis is one of the popular forms of spontaneous colitis models. In this model, the inflammation is limited to the right side of the colon and lasts between 1 month to 1 year of life (Goyal et al., 2014). Genetically engineered models of colitis have gained more attention in recent years for their effectiveness in producing spontaneous colitis. Based on the gene construction strategies, genetically engineered murine models of IBD are classified into several subcategories. In particular, conventional knock-out mice, which are genetically

engineered to lack a particular gene of interest in all cell types, are commonly used to study the pathogenic/regulatory factors during the development of spontaneous chronic colitis (Mizoguchi et al., 2020). IL-10 $^{-/-}$, IL-2 $^{-/-,}$ and TGF- β $^{-/-}$ are a few examples of conventional gene knock-out models (Jamwal & Kumar, 2017). Salmonella-induced colitis is one of the models that fall under bacterial induction of colitis. Colitis is usually initiated within 5-7 days after the infection (Low et al., 2013). However, selecting the most suitable experimental model for assessing colitis always depends on practical criteria such as accessibility, easy experimental manipulation, cost-effectiveness, and % similarity with mirroring the human disease.

### 2.4.2 DSS-induced acute colitis

DSS is a water-soluble, negatively charge sulfated polysaccharide which has a highly variable molecular weight range from 5-1,400 kDa (Figure 4). Among currently used chemical models of colitis, the DSS-induced colitis model is the most used model which brings in severe epithelial damage and mimics the human UC. It has the advantage of being manipulated and used to demonstrate both acute and chronic colitis in which the latter is produced via the application of repeated cycles of DSS. Being rapid in completion, having a higher percentage of reproducibility, and possessing simplified protocols have made it well accepted (Eichele & Kharbanda, 2017). The concentration of the DSS solution, duration, and frequency of the administration mainly affect the nature of the model. However, responses also varied with the molecular weight of the DSS, manufacturer, batch number, genetic markup of the subjective animal, and gut microbiome of the animal (Perše & Cerar, 2012). Animal models are currently implemented to use DSS in the 40-50 kDa molecular weight range in drinking water (Eichele & Kharbanda, 2017).

In a study conducted using three different molecular weights of DSS in inducing acute colitis in mice, only the molecular weights of 5 kDa and 40 kDa were able to produce the colitis but not the 500 kDa. The main reason why the higher molecular DSS was not potent in inducing inflammation is the inability of DSS to pass through the mucosal membrane (Kitajima et al., 2000).

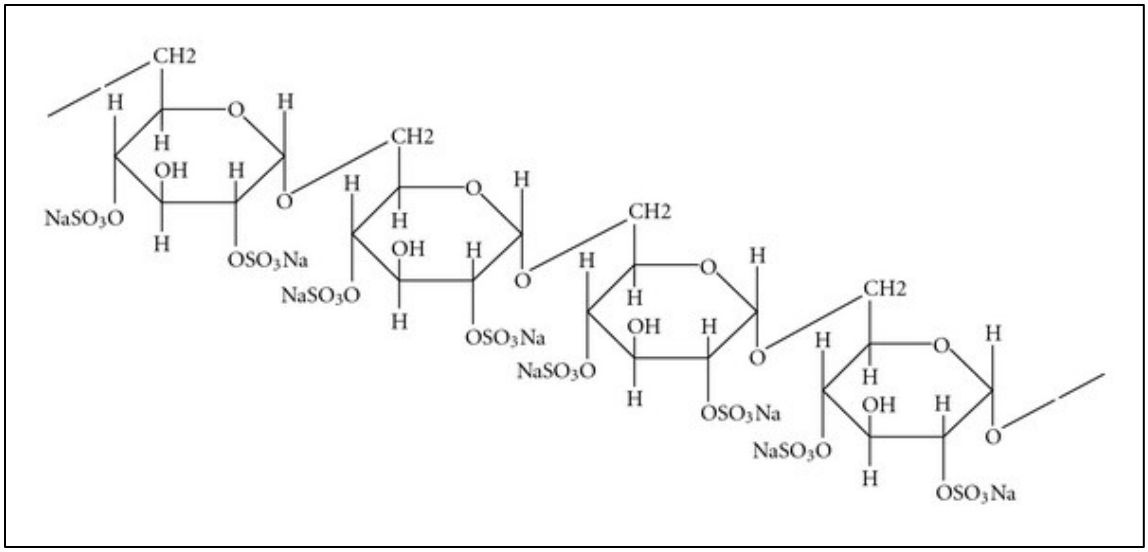


**Figure 4: Chemical structure of a part of DSS macromolecule.** DSS is a sulfated polysaccharide which uses for inducing acute and chronic colitis in animal models.

DSS is highly toxic to epithelial cells and causes a collapse in epithelial integrity and increases colonic mucosal permeability (Biton et al., 2018). Additionally, it facilitates the passage of luminal microorganisms into the mucosa (Perše & Cerar, 2012). DSS is recognized for its ability to inflame the animal's colon which has characteristic features of colitis more similar to that of humans. For instance, administration of ≥2.5% w/v DSS in drinking water for less than 7 days was potent in inducing colitis in mice with remarkable similarities to that of colitis patients resulting in mucosal edema, lesions, observable ulceration, occult blood and neutrophil infiltration (Randhawa et al., 2014). Typically,

acute colitis is induced by the administration of one cycle of DSS. On the other hand, chronic colitis results from the application of repeated cycles of DSS which includes 1 week of DSS followed by 7-14 days of sterile water (Figure 5) (Okayasu et al., 1990).

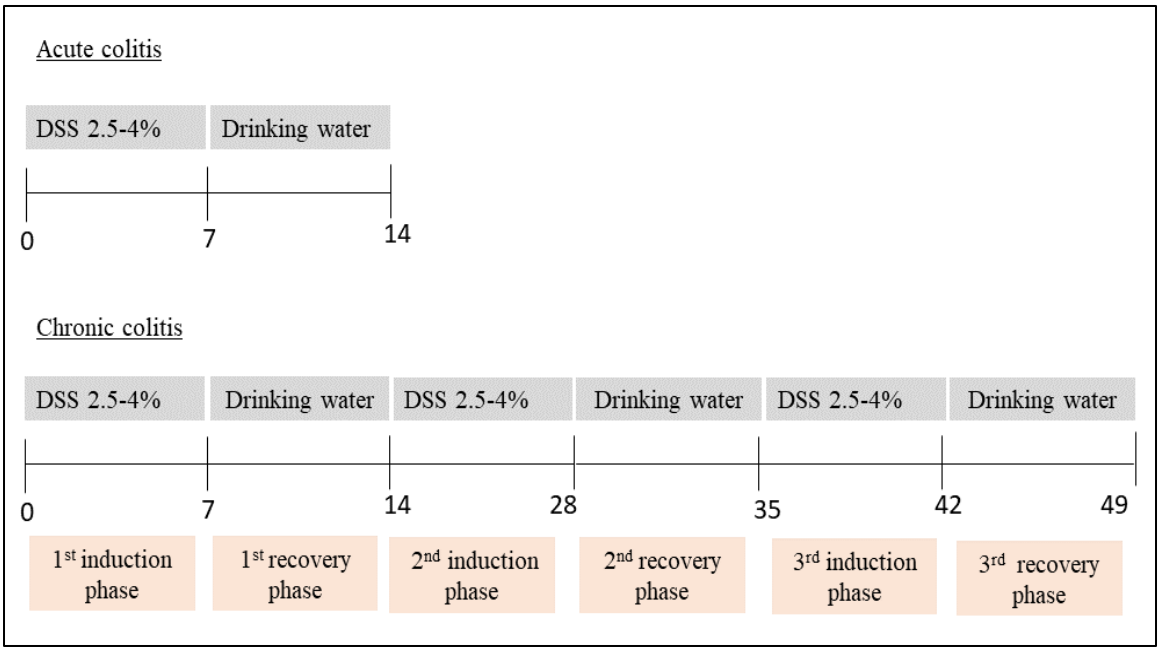


**Figure 5: Schematic diagram for acute and chronic colitis by DSS.** Acute colitis can be induced by DSS administrating a single cycle of DSS for a week followed by normal drinking water. On the other hand, chronic colitis is induced by administrating DSS more than 1 time which is indicated by having more induction and recovery phases.

## 2.5 Anti-inflammatory actions of dietary interventions

Positively addressing the modifiable risk factors such as lifestyle practices including smoking, unhealthy diet, and physical inactivity could potentially prevent 70-90% of various chronic disease conditions including inflammation (Wagenaar et al., 2021). As for the research findings, Mediterranean diets, diets rich in fruits and vegetables, diets with plant-based ingredients, whole grains, and a high amount of dietary fiber are associated with reducing the risk of persistent inflammation (Smidowicz & Regula, 2015). According to the data obtained from a meta-analysis, vegetarian-based dietary patterns are

found to be associated with a significantly lower concentration of C-reactive protein, total leukocytes, and fibrinogen compared to non-vegetarian diets (Craddock et al., 2019). Energy received from plant sources has been associated with favorable biomarkers of anti-inflammation and current findings show that the inflammatory marker profiles are subjected to alteration by the changes in dietary patterns highlighting the therapeutic role of food (Barros et al., 2021). Anti-inflammatory diets involve regulating the composition and metabolic activity of the gut microbiome, which directly affects the initiation and progression of inflammatory conditions in GIT. Dysbiosis of the gut microbiome facilitates intestinal permeability by disrupting the intestinal barrier integrity and altering the expressions of TJ proteins (Zheng et al., 2020). Changes in intestinal permeability aid in harboring the pathogenic microbes into the lumen which later enables the onset of an inflammatory response. Therefore, maintaining the natural balance of the gut microbiome and having diets that increase the count of healthy gut bacteria is one of the promising and effective ways of managing intestinal inflammation.

In addition to nutrients that are found in fruits and vegetables, such as essential vitamins and minerals, there are several plant-derived components commonly named phytochemicals. In particular, one of the major groups of phytochemicals, known as polyphenols has been extensively studied for their anti-inflammatory and anti-cancer properties (Fraga et al., 2019). Furthermore, there is a bi-directional relationship between polyphenols and the microbiome of the human gut in which polyphenols can modulate the composition of an individual's microbiome in the direction of improving healthy gut bacteria (Oteiza et al., 2018). Scientific evidence has demonstrated that flavonoids, a sub-class of polyphenolic compounds extensively present in plants hold anti-inflammatory

properties through different mechanisms such as inhibition of regulatory enzymes and transcription factors which serve as controllers of inflammatory mediators. Moreover, having pronouncing anti-oxidant properties, modulating the gene expression and immune cells, and having a direct impact on arachidonic acid metabolism make the flavonoids a potent candidate for controlling the inflammatory response (Maleki et al., 2019). Out of the seven sub-classes of flavonoids, anthocyanin has been widely investigated for its potential in controlling intestinal inflammation (Verediano et al., 2021).

### 2.5.1 Chemistry and dietary sources of anthocyanin

Anthocyanins, which are a glycosidic form of anthocyanidins, possess a basic structure of C6-C3-C6 composed of two aromatic rings (A and B) and one heterocyclic ring (C) (Jackman et al., 1987) (Figure 6). Anthocyanins are differentiated based on the number of hydroxyl groups, the number and type of sugar moieties, and the presence or absence of acyl groups. Out of over 600 anthocyanins identified in nature, six main anthocyanin classes are well distributed in fruits and vegetables (Figure 6). The C3G is highly abundant among anthocyanins, and more than 90% of anthocyanins are conjugated with glucose (He & Giusti, 2010). Families of Vitaceae (grape), Rosaceae (cherry, plum, raspberry, strawberry, blackberry, apple, and peach), Solanaceae (tamarillo and eggplant), Saxifragaceae (red and black currant), Caprifoliaceae (haskap), Cruciferae (red cabbage) and Ericaceae (blueberry and cranberry) are primary sources of dietary anthocyanin (D. Li et al., 2017; Rupasinghe et al., 2018).

#### 2.5.1.1 Haskap berry anthocyanin

Haskap berry (*Lonicera caerulea),* a variety of edible honeysuckle species containing very high levels of phenolics, is a plant native to low-lying wet areas and

mountains of Siberia and northeastern Asia, Europe, and North America (Bell & Williams, 2018). Haskap is fairly new to Canada, with only three major varieties in production, namely Borealis, Indigo Gem, and Tundra (Bors, 2009). Although many berry species are claimed to have a higher content of polyphenols, haskap has been identified as having a significantly higher amount of flavonoids (Celli et al., 2014). Haskap berry is rich in anthocyanins primarily having higher contents in the forms C3G, cyanidin-3,5-*O*-diglucoside, and cyanidin-3-*O*-rutinoside. Haskap berries contain high total phenolic content (141–1,142 mg gallic acid equivalent/100 g fresh weight, FW), total anthocyanin content (1,300 mg C3G equivalent/100 g FW), total flavonoid content (595–699 mg quercetin equivalent/100 g FW), and have the strong antioxidant capacity (Bors, 2009; Celli et al., 2014; Rupasinghe et al., 2012). The anthocyanin content of haskap berries is greater than that of raspberry (22.2-437 mg C3G equivalent/100 g FW), blackberry (126-152 mg C3G equivalent/100 g FW), red currant (1.4-7.8 mg C3G equivalent/100 g FW) and blueberry (99.9 mg C3G equivalent/100 g FW) (Celli et al., 2014). As haskap is a promising source of anthocyanin specifically, C3G, it has been widely investigated for its anti-inflammatory properties (Rupasinghe et al., 2015).

### 2.5.2 Bioavailability of anthocyanin

Intact forms of anthocyanins that are absorbed from the stomach, as well as the intestine via an active transport mechanism, are then subject to hepatic Phase 2 metabolism. The resulting anthocyanin metabolites enter the systemic circulation. Unabsorbed anthocyanins reach the large intestine and undergo microbial biotransformation into

decomposed products that contribute to anti-inflammation and cancer chemoprevention (J. Fang, 2014).

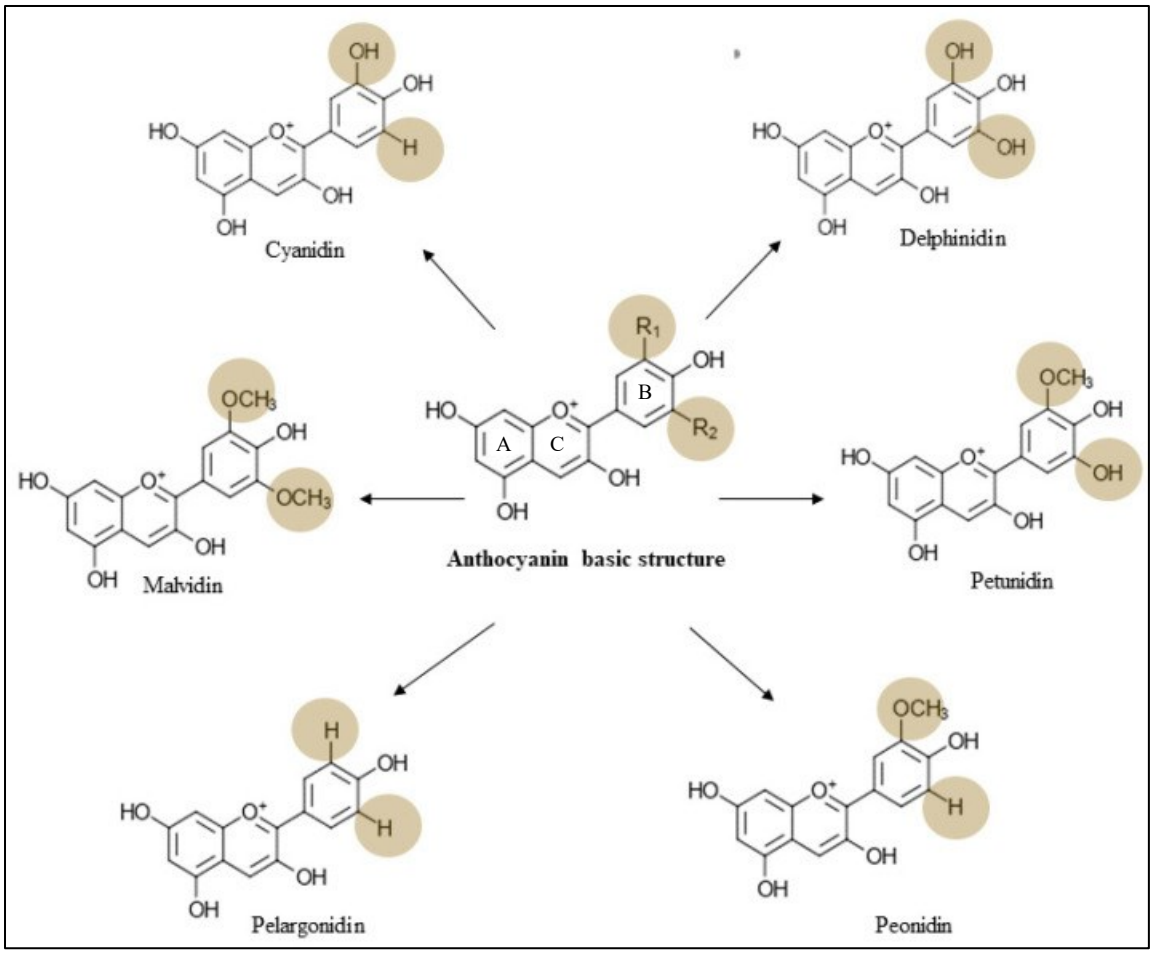


**Figure 6: Basic chemical structures of anthocyanidins.** Anthocyanin is derived from anthocyanidins and has the basic structure of flavylium ion which lacks the ketone oxygen at the 4$^{th}$ position of the C-ring. There are six different anthocyanidins that have been identified from plants.

Gastric digestion does not significantly affect anthocyanin composition; however, approximately 42–76% of total anthocyanins and 29% of their antioxidative activity are lost during passage through the intestines (Y. Liu et al., 2014; D. Sun et al., 2015). A $^{13}C$ traceability study that utilized eight healthy male participants revealed 12% relative bioavailability of C3G after receiving a 500 mg oral dose of anthocyanin (Czank et al.,

2013). In contrast, a recent human intervention study showed that only 0.02% of ingested bilberry anthocyanin is detectable in plasma over 8 h after ingestion (Mueller et al., 2017). These controversial findings indicate that further investigations of the bioavailability, absorption and excretion of anthocyanins are warranted. The maximum plasma concentration is attained within 0.5–2 h after the consumption of anthocyanin-rich foods (J. Fang, 2014). Around 20–25% of the ingested anthocyanin is absorbed by the gastric mucosa, although this varies according to the structure of the anthocyanin (Felgines et al., 2006; Talavéra et al., 2003). The majority of glycosidic forms, anthocyanin monoglucosides, and non-acylated compounds are well absorbed (Novotny et al., 2012; Passamonti et al., 2003). Glucose transporters are not involved in the gastric absorption of anthocyanin; hence, absorption is facilitated by bilitranslocase, an organic anion membrane carrier (Felgines et al., 2008). Absorbed anthocyanin is then metabolized into glucuronidate, sulfate, or methyl derivatives in the small intestine. The greatest amount is absorbed in the jejunum and the lowest is absorbed by duodenal tissue (Talavéra et al., 2003). Anthocyanins that pass down to the large intestine are subjected to spontaneous or microbial bioconversion (Valdez & Bolling, 2019). In vitro studies prove that upon bacterial metabolism, cleavage of glycosidic linkage and breakdown of the anthocyanidin heterocycle is possible while producing 4-hydroxybenzoic acid, PCA, gallic acid, vanillic acid, and syringic acid as the major microbial metabolites (Fernandes et al., 2015). Incubation of a mixture of anthocyanins with fecal bacteria results in the formation of gallic, syringic, and p-coumaric acids (Hidalgo et al., 2012). The metabolism of C3G and cyanidin-3-*O*-rutinoside by rat gut microflora gives rise to protocatechuic, vanillic, p-coumaric acids, and 2,4,6-trihydroxybenzaldehyde. Gallic acid, syringic acid, and 2,4,6-

trihydroxybenzaldehyde are the primary metabolites of delphinidin-3-*O*-rutinoside (Y. Chen et al., 2017). Therefore, microbial metabolism of anthocyanins may contribute to their pronounced anti-inflammatory properties, as the microbiome enhances anthocyanin metabolite concentrations (Hanske et al., 2013).

### 2.5.3 Anti-inflammatory properties of anthocyanin

Under chronic inflammatory conditions, intestinal barrier function is impaired by the loss of the mucosal epithelial layer integrity layer due to decreased production and assembly of the TJ proteins and translocation of invasive microbial species and microbial products to the internal tissue environment (S. Li et al., 2019). In various systems, anthocyanins improve the intestinal TJ barrier integrity by promoting the expression of crucial barrier-forming TJ proteins such as occludin, claudin-5 and, zonnula occuldin-1 via upregulation of glucagon-like peptide (GLP)-2 intestinal hormone levels (Cremonini et al., 2019; Nunes et al., 2019). In addition, anthocyanins tend to improve barrier function by regulating TJ and epithelial cell permeability (X. Sun et al., 2018). Anthocyanins also down-regulate the expression of major pro-inflammatory biomarkers such as TNF-α, IL-6, IL-1β, IFN-γ, PGE2, monocyte chemoattractant protein (MCP)-1, cyclooxygenase (COX) -2, and NF-κB (Ferrari et al., 2016; Peng et al., 2019). For example, a combination of lycopene and anthocyanin inhibits the expression of the cytokine IL-8, whereas anthocyanin-rich wild blueberry extract reduces the activity of NF-κB in Caco-2 cells (Phan et al., 2019; Rupasinghe et al., 2015). Anthocyanins extracted from red clover (Lee et al., 2020), and black rice (Limtrakul et al., 2015), inhibit the translocation of NF-κB into the nucleus of lipopolysaccharide (LPS)-activated RAW264.7 macrophages. Furthermore, the production of NO, expression of COX-2, and secretion of TNF-α and IL-6 were also

diminished by black rice extracts (Limtrakul et al., 2015). Overexpression of the pro-inflammatory enzyme, iNOS, is another general feature of epithelial tissue inflammation and carcinoma development (Domitrovic, 2011). In this regard, Peng et al. (2020), reported that the long-term consumption of anthocyanin from *Lycium ruthenicum* Murray reduces inflammation of the colon by reducing the expression of iNOS, Cox-2, TNF-α, IL-6, IL-1β, and IFN-γ mRNAs in C57BL/6 male mice. Additionally, cocoplum extract, which is rich in the anthocyanins delphinidin, cyanidin, petunidin, and peonidin, downregulates IL-1β, IL-6, and NF-κB expression in HT-29 colorectal adenocarcinoma cells while decreasing TNF-α-induced intracellular ROS production (Venancio et al., 2017). Moreover, anthocyanins from various sources, for example, fruits of *L. ruthenicum* Murray (Peng et al., 2019), red raspberry (L. Li et al., 2014), black rice (L. Zhao et al., 2018), and strawberry (Ghattamaneni et al., 2020), are able to attenuate DSS-induced gut inflammation in mouse models of IBD.

### 2.5.4 Anthocyanin in the regulation of gut microbial dysbiosis

Healthy gut bacteria or probiotics are involved in activating anti-tumor immunity and boosting the efficacy of immunotherapy, whereas harmful bacteria induce inflammation-driven deoxyribose nucleic acid (DNA) alterations (Wroblewski et al., 2016). Anthocyanins and gut microbiota exhibit a two-way interaction that impacts host physiology. There is a broad agreement that dietary anthocyanins are involved in the modulation of gut microbiota, increasing the ratio of healthy/unhealthy bacteria (S. Li et al., 2019). For example, oral administration of 5 g/kg body weight of black raspberry to the diet for six weeks increased the abundance of healthy microbial species such as *Akkermansia* and *Disulfovibrio* (known to have anti-inflammatory effects) in F-344 rats

(Wroblewski et al., 2016). C57BL/6J mice with colitis that were fed malvidin-3-glucoside at a dose of 24 g/kg body weight also showed a decrease in the number of pathogenic bacteria such as *Ruminococcus gnavus*, thereby restoring the gut microbial balance (F. Liu et al., 2019). In a recent study, oral gavage of malvidin-3-galactoside (40–80 mg/kg body weight) increased butyric-producing bacteria and reduced the abundance of pathogenic bacteria in C57BL/6J mice with liver carcinogenesis (Cheng et al., 2020). As pathogenic microbes are involved in intestinal inflammation, regulation of gut microbial composition by anthocyanin is directly linked with the reduction of inflammation.

### 2.5.5 Probiotics in the prevention of inflammation

The microbial ecosystem in our gut has a dramatic role in human health and has particularly gained much attention recently for the heath-restoring properties of healthy gut bacteria or probiotics (Prescott, 2013). According to the definition given by Nutrition Division, Food and Agriculture Organization (2006) probiotics are "live microorganisms which confer a health benefit on the host, when administered in adequate amounts". The difference in the composition and activity of gut microflora shown by an increase in the number and species type of harmful bacteria and a decrease in the number and species types of healthy bacteria have been identified as a major factor affecting an individual's overall health (Levy et al., 2017). Therefore, the incorporation of probiotics in regular diets has now become an effective way of restoring gut microflora imbalance.

Probiotics are capable of producing critical anti-inflammatory metabolites such as short-chain fatty acids (SCFAs: acetate, butyrate, and propionate) produced by probiotics bifidobacilli, and lactobacilli bind and activate receptors (free fatty acid receptor 2 - FFAR2, free fatty acid receptor 3-FFAR3) on intestinal epithelial cells to inhibit the NF-

κB pathway to prevent inflammation (Y. Liu et al., 2018). Apart from this, SCFAs play an important role in maintaining colonocyte homeostasis and are involved in the reduction of neutrophil cytokine production as well (Vinolo et al., 2011). Besides, probiotics are found to be effective in activating the TLRs thereby influencing important signaling pathways and DCs which transport the antigens to local lymph nodes with the following release of IL-10 and IL-12 (Cristofori et al., 2021). TLR-2 and TLR-4 activation by probiotic microorganisms are recognized as particularly important receptors mediating the direct influence of probiotic and commensal bacteria on inflammatory signaling pathways (Bermudez-Brito et al., 2012).

A recently published mechanistic overview confirms the potential of probiotics in the reduction of levels of inflammation and oxidative biomarkers including C reactive protein P, TNF-α, IL-6, and IL-12, and involvement in improving the intestinal barrier integrity and reduction in leakage of harmful metabolites (Mahdavi-Roshan et al., 2022). Furthermore, probiotics have shown beneficial effects on attenuating gut inflammatory conditions by inhibiting the growth of microbial pathogens, increasing the epithelial TJ protein activity, modulating immune responses of epithelial mucosal immune cells, secreting the antimicrobial products, and decomposing luminal pathogenic antigens (Bai & Ouyang, 2006). TNF-α, causes leaky barriers in intestinal epithelial by directly impairing the integrity of TJ proteins between epithelial cells. Hence, the reduction of TNF-α by probiotics facilitates the maintenance of endothelial integrity (Lescheid, 2014). Moreover, probiotics directly affect the expression of zonulin-1, occludin, and cingulin, a few of the principal TJ proteins (Ukena et al., 2007).

## 2.6 Need for encapsulation to protect probiotics and anthocyanins

Despite the perceived health benefits, the low viability, and stability of probiotics in foods as well as in the human GI tract is found to be one of the main technological challenges in using them as healthier remedies and functional ingredients (Mattila-Sandholm et al., 2002). Microorganisms are continuously exposed to extreme temperatures, high pressure, and shear forces during the production process (Thantsha et al., 2012) and the remaining viable cells in the product will experience further stress conditions during the gastric transition on account of low pH in the stomach and high bile salts concentration in the intestine (Haffner et al., 2016). To achieve the desired health effects, it is recommended to have at least $10^8$-$10^9$ CFU/g of viable cells at the time of consumption (Haffner et al., 2016). However, about 60% of the bacteria is being killed in the gastric environment before it reaches the intestine (Clemente et al., 2012) and about 90% of the active microorganisms in formulated products tend to be non-functional during one year storage period (Viernstein et al., 2005).

On the other hand, the use of anthocyanin as a functional food ingredient or a nutraceutical is also restricted due to its high instability in food processing conditions and susceptibility to degradation in GIT (Giusti & Wrolstad, 2003). Moreover, the bioavailability of anthocyanin compounds is very low due to their low absorption and fast metabolization in the body (Fidan-Yardimci et al., 2019). As Y. Liu et al. (2014) reported, 42% of total anthocyanins are lost during passage through the gastrointestinal tract, and stability is increased with an increasing number of methoxy groups in ring-B. Additionally, anthocyanin bioavailability is low because of its sensitivity to low pH conditions in the stomach. Generally, anthocyanin is stable at pH 3.5, and pH levels below that, they undergo

continuous degradation which results in less biochemical activities (Robert & Fredes, 2015). In this context, scientists investigate a multitude of technological approaches such as encapsulating techniques to improve probiotic cell viability and anthocyanin bioavailability.

### 2.6.1 Microencapsulation

Microencapsulation (ME), one of the most common methods of bioactive and cell stabilization in the fields of food and pharmaceuticals (Trelles & Rivero, 2013). As encapsulation itself is a broader area, generally it is identified as a separate technique of stabilization of active compounds through the structuring of systems capable of preservation of their chemical, physical, and biological properties, as well as their release or delivery under established or desired conditions. The term ME is defined as a "technology of formation of a continuous coating around an inner core of sensitive ingredient/s (solid, liquid, or gaseous) by means of physicochemical or mechanical ways to produce particles with a diameter in the range of 20 μm-1 mm (Figure 7) (Shori, 2017). However, according to some authors, the final particle size of the microcapsules can be extended up to 5 mm which is attributed to the respective technologies used (Sarao & Arora, 2017). To date, there is a rising interest in probiotic encapsulation technology (PET) in the field of bio-pharmacy focusing on the controlled release of probiotics at the colon to restore gut microbial dysbiosis (Gbassi & Vandamme, 2012). Aligning the same with the PET, encapsulation of plant bioactive such as anthocyanin has also gained broader attention primarily focused on providing protection from environmental conditions (light, oxygen, temperature, and water), avoiding oxidation and increasing the shelf life, improving their permeability through the intestinal mucus and epithelium by protecting these compounds

from degradation in the gastrointestinal tract (Chai et al., 2018; Tarone et al., 2020). Generally, an encapsulated system contains a matrix in which the core material is suspended and a wall material in which the entire core is surrounded. However, as per encapsulating the probiotics reservoir-type microcapsules are generated (Figure 7).

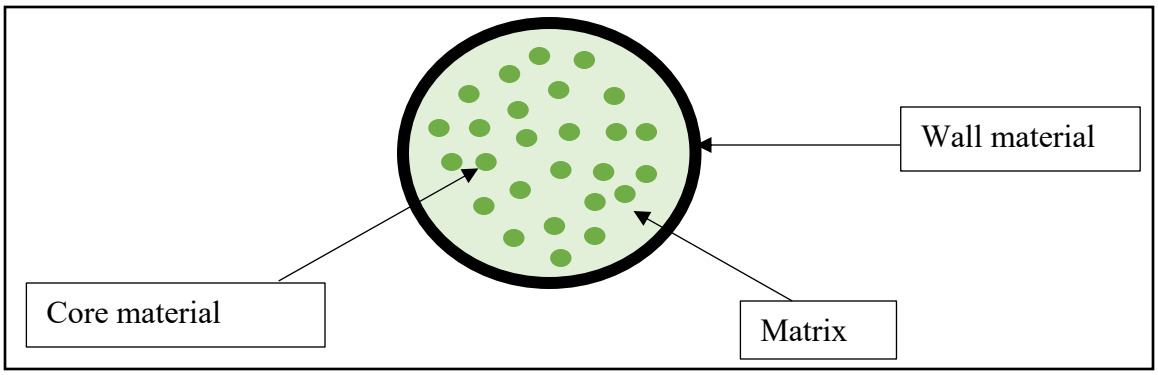


**Figure 7: Schematic diagram of an encapsulated system.** For example, probiotics or anthocyanin is the core material and is usually suspended in encapsulating matrix coated by wall or shell material.

### 2.6.2 Encapsulating agents

The use of wall materials or encapsulating agents in the encapsulation process depends on the nature of the material, capsule characteristics, and the desired environment of disintegration (Mortazavian et al.,2007). Those wall materials can be used either alone or in a composite form. Generally, in the pharmaceutical industry, composite wall materials are much favored, as single wall material doesn't possess all the desired characteristics. These materials can be either organic or inorganic. Based on the molecular configuration and functional groups present, those monomers and polymers exhibit specific functionalities such as the ability to form gels (Krasaekoopt, 2013). The choice of encapsulating agent is very important for the proper encapsulation efficiency (EE), the stability of the active compounds in the microparticles during storage, and the release properties in foods and the gastrointestinal tract (Robert & Fredes, 2015).

### 2.6.2.1 Maltodextrin and inulin as anthocyanin encapsulating agents

In the microencapsulation of anthocyanins, maltodextrin (MD) is essential for preserving the integrity of anthocyanins for encapsulation (Ibrahim Silva et al., 2013). MDs are starch hydrolysates produced by partially hydrolyzing starch with acid or enzyme ( Figure 8a) and possess good water solubility, low sugar content, and low viscosity values even at high concentrations (Akdeniz et al., 2017). Besides, MD produces colorless solutions and therefore, the original color of the bioactives is less altered. However, MD is a digestible polymer, and the encapsulated bioactive compounds tend to release quickly upon digestion exposing them to harsh gastric conditions (González et al., 2020). Moreover, MD is deficient in terms of emulsification properties and surface-active features (Nguyen et al., 2022). Therefore, to produce stable micro-capsules, MD is usually combined with other wall materials such as gum Arabic (Lopes et al., 2019), xanthan gum (Antigo et al., 2020), and inulin (Lacerda et al., 2016).

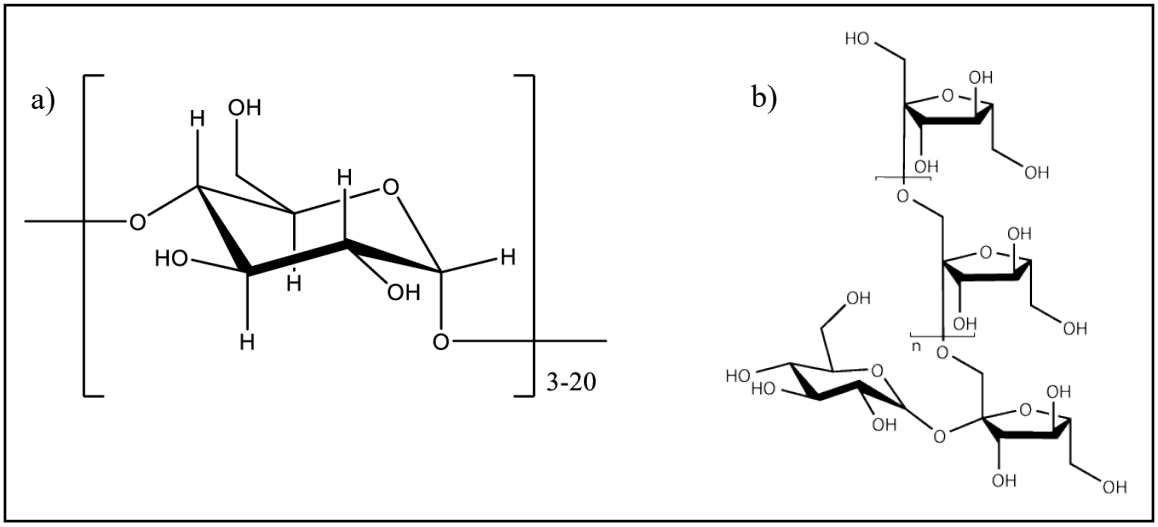


**Figure 8: Chemical structures of a) maltodextrin and b) inulin**

Inulin (IN) is a slightly branched (<5%) fructo-oligosaccharide, composed of β-(2-1) linked fructose units (Figure 8b). Although IN is moderately water soluble, its β-(2-1) glycosidic

bonds make it indigestible by humans, in contrast with maltodextrin, but largely digestible by certain microorganisms in the gut. Therefore, IN has been reported as a colonic delivery biopolymer, since it can pass relatively intact through the upper part of the gastrointestinal tract, reaching the colon where the bioactive compounds can be released (de Vos et al., 2010).

#### 2.6.2.2 Freeze-drying as an encapsulating technology

Encapsulating techniques can be classified into three types, chemical, physicochemical and physicomechanical methods and are widely used for microencapsulation of several pharmaceuticals and plant bioactives (Kandasamy & Naveen, 2022b). Spray drying, freeze-drying, extrusion, coacervation, gelation, spray freeze-drying, fluidized bed coating, anti-solvent precipitation and layer-by-layer deposition are some of the examples of the above categories. However, the encapsulation technique that will be utilized should provide high loading capacity, high encapsulation efficiency, improved stability of the compound with high shelf-life, and high bioavailability (Basar et al., 2021). Even though spray drying is still popular in encapsulating bioactives, the use of high temperatures in evaporation can promote the degradation of core materials (Rezvankhah et al., 2019). In contrast to that, freeze-drying or lyophilization has been engaged in encapsulating heat-sensitive bioactive compounds (Pudziuvelyte et al., 2020). Freeze-drying-based encapsulation involves the generation of an emulsion solution formed by the target compound and the encapsulating materials to later convert them into microcapsules applying the freeze-drying technique. Lyophilization includes three stages: freezing, primary drying, and secondary drying (Kandasamy & Naveen, 2022a). To carry out this process, firstly the material of interest is frozen, and then,

a high-pressure vacuum is applied to sublimate the water, obtaining a dry final product. Since this process is performed in a vacuum and at a low operating temperature, the number of deterioration reactions is dramatically reduced. The freeze dryer consists of sets of units including a drying chamber, a vacuum system, a refrigeration or cooling system, a heating system, and an electronic control unit (Carpena, et al., 2021). Since freeze-drying is a combination of sophisticated units, usually freeze-dried products are considerably expensive. However, freeze-dried products have a high quality because the process takes place under moderate conditions contributing to the formation of highly porous solids with good sensory attributes (Abascal et al., 2005). The maintenance of these natural properties enhances the self-protection of the molecules and improves their delivery (Carpena et al., 2021). However, the use of sugars (glucose, sucrose, oligosaccharides such as inulin), polysaccharides (starch, alginate, maltodextrin) or gums (Arabic, guar, carrageenan) is essential in enhancing the cell viability of probiotics and preserving the biological activity of heat-sensitive compounds such as anthocyanins (Abascal et al., 2005; Gul & Atalar, 2019). The freeze-dried powders are most noticeable with irregular agglomerates and a thin porous sheet-like material and have lower storage stability as they are highly hygroscopic in nature (Laokuldilok & Kanha, 2017). The EE, stability, and physical properties of the powder can be profoundly impacted by the composition and type of wall material. Maltodextrin is the most popular wall material that has been widely used in this technique. Mixing this wall material with other encapsulating agents has been examined to effectively preserve anthocyanins and produce better physical properties (Mohammadalinejhad & Kurek, 2021).

# CHAPTER 03: MATERIALS AND METHODS

## 3.1 Instruments and chemical reagents

Water bath (ISOTEMP 205, Fisher Scientific, Mountain View, CA, USA), centrifuge (Sorvail Legend Micro 21 R, Thermo Fisher Scientific Inc., Waltham, MA, USA), large capacity centrifuge (Damon/ IEC model CU-5000, San Diego CA, USA) microplate reader (Tecan Infinite® M200 PRO, Morriscille, NC, USA), nitrogen evaporator (N-EVAP™ 111, Organomation Associates Inc., Berlin, MA, USA), micro centrifuge (Sorvail ST 16, Thermo Fisher Scientific Inc., Waltham, MA, USA), freeze dryer (Dura-Dry™ MP FD-14-85BMP1, DJS Enterprises, Markham, ON, Canada), commercial blender (HBB909, Hamilton Beach Brands Inc., Glen Allen, VA, USA), coffee grinders (Black & Decker smart grind, Towson, Maryland, USA), rotary evaporator (Heidolph RotaChill, UVS400-115, Thermo Electron Corporation, Milford, MA, USA), ultrasonic bath of 20 kHz/1000 Watts (model 750D, VWR, West Chester, PA, USA), digital hand-held refractometer (Digital refractometer 300016, SPER SCIENTIFIC, Scottsdale, AZ, USA), mini shaker (980334, VWR International, Edmonton, AB, Canada), heat block (Isotemp® 2001, Fisher Scientiic, Ottawa, ON, Canada), gel electrophoresis unit (BIO-RAD Mini PROTEIN® Tetra cell gel electrophoresis unit with Bio-Rad powerpal ™ Basic- Singapore), electro transfer system (BIO-RAD Trans- Blot® Turbo™ system, Hercules, CA, USA), Digital imaging system (BIO-RAD chemidoc MP™ imaging system-unversal hood III, Bio-Rad Laboratories, Inc. Hercules, CA, USA), magnetic stirrer ( 410N0046, Fisher Scientific, Ottawa, ON, Canada), water activity meter (AQUALAB 4TE, Metergroup, Pullman, WS,USA), moisture analyzer (A&D MF-50, Wood Dale, IL, USA), scanning electron microscope (8211011147, ZEISS Sigma 300 VP FESEM, Carl

Zeiss Microscopy, Munich,Germany), particle size distribution analyzer (HoriBA, Partica LA-950 V2, Minami-ku Kyoto, Japan), and Fourier transmission-Infrared Spectrophotometer (Spectrum Two, PerkinElmer, Waltham, MA, USA) were used for the experiments.

Maltodextrin was purchased from ProteinCo (Quebec, Canada) and inulin (08648, Fruitafit, HD, chicory root fiber) was purchased from Sensus, Royal cosun company (Lawrenceville, NJ, USA). Dextran sulfate sodium - colitis grade (MFCD0008155, Molecular weight 36,000-50,000) was purchased from MP biomedicals, Santa Ana, CA, USA). 11 strain probiotic powder was purchased from Custom Probiotics Inc. (Glendale, CA, USA). Primary antibodies required in western blot analysis, , claudin-2 (E1H90) Rabbit, mAb 48120, BCL-2 (D17C4) rabbit mAb (mouse preferred) 3498, BAX ( D3R2M) rabbit mAb (Rodent preferred) 14796, IL-6 (D5W4V)XP® ) rabbit mAb (Mouse specific) 12912, TNF-α (Cat: 3707) and anti-rabbit IgG, HRP-linked Antibody (Cat: 7074) were purchased from Cell Signaling Technology (Danvers, MA, USA) whereas, claudin-3 (ab15102), claudin-4 (ab15104), occludin (ab222691), and HRP anti-beta actin antibody (mAbcam 8226) - loading control (ab20272) were purchased from Abcam Inc. (Toronto, ON, Canada). Alanine transaminase colorimetric activity assay kit (700260-96), and aspartate aminotransferase colorimetric activity assay kit (701640-96) were purchased from CEDARLANE (Burlington, ON, Canada).

## 3.2 Animals

Ethical approval for animal use was obtained from the Dalhousie University Committee on Laboratory Animals (UCLA) (Protocol number: 19-098). Six weeks old male Balb/c mice were purchased from Charles River Canada (Lasalle, QC, Canada).

Animals were housed under sterile conditions in the Carleton Animal Care Facility, Tupper Building, Dalhousie University, Halifax, NS, Canada. and fed on a sterilized regular chow diet and water was supplied ad libitum.

## 3.3 Laboratory analysis

The experiment was conducted in three main phases: i.) extraction and concentration of haskap berry anthocyanin, ii.) microencapsulation of haskap berry anthocyanin, and iii.) animal experimental model of acute colitis.

### 3.3.1 Extraction and concentration of haskap berry anthocyanin

Well-ripen haskap berry fruits (°Brix value of 16.8, variety Tundra) frozen at -20°C were used in the process of extraction of anthocyanin. First, the berries were freeze-dried in a freeze-dryer (Dura-Dry™ MP FD-14-85BMP1, DJS Enterprises, Markham, ON, Canada), ground using a coffee grinder (Black & Decker smart grind, Towson, MD, USA), and the resulted powder was stored in airtight boxes at -80°C. The anthocyanin extracts were prepared according to the method described previously (Celli et al., 2015). The ground berry powder was mixed with extraction solvent (80% ethanol, 0.5% formic acid, 19.5% distilled water) at a ratio of 1: 25 (w/v) and sonicated for 20 min at a constant temperature of 35 ºC in an ultrasonic bath of 20 kHz/1000 Watts (model 750D, VWR, West Chester, PA, USA). The resulting ethanolic extract was filtered through P2 grade filter papers (09-805-5C, Fisher Scientific, Ottawa, ON, Canada) under a vacuum in semi-dark conditions. The remains were washed with ethanol until a clear filtrate was obtained and then filtrates (a volume of 17 L) was concentrated (brought down to 2.4 L) in dark using a rotary evaporator (Heidolph RotaChill, UVS400-115, Thermo Electron Corporation,

Milford, MA, USA) maintaining a temperature of 45 ºC in the water bath and -9 ºC chiller temperatures at a speed of 80 - 100 rpm.

The concentrated extracts were further purified to obtain sugar-free anthocyanin extracts by solid-phase column chromatography. The column loaded with Sepabeads Resin (cat # 207-1, Sorbent Technologies, Atlanta, GA, USA) was preconditioned with deionized water and equilibrated overnight using 50% aqueous ethanol. About 1 L of concentrated anthocyanin extract was loaded into the column. The water-soluble sugar fraction was slowly eluted with deionized water. °Brix value of eluent was measured (≤ 0.1) by refractometer (Digital refractometer 300016, SPER SCIENTIFIC, Scottsdale, AZ, USA) to confirm the removal of sugar. The non-sugar fraction was eluted with 20%, 70%, and 95% in an ethanol gradient. The elute was collected as °Brix reached zero. It was then rotary evaporated and freeze-dried, as described before, to obtain sugar-free anthocyanin-rich haskap berry fraction (AHF). Powdered anthocyanin-rich fractions were stored at -80 ºC in dark airtight containers.

### 3.3.2 Microencapsulation of sugar-free anthocyanin

For microencapsulation, MD and IN were selected as the wall materials and anthocyanin extraction as the core material. The microencapsulation process was adopted from Mahdavi et al. (2016) while increasing the final solid content of the encapsulation mixture from 20% to 40%. Briefly, MD and IN at a ratio of 3:1 (Michalska et al., 2019) were added in 5 mL of deionized water, mixed using a magnetic stirrer (410N0046, Fisher Scientific, Ottawa, ON, Canada) for 90 sec, and kept overnight at 4±2 °C for rehydration. The wall material solution was then mixed with anthocyanin powder (adhering to four different wall/core material ratios- 1:1, 1:1.5,1:2, and 1:3) to get 40% of final solid content

and stirred till the content was well dissolved. The resulting mixture was subsequently frozen at -20°C and freeze-dried (-45 °C for 72 h). The freeze-dried powders prepared in quadratic samples were then weighted, carefully collected into airtight containers, and stored in a desiccator at -20°C until further analysis.

**3.3.2.1 Encapsulation efficiency**

To determine the encapsulation efficiency, total anthocyanin content (TAC), and surface anthocyanin content (SAC) were calculated according to the method of Idham et al. (2012). To obtain the TAC, about 100 mg of microparticles were weighted and 1 mL of deionized water was added. It was mixed well and sonicated at 35 °C for about 1 min. It was then added with 1 mL of formic acid and 9 mL of absolute ethanol followed by sonication for 5 min at the same temperature mentioned earlier. The content was thoroughly mixed and centrifuged (Damon/ IEC model CU-5000, San Diego CA, USA) at 5000 rpm for 10 min. The supernatant was carefully collected, and a 10% diluted sample was prepared by adding absolute ethanol. To determine the SAC, microparticles (100 mg) were added with 10 mL of absolute ethanol and vortex for 10 seconds, followed by centrifugation at 3,000 rpm for 3 min. The supernatant was collected and used in TAC quantification.

<u>TAC determination by pH differential spectrophotometric method</u>

TAC and SAC were determined using the pH differential method as stated in AOAC International (2006) using potassium chloride buffer at pH 1.0 (0.025 M) and sodium acetate buffer at pH 4.5 (0.4 M). The samples and buffers were mixed in a ratio of 1:4, vortex for a few seconds, and the absorbance was measured at 520 and 700 nm using the

microplate reader (Tecan Infinite® M200 PRO, Morriscille, NC, USA). The samples were diluted accordingly.

The TAC was calculated as the equivalents of C3G according to the following equation:

$$TAC\ (mg/L) = \Delta A\varepsilon \times 1 \times M \times 103 \times D$$

Where ΔA= (A520 pH 1.0–A700 pH 1.0) − (A520 pH 4.5–A700 pH4.5); ε (molar extinction coefficient) = 26,900L/mol/cm for C3G; 1, path length in cm; M (molecular weight) = 448.8 g/mol for cyanidin-3-glucoside; D, dilution factor; $10^3$, conversion from gram to milligram. The following equations were used to calculate the encapsulation efficiency (% EE) using the results from the TAC and SAC contents.

$$EE\ \% = \frac{(TAC - SAC)}{TAC} * 100$$

**3.3.2.2 Encapsulation yield, anthocyanin recovery, and retention**

The encapsulation yield and anthocyanin recovery were calculated according to the following equations (Fredes et al., 2018).

$$Encapsulation\ yeild\ \% = \frac{Amount\ of\ anthocyanin\ entrapped\ in\ microparticles\ (mg)}{Total\ powder\ weight\ (mg)} * 100$$

$$Anthocyanin\ recovery\ \% = \frac{Total\ anthocyanin\ in\ microparticles\ (mg)}{Anthocyanin\ in\ the\ feed\ solution\ (mg)} * 100$$

The anthocyanin retention % was calculated using the equations adopted from Norkaew et al. (2019).

$$Anthocyanin\ retention\ \% = \frac{Actual\ loading}{Theoretical\ loading} * 100$$

$$Actual\ loading = \frac{Mass\ of\ anthocynain\ in\ dried\ powder\ (mg)}{Toal\ mass\ of\ the\ powder\ (mg)}$$

$$Theoretical\ loading = \frac{Mass\ of\ anthocynain\ in\ the\ feed\ solution\ (mg)}{Toal\ mass\ of\ the\ feed\ (mg)}$$

### 3.2.2.3 Anthocyanin quantification by UPLC-ESI-MS

Microencapsulated AHF powder and original freeze-dried powder were analyzed using ultra-pressure liquid chromatography (UPLC) coupled with electrospray ionization (ESI) and mass spectrometry (MS) (Waters, Milford, MA, USA) for the identification and quantification of major individual anthocyanin (Rupasinghe et al., 2008). Briefly, powders were dissolved (1 mg/1 mL) in ethanol containing 0.5% formic acid to obtain a final concentration of 1,000 mg/ L. It was mixed well and sonicated at 35 °C for about 5 min and then centrifuged (Damon/ IEC model CU-5000, San Diego CA, USA) at 5,000 rpm for 10 min. The supernatant was carefully collected and filtered through 0.22 µm nylon syringe filters. An Aquity BEH $C_{18}$ (100 mm × 2.1 mm, 1.7 µm) column (Waters, Milford, MA, USA) was used. For the analysis of anthocyanin compounds, ESI in positive ion mode (ESI+), with a capillary voltage of 3000 V, nebulizer gas 375 °C, and a flow rate of 0.35 mL/min was used. Individual compounds were identified using the single ion monitoring mode using specific precursor-production transition: m/z 449 for C3G, 661 for cyanidin-3,5-diglucoside, 463 for peonidin-3-glucoside and 595 for cyanidin-3-*O*-rutinocide (Gouvêa et al., 2012, Razgonova et al., 2021, De Silva & Rupasinghe, 2020).

### 3.3.2.4 Determination of the physical properties of microparticles

The moisture content of the microparticles was determined using a moisture analyzer (A&D MF-50, Wood Dale, IL, USA) and water activity was determined using a water activity meter (AQUALAB 4TE, Metergroup, Pullman, WAUSA). The hygroscopicity of powder was measured under saturated sodium chloride (NaCl) solutions (Relative humidity of 75%) in desiccators. Samples were weighted after 1 week and the

hygroscopicity was expressed as grams of absorbed moisture per 100 g of dry solids (Khazaei et al., 2014). The water solubility index (WSI) of powders was measured by weighing 0.5 g of samples dissolving in 50 mL of distilled water and stirring at room temperature for 30 min. The suspension was then transferred to a 50 mL falcon tube and centrifuged at 3,000 rpm for 5 min. Aliquots of the supernatant were then transferred to pre-weighted Petri dishes and dried at 105°C for 5 h and final weights were taken. The bulk density (ρbulk) of the powders was measured by weighing 1 g of the sample and placing it in a 10 mL graduated cylinder. The cylinder was tapped by hand and the bulk density was calculated as the ratio between the mass of powder contained in the cylinder and the volume occupied (Ferrari et al., 2013).

#### 3.3.2.5 Powder morphology and particle size

A scanning electron microscope (SEM) was used to study the outer structural appearance of the microparticles. The samples were attached to stubs using a two-sided adhesive tape and sputter coated with gold/palladium combination (4-10 nm) for 100 s at 30 mA which was operated at 15 kV. The size of the microparticles was analyzed using the particle size analyzer (HoriBA, Partica LA-960 V2, Burlington, ON, Canada) at the Department of Physics and Atmospheric Science, Dalhousie University.

#### 3.3.2.6 Fourier-transform infrared (FTIR) spectroscopy

FTIR analysis of microencapsulated particles and wall materials was performed using FTIR spectrophotometer (Spectrum Two, PerkinElmer, Waltham, MA, USA ). The wavelength range was set from 4,000 to 400 $cm^{-1}$, while the resolution was 4 $cm^{-1}$.

### 3.3.3 DSS-induced acute colitis model *in vivo*

In the final phase of the study, the effect of dietary supplementations of non-encapsulated AHF and encapsulated AHF with or without probiotic supplementations (*Lactobacillus acidophilus, Lactobacillus rhamnosus, Lactobacillus salivarius, Lactobacillus plantarum, Lactobacillus casei, Lactobacillus lactis, Bifidobactium breve, Bifidobactium infantis, Bifidobactium longum, Bifidobactium bifidum, Bifidobactium lactis*) on the DSS-induced acute colitis model of mice was investigated. According to the results obtained from the microparticle analysis, the wall material/core ratio of 1:1.5, was selected to produce the anthocyanin microparticles used in vivo.

#### 3.3.3.1 Determination of dietary supplementary doses

To the best of current knowledge, there is no recommended dietary allowance (RDA) value for anthocyanin consumption. Therefore, based on the reported literature, an intake of 2 g of anthocyanin/human/day was considered the safe limit for anthocyanin consumption with therapeutic effects (Thomasset et al., 2009). Therefore, a dietary supplement for a 20 g weight Balb/c mouse was estimated to be 6.2 mg C3G equivalents/mouse/day, which is calculated according to the following formula below; where the Km factor for mice and adult humans is 3 and 37, respectively (Nair & Jacob, 2016).

$$Human\ equivalent\ dose\ \left(\frac{mg}{kg}\right) = Animal\ dose\ (\frac{mg}{kg}) \times \frac{Animal\ Km}{Human\ Km}$$

The powder weight of the probiotic supplementation was determined considering the dose of live bacteria originally present in the mixture ($2.6 \times 10^{11}$ / g), which satisfied the safe dosage of $1 \times 10^{9}$ CFU/g of probiotics/mouse/day (L. L. Chen et al., 2009; Suwal et al., 2018). The measured amounts were mixed accordingly into regular mouse chow

(Prolab®RMH 3000 from LabDiet, St. Louis, MO, USA) and formed into a 2 g (dry weight) pellet. Regular mouse chow hard pellets were ground using a commercial blender (HBB909, Hamilton Beach Brands Inc., Glen Allen, VA, USA). Pellets were prepared every three days and stored in sealed containers in the dark at 4 °C.

#### 3.3.3.2 Experimental design

The experiment was designed to investigate the effect of five different dietary interventions on DSS-induced acute colitis in mice compared to the control (regular chow with no DSS administration), and the disease model (regular chow with DSS administration) groups (Figure 9). Mice were housed individually in filter-topped plastic cages and maintained under 12-h light-dark cycles. After one week of acclimation, mice were randomly divided into seven dietary groups (n=5 in each). Respective diets were introduced on day $8^{th}$ and besides the control group, which received the sterile drinking water, all other groups were supplied with 3% DSS-added sterile drinking water from day $13^{th}$ to day $19^{th}$. The initial body weight of the mice was taken at end of the acclimation period and continued till they were sacrificed. Feed intake and water consumption were monitored throughout the experimental period. Starting from the 3% DSS administration, stool consistency was recorded and evaluated for occult blood using Hemoccult blood test strips (Hemoccult II, Beckman-Coulter, Brea, CA, USA). Finally, mice were euthanized by overdosing on isoflurane in an anesthetic chamber supplemented with sufficient oxygen after the fecal matter was collected.

#### 3.3.3.3. Organ and blood harvesting

Portal vein blood was collected using a 1 mL needle. Blood samples were incubated at room temperature for 1 h to separate the serum by spinning down at 2,000 rpm × g for 15

min at 4°C and then stored at -80 °C for further analysis. The colon was isolated by trimming at the ileocecal junction and the distal end of the rectum and the total length was measured. Colon contents were removed, weighed, and partitioned into two sections longitudinally. One section was processed into Swiss Roll and the rest was snap-frozen and stored at -80 °C until further processing. The spleen was harvested, weighed, snap frozen, and stored at -80 °C and the spleen index was calculated as spleen weight (mg) to body weight (g) ratio (Xiong et al., 2012).

#### 3.3.3.4 Disease activity index (DAI)

The DAI was used to evaluate the grade and extent of intestinal inflammation; a composite score derived from a compilation of relative body weight loss, stool consistency, and occult blood in the stool measurements (Table 1).

**Table 1.** Clinical symptoms of colitis were used to calculate the DAI (Qian et al., 2020).

| Score | Weight loss % | Stool consistency | Occult blood |
|---|---|---|---|
| 0 | None | Well-formed pellets | Negative |
| 1 | 1-5% | | |
| 2 | 5-10% | Loose stools | Hemoccult positive |
| 3 | 10-20% | | |
| 4 | >20% | Diarrhea | Gross bleeding |

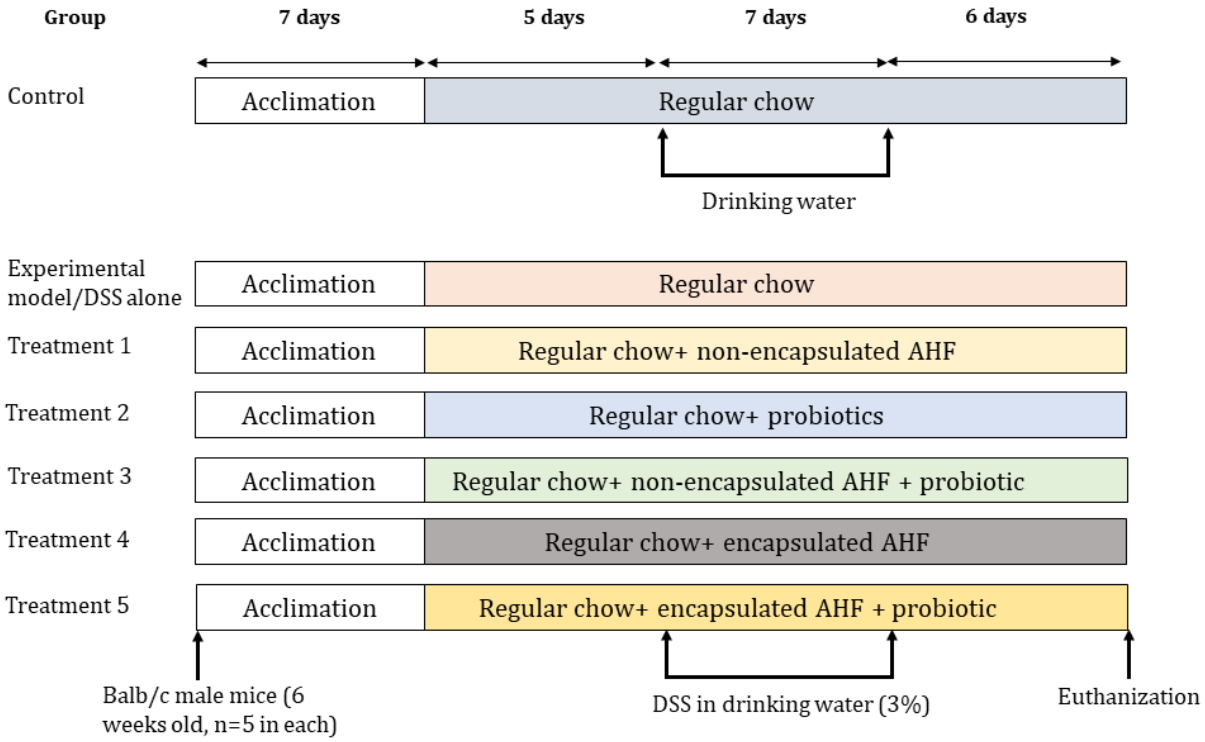


**Figure 9: Schematic representation of DSS-induced acute colitis experimental model of male Blab/c mice.** All experimental groups (n=5 in each) were housed with 12 h light/dark cycle facilitating regular chow diet and water ad libitum for 1 week of acclimation period. All groups were introduced either drinking water or 3% DSS in drinking water at day 12 for 1 week. Dietary supplementary groups were, control (regular chow + drinking water), experimental model (regular chow + 3% DSS in water), Treatment 1 (regular chow + non-encapsulated AHF + 3% DSS in drinking water), Treatment 2 (regular chow + probiotics + 3% DSS in drinking water), Treatment 3 (regular chow + non-encapsulated AHF + probiotics + 3% DSS in drinking water), Treatment 4 (regular chow + encapsulated AHF + 3% DSS in drinking water), and Treatment 5 (regular chow + encapsulated AHF + probiotics + 3% DSS in drinking water).

### 3.3.3.5 Liver toxicity tests

The levels of alanine aminotransferase (ALT) and aspartate aminotransferase (AST) in mice serum were measured using the ALT colorimetric activity assay kit (700260, Cayman CHEMICAL, Ann Arbor, MI, USA) and AST colorimetric activity assay kit (701640, Cayman CHEMICAL, Ann Arbor, MI, USA) respectively by following the manufacturer's

instructions. All reagents were equilibrated to room temperature before beginning the assays and the final volume of the wells was 210 µL. The assays were conducted in triplicates. Respective reagents provided with the assay kits were mixed accordingly to obtain positive control wells (150 µL of the substrate, 20 µL of the cofactor, 20 µL of positive control) and sample wells (150 µL of the substrate, 20 µL of the cofactor, 20 µL of mouse serum). Plates were covered and incubated at 37 °C for 15 min. The reactions were initiated by adding respective initiator reagents (20 µL) and absorbance was measured at 340 nm using a microplate reader (Tecan Infinite® M200 PRO, Morriscille, NC, USA) once every min for 10 min at 37°C. Change in the absorbance respective to the time was calculated and ALT and AST activities were determined using the following equation.

$$ALT\ or\ AST\ activity\ (UmL^{-1}) \frac{\Delta A340/\min * 0.21\ mL}{4.11\ mM^{-1}\ * 0.02\ mL}$$

**3.3.3.6 Western blot analysis**

The presence of TJ proteins (Occludin, claudin 2, claudin 3, and claudin 4), IL-6, TNF-α, bcl-2-like protein 4 (BAX), and B-cell lymphoma 2 (BCl-2) expression in mouse colon tissues were measured by western blot analysis. A composite sample of mice colon tissues from each dietary group was prepared (n=5 per group, weight of the composite sample ≈ 500 mg) by finely grounding the tissues using pallet pestle Eppendorf tubes. Tissue samples were kept on ice during the preparations. An aqueous solution of radio-immunoprecipitation assay (RIPA) buffer was prepared by combining 50 mM Tris HCl, 150 mM NaCl, 1% Triton X-100, 0.5% sodium deoxycholate,1 mM ethylenediaminetetraacetic acid (EDTA), and 10 mM sodium fluoride (NaF). RIPA buffer was mixed with the ×100 protease inhibitor cocktail (10 µL/1 mL of RIPA) and mixed

thoroughly with ground mice tissues (500 mg of tissue/3 mL of RIPA). Eppendorf tubes were immediately placed on ice and incubated for 30 min followed by centrifugation at 12,000 × g for 20 min (at 4 °C) using a micro-centrifuge (Legend MICRO 21R, Cat: 75002446, Thermo Fisher Scientific, Osterode, Germany) to collect the protein-rich supernatant. Protein concentrations of the supernatants were estimated by Bradford assay using Pierce™ Coomassie (Bradford) protein assay kit (Cat: 23200, Thermo Fisher Scientific, Rockford, IL, USA). A series of albumin protein solutions (0, 25, 125, 250, 500, 1,000, 1,500, and 2,000 µg/mL) were prepared using the stock solution vial (2 mg/mL) provided with the assay kit. A volume of 5 µL of each protein sample + RIPA buffer and prepared protein standards were pipetted on a clear fat bottom 96-well plate in triplicates and wells were added with 200 µL of Coomassie solution. The plate was shaken thoroughly to mix the contents and incubated for 30 min at 37 °C. The absorbance values were read at 595 nm using the microplate reader (Infinite® 200 PRO, Tecan Trading AG, Mannedorf, Switzerland), and protein content in samples was determined by a standard curve. Extracted protein samples were denatured using a blue loading buffer pack (Cat: B7703S, New England BioLabs$^{TM}$ Inc., Ipswich, MA, USA). In brief, 3× reducing blue loading buffer was prepared by mixing 30× reducing agent and 3× blue loading buffer at a ratio of 1:10. Protein solutions and 3× reducing buffer were mixed in 2:1 ratio in Eppendorf tubes and heated for 5 min at 95°C on a heating block. Denatured protein samples were further diluted with a mixture of RIPA buffer and 3× reducing blue protein loading dye (2:1 ratio) to obtain a similar protein concentration in each sample. Denatured proteins were separated on a 4–20% precast polyacrylamide gels (#4568095, Mini-PROTEAN® TGX Stain-Free™ Protein Gels, Bio-Rad Laboratories Inc., Hercules, CA, USA) by electrophoresis.

Polyacrylamide gels were set with the running module of BIO-RAD Mini PROTEAN® Tetra Cell unit. The running module was then filled with 1 × SDS running buffer (25 mM Tris base, 192 mM glycine, and 0.1 % SDS). An amount of 7 µL of Precision Plus Protein™ Dual Color Marker (Precision Plus Protein™ Dual Color Standards, Cat: 161-0374, Bio-Rad Laboratories Inc., Hercules, CA, USA) and protein extracts containing 150 µg of proteins were loaded into the wells accordingly. The SDS-PAGE gel electrophoresis was performed for 1.5 h at 90 V and 400 mA. Proteins which were separated on precast gels were then transferred onto a polyvinylidene difluoride (PVDF) membrane (Cat: 88518, Thermo Fisher Scientific, Rockford, IL, USA) using a Trans-Blot® Turbo™ Transfer System (Cat: 1704150, Bio-Rad Laboratories, Inc. Hercules, CA, USA). Activation of PVDF membranes was done by immersing in 100 % methanol for 10 seconds followed by equilibrating in transfer buffer (pH-8.3, 25 mM Tris, 192 mM glycine, and 20% methanol) for 20 min by subjecting to gentle rocking. Thick blotting papers (Cat: 1703966, Bio-Rad Laboratories Inc., Hercules, CA, USA) were also equilibrated in a transfer buffer under the same conditions. A transfer sandwich was built placing PVDF membrane and mini-gel in between two thick blotting papers. Protein transfer was carried out for 30 min at 20 V and 1 A in Trans-Blot® Turbo™ Transfer System. Electro-transferred PVDF membranes were then blocked with commercially available 5% non-fat milk in 1× Tris-buffered saline (20 mM Tris-HCl, pH 7.6, 200 mM NaCl) containing 0.1% Tween 20 (TBST) (Cat: 9997S, Cell signaling Technology, Danvers, MA, USA) for 1 h at room temperature with gentle shaking on a rocker. Blocked PVDF membranes were incubated with primary antibodies in 5% aqueous bovine serum albumin (BSA) solution at 4 °C for overnight while shaking. BAX, BCL-2, TNF-α, IL-6, occludin, claudin-2, claudin-

3 and claudin-4 primary antibodies were diluted at 1:500 (v/v) ratio. β-Actin levels in protein samples were measured as the housekeeping protein (1:3,000 v/v antibody dilution) to normalize the levels of measured primary antibodies. PVDF membranes incubated with primary antibodies were washed with TBST (10 min × 3) and probed with HRP (Horseredish peroxidase)-linked anti-rabbit secondary antibodies (1:2,000 v/v antibody dilution) in 5% aqueous BSA solution for 1 h at room temperature. PVDF membranes were then washed with TBST (10 min × 3) and developed by using enhanced chemiluminescence (ECL) based ClarityTM and Clarity MaxTM Western ECL substrate Kit (Cat: 1705060, Bio-Rad Laboratories Inc., Hercules, CA, USA) which mixed in 1:1 ratio. PVDF membranes were incubated for 5 min with ECL substrate solution, placed in two transparent plastic sheets and imaged using BIO-RAD Chemidoc MP™ imaging system (Universal hood III, Bio-Rad Laboratories Inc., Hercules, CA, USA) under chemi-hi sensitivity blot settings in signal accumulation mode. The blot images were analyzed for protein band intensities by Image lab version 6.0.1 software (Bio-Rad Laboratories Inc., Hercules, CA, USA) and protein levels were normalized by comparing with *β*-actin levels and control.

#### 3.3.3.7 Enzyme-linked immunosorbent assays (ELISA)

Inflammatory markers (TNF-α, IL-1β, and IL-6) in mouse serum were measured using mouse TNF-α, SimpleStep ELISA® Kit (ab208348), mouse IL-1β, SimpleStep ELISA® kit (ab197742), and IL-6 Mouse ELISA Kit (ab46100), respectively (Abcam Inc. Toronto, ON, Canada) according to the manufacturer's instructions. All reagents were equilibrated to room temperature prior to use. TNF-α and IL-1β assays were conducted in a similar way. In brief, a volume of 50 µL of serum samples (with no dilution) and standards (prepared

by reconstituting the respective protein standards by adding 100 µL of deionized water) were added to appropriate wells in a 96-well microplate. An amount of 50 µL of antibody cocktail was also added to each well. It was sealed and incubated for 1h at room temperature on a plate shaker at 400 rpm. Each well was washed with 3 × 350 µL 1 × wash buffer until the liquid is completely removed. TMB development solution (100 µL) was added to each well and incubated in dark on the plate shaker at 400 rpm. A 100 µL of stop solution was added to each well and absorbance was measured at 450 nm. Sample concentrations were calculated by plotting a standard curve. To determine the IL-6 in mice serum samples, 100 µL of each standard and 4-fold diluted serum sample were added in appropriate wells in 96 well microplates. 1 × Biotinylated anti-IL-6 (50 µL) was added to each well and the covered plate was incubated for 3 h at room temperature. The plate was then washed with 1 × wash buffer 3 times. A 100 µL of 1 × streptavidin-HRP solution was added to each well and incubated again for 30 min. The wells were washed as described earlier. A 100 µL of chromogen TMB substrate solution was added and incubated at the dark for 25 min at room temperature. Finally, the reaction was terminated by adding a stop reagent (100 µL). Absorbance reading was taken at 420 nm and sample concentrations were determined using the standard curve method.

#### 3.3.3.8 Histological evaluation

Mice colon tissue samples made into Swiss rolls were used in histological analysis. Cassettes with tissue samples were immersed in containers filled with fixative agents i.e., 10% acetate buffered formalin (37% formaldehyde, distilled water, and sodium acetate-$3H_2O$) for 48 h. Formalin was replaced with 2 washes of 70% ethanol. Fixed specimens were dehydrated by immersing them in a series of ethanol concentrations (70%, 2 × 95%

and 3 × 100%) for 1.5 h in each. Clearing of the specimens was done to replace the alcohol in tissues using a clearing agent, xylene. Specimens were immersed in 50:50 xylene (100% ethanol: xylene) and twice in pure xylene (1 h in each solution). Tissues were then infiltrated with paraffin wax (Cat: 22-900-700, Fisherbrand™ Histoplast Paraffin Wax, Waltham, MA, USA) for 1 h and embedded in paraffin using embedding rings and orienting tissue as the swiss roll is captured. Blocks were placed at 4 °C for 15 min to solidify. Blocks were cut using a microtome (Leica Rm 2255, Leica Biosystems, ON, Canada) to obtain 5 µm sections, and cut sections were placed in a water bath (45 °C) and placed on immunostaining slides and dried at 37 °C in an oven for overnight. Slides containing paraffin sections were placed in a glass slide holder and deparaffinized by submerging them in xylene. Rehydration of the slides was carried out by placing them in 100% ethanol for 3 × 5 min, 95% ethanol for 2 × 5 min, and 70% ethanol for 2 × 5 min. Slides were rinsed with running water to remove the excess ethanol. Slides were dipped in Harris hematoxylin solution for 2 min. They were dipped in Scott's water for another 2 min, in 0.2% nitric acid for a few seconds and again in Scott's water (2 min). In between two dippings, slides were rinsed off with running water to remove the excess dye. Finally, slides were submerged in eosin dye (10 dips) and excess dye was removed by submerging in aqueous ethanol (a series of 70 – 100 %) and xylene several times. Processing of the samples for hematoxylin and eosin (H&E) staining was carried out at the Histology and Research Services Center, Faculty of Medicine, Dalhousie University. The colitis severity was measured in a blinded manner by a professional pathologist from the Department of Pathology at Dalhousie University. Briefly, the stained tissue sections were visualized under a bright-field microscope at 200 × and the histopathologic score was calculated by

combining the scores given for (a) leukocyte infiltration, (b) crypt damage, (c) ulceration, (d) edema, and (e) crypt hyperplasia (Appendixes b).

#### 3.3.3.9 Composition of fecal microbiota

Effects of dietary supplementations on mouse gut microbiota were investigated by the 16S rRNA sequencing technology at the Integrated Microbiome Resources facility of Dalhousie University (Halifax, NS, Canada). Bacterial DNA was extracted and purified from the feces samples collected on the final day of the experiment by using QIAmp 96 PowerFecal QIAcube HT (Catalog number: 51531, QIAGEN, Toronto, ON, Canada) commercial microbial DNA extraction kit according to the instructions given by the manufacturer. The polymerase chain reaction (PCR) was used to amplify the V4-V5 region of the extracted microbial DNA. The 16S rRNA gene V4 – V5 fusion primers (515FB – 926R) and high-fidelity Phusion polymerase enzyme were used in the amplification process. Amplified V4 – V5 region was sequenced by Illumina MiSeq to produce 300 base pair paired-end reads. Raw data from DNA sequencing were analyzed by Qiime 2 (version 2020.8) microbiome bioinformatics software (Caporaso et al., 2010; Comeau et al., 2017) and Shannon index, observed operational taxonomical units (OTUs), Faith's phylogenetic diversity (PD), and Pielou's evenness were calculated.

## 3.4 Statistical analysis

Data were analyzed by one-way analysis of variance (ANOVA) and two-way analysis of variance using Minitab statistical software (version 17) at 0.05 % significance level ($p < 0.05$). Results were expressed as the mean ± standard deviation of three individual experiments performed in triplicates. Means were compared by Tukey's and Bonferroni's multiple mean comparisons at $p < 0.05$ level.

# CHAPTER 04: RESULTS

The study consisted of three main phases: (i.) extraction, fractionation, and concentration of haskap berry anthocyanin; (ii.) microencapsulation of haskap anthocyanin-rich fraction, and (iii.) investigation of the effect of anthocyanin-rich haskap fraction (non-encapsulated or encapsulated form) with or without combining with probiotics in attenuating the severity of DSS-induced acute colitis in Balb/c mice. During the initial phase, haskap berry anthocyanin was extracted using ultrasonic-assisted extraction with ethanol as the solvent. After fractionation using column chromatography, anthocyanins were concentrated and freeze-dried to generate microparticles. Maltodextrin and inulin (MD-IN) in a ratio of 3:1 was used as wall materials (WM) in the encapsulation process. According to the physicochemical parameters assessed, the most reliable ratio of wall material to AHF was selected and subsequently used in the acute colitis model in vivo.

## 4.1 Microencapsulation of AHF using four different WM:AHF ratios

AHF was microencapsulated in an MD-IN matrix using freeze-drying. Assessments were taken to investigate the physical properties of particles and encapsulation productivity.

### 4.1.1 Anthocyanin profiling and physical properties of microparticles

The UPLC-ESI/MS analysis was conducted to profile anthocyanin in microparticles and freeze-dried AHF powder (Table 2). Four main different anthocyanins were detected; cyanidin-3-rutinoside, cyanidin-3-glucoside, cyanidin-3,5-diglucoside and peonidin-3-glucoside. All types of anthocyanins were significantly higher in the freeze-dried AHF powder ($P<0.05$). The amount of anthocyanins increased with the increase of the amount added to microparticles. Among the four tested anthocyanins, cyanidin-3-

glucoside was observed in higher amounts than other types. Different physical parameters of microparticles were tested to select the most reliable WM: core material ratio (WM: AHF-1:1, 1:1.5, 1:2, and 1:3) (Table 2). The moisture content of microparticles was between 6.9±0.07- 8.4±0 %. WM:AHF ratio of 1:1.5 showed a significantly lower moisture % ($P<0.05$), whereas WM:AHF ratio of 1:3 showed the highest. However, all tested ratios showed similar water activity ($a_W$) in resulted microparticles. The least solubility was obtained for the microparticles produced using the 1:2 WM:AHF ratio and the highest was observed with 1:1.5 ratio ($P<0.05$). Statistically similar solubilities were observed for the ratios 1:1 and 1:3. Apart from the ratio of 1:1 ($P<0.05$) all three other ratios produced particles with similar bulk density. The hygroscopicity of the particles was also similar in all tested ratios ($P>0.05$). Comparatively, the highest particle diameter was observed with 1:1 ratio of WM:AHF. The lowest particle diameter resulted in the 1:2 WM:AHF ratio. Similarly, the same ratio resulted in the lowest values for $D_{10}$, $D_{50,}$ and $D_{90}$ cumulative distribution indexes.

### 4.1.2 AHF was successfully entrapped in MD and IN matrix

Entrapment of anthocyanin in MD-IN matrix was investigated by analyzing FT-IR spectrum. Pure wall materials and wall materials + core material were tested separately (Figure 10). Pure wall materials resulted with characteristic peaks at <1,000 $cm^{-1,}$ indicating the main infrared regions of MD and near 1,072 $cm^{-1}$ and 1,145 $cm^{-1}$ indicating the C-O-C stretching ring vibrations of carbohydrates. In contrast to that, microparticles with AHF, showed novel peaks around the regions of 1,152 $cm^{-1}$, 1,231 $cm^{-1}$, 1,330 $cm^{-1}$, 1,440 $cm^{-1}$, 1,608 $cm^{-1}$, 2,924-2,926 $cm^{-1}$ and broader and deep peaks around 3,000-3,600

$cm^{-1}$ wavelengths. These results indicate that AHF was successfully loaded into the wall material matrix of MD and IN.

### 4.1.3 SEM images of microparticles

The external structure and morphology of microparticles of AHF (in three different magnifications) were displayed in Figure 11. Microparticles produced with all four WM: AHF ratios resembled the broken glass structure of variable sizes which is a common feature of freeze-dried powders. The particles showed irregular shapes, sharp edges, and deep grooves.

### 4.1.4 Assessment of the encapsulation productivity

The encapsulation productivity of microparticles was determined using four different parameters: encapsulation efficiency % (EE%), encapsulation yield % (EY%), encapsulation retention% (ERT%), and encapsulation recovery % (ER%) (Figure 12). These parameters aid in determining the powders with minimum surface anthocyanin and the maximum capacity of the anthocyanin loading. The WM: AHF ratio of 1:1.5, showed the highest EE% (59.9 ±4.04%). However, all powders produced statistically similar encapsulation efficiencies. EY% was increased with incorporated AHF amount producing the highest yield (12.2±0.68%) at WM:AHF ratio of 1:3. Besides, the least EY% (7.92±1.17%, $P<0.05$) obtained which resulted in 1:1 ratio, EY% of particles of WM: AHF 1:1 was different from the rest ($P<0.05$). WM:AHF ratio of 1:1 produced the least ERT% (81.6±1.85%, $P<0.05$) microparticles whereas, other ratios produced a similar ERT%. ERT% also tends to increase with AHF amount in the encapsulation mixture. Considering the ER%, particles resulting from 1:1 ratio was lower than that of 1:1.5 and 1:2 ($P<0.05$).

However, the highest ER% (88.9±1.24%) was observed with microparticles with WM:AHF ratio of 1:1.5.

## 4.2 DSS-induced acute colitis model in vivo

WM: AHF of 1:1.5 was selected as the suitable ratio of microparticles based on physical properties (low moisture content, higher solubility, less bulk density, and average particle size) and encapsulation productivity (higher EE%, ERT%, and ER%). It was then used as one of the dietary supplements in the DSS-induced acute colitis model. Attenuation of the severity of colitis was assessed by clinical observations, western blot analysis for colonic inflammatory proteins, presence of serum inflammatory markers, histopathology evaluation, and feces microbiome analysis.

### 4.2.1 Food and water intake, and body weight changes during DSS administration

Food intake during the DSS treatment followed the same fluctuating pattern in all treatment groups (Figure 13-A). No significant difference was observed between the control group and the rest ($P>0.05$). Food intake started to reduce by day 3 and the least food intake was recorded on day 5 in all groups. Dietary supplementations with probiotics alone showed the lowest food intake during the recorded period in which it was significantly lower than the amount of the group free AHF + probiotics group at days 5, 6 and 7 ($P<0.05$). Similarly, probiotics alone showed less food intake compared to the encapsulated AHF+ probiotics group ($p<0.05$). In addition to that, on day 6, free AHF + probiotics showed higher food intake than the free AHF alone group ($p<0.05$). Water consumption by each group during the exposure to DSS was measured to ensure that each mouse was exposed to the equivalent quantity of the disease-causing chemical, DSS. Figure 13-B shows the average consumption of water by each dietary group, which is

averaged over the period of DSS exposure. All DSS groups consumed about the same quantity of water ($P<0.05$) varying from 1.88 mL to 10.17 mL. However, the water intake of the control group did not differ from the DSS-treated groups ($P>0.05$). Body weight (g) of mice administered with DSS and fed with regular chow (disease model group) showed lower values than the healthy control during the assessment period (Figure 13-C). The bodyweight of mice in the control group was gradually increased, while the bodyweight of DSS group was sustainably and substantially reduced compared to the control group ($P<0.05$). All dietary groups that received DSS showed a fairly similar pattern in body weight reduction and the weight started to decline on day 4. The disease model group and other dietary groups that received DSS showed no difference in body weight ($P>0.05$). However, there is a significant drop in the body weight of mice in dietary groups (free AHF, probiotics, free AHF + probiotics, encapsulated AHF and encapsulated AHF + probiotics) compared to the healthy control group on days 5, 6, and 7 ($P<0.05$). The model group resulted in the lowest body weight on the final day of the DSS exposure period.

### 4.2.2 AHF mitigated the clinical symptoms in DSS-induced colitis mice

There was no mortality among the experimental groups. Colons from all groups of mice were isolated and measured (length and weight) after the animals were sacrificed. The mice in the healthy control group had the significantly largest average colon length of 10.5±0.79 cm ($P<0.05$) while mice in the experimental model group had the smallest average length of 7.28±0.13 cm (Figure 14-A). Free AHF and free AHF + probiotics groups had a significantly larger average colon length (8.52±0.53 cm and 8.38±0.44 cm, respectively) than the disease control but significantly smaller than that of the healthy control ($P<0.05$). However, there was no significant change in the colon weight and colon

weight to length ratio of the mice among experimental groups (Figure 14-B and 14-C, respectively). However, it was prominent that, the colon weight-to-length ratio was increased in all DSS-treated groups than in the control group. The ratio between the spleen weight to the final day body weight was calculated and represented as the spleen index (Figure 14-D). Compared to the control, DSS alone group showed a significant increase in spleen index ($P<0.05$). The spleen index of other groups was not different from the control group or the DSS alone group. However, all the groups administered with DSS showed higher spleen index values than that of the control group. Disease activity index (DAI), which is scored using, weight loss%, stool consistency, and occult blood presence is an indicator of the colitis severity (Figure 14-E). The disease model group showed the highest DAI on all days and was significantly higher than the healthy control group ($P<0.05$). DAI of the disease model group was higher than the groups of free AHF and probiotics on day 4 and with all the treatment groups on days 5, 6, and 7 ($P<0.05$). However, the lowest DAI score on all days except on day 3 was received by the free AHF+ probiotics supplementary group.

### 4.2.3 Supplementary diets and DSS did not cause hepatotoxicity

To assess whether the DSS administration or dietary supplementations cause any liver injury, serum ALT and AST amounts were examined (Figure 15-A and 15-B respectively). ALT (U/mL) levels were below the upper limit (0.06 U/mL) recorded for mouse serum in all treatment groups (Sher & Hung, 2013). However, the disease model group demonstrated the highest mean value (0.055±0.022 U/mL) for ALT activity. Considering the levels of AST (U/mL) in mouse serum, the disease model group showed a significantly elevated level (0.047 ±0.006 U/mL) than the healthy control, probiotics, and

free AHF+ probiotics group ($P<0.05$). Moreover, AST levels in the healthy control group were lower than in the mice fed with free AHF ($P<0.05$). Free AHF+ probiotics supplementation was more potent in reducing the serum AST levels than free AHF alone in DSS experimental mice. Apart from the disease model and the free AHF groups, other treatment groups showed no significant difference in serum AST levels compared to the healthy control group ($P>0.05$).

### 4.2.4 Supplementary diets numerically reversed the effect of DSS on BCl-2, BAX, IL-6, and, TNF-α level

The DSS administration increases colonic apoptosis by upregulating the BAX expression, downregulating the BCL-2 protein expression, and elevating the inflammatory cytokine expression. Colonic expressions of BCL-2, BAX, TNF-α, and, IL-6 (Figure 16-A, B, C, and D, respectively) were analyzed by western blotting, normalized to housekeeping protein β-actin, and presented as compared to the healthy control group. The disease model group showed considerably lower expression of BCL-2 compared to the control. Dietary supplementations were unable to reverse the effect of DSS on BCL-2 expression significantly. However, there was a trend in improving the BCL-2 expression in groups with dietary supplementations. DSS upregulated the BAX protein expression compared to healthy control and supplementary diets only observed with a trend of reversing the effect of DSS on BAX expression ($P>0.05$). There was numerical increase in the TNF-α and IL-6 cytokine levels in colonic tissue in all groups administered with DSS compared to healthy control ($P>0.05$). Besides the free AHF+ probiotics diet, other supplementary diets failed to downregulate the TNF-α levels ($P>0.05$). However, there was

an effect of supplementary diets on downregulating the expression of IL-6 levels which was not statistically significant.

### 4.2.5 Effect of DSS and supplementary diets on colonic TJ proteins

The effect of dietary supplementations on TJ protein expressions in terms of occludin, claudin-2, claudin-3, and claudin-4 (Figure 17-A, B, C, and D respectively) in colitis mice were determined using western blotting, normalized to housekeeping protein β-actin and presented with relevant to the healthy control group. None of the diets were able to significantly mitigate the effect of DSS on TJ protein expressions ($P>0.05$). However, there was a trend in modulating the TJ expressions in dietary supplementary groups.

### 4.2.6 Supplementary diets restored the DSS-induced serum inflammatory cytokine expressions

Serum inflammatory cytokine levels in terms of IL-1β, IL-6 and TNF-α were analyzed using the ELISA method (Figure 18-A, B, and C respectively). The mean serum level of IL-6 and TNF-α was higher in DSS alone group compared to the healthy control group ($P<0.05$). The IL-6 level of encapsulated AHF group was significantly higher than the healthy control group ($P<0.05$). However, the supplementary diets of probiotics and free AHF + probiotics reduced the serum IL-6 levels ($P<0.05$), which were not different from the control group. Further, diets of free AHF, probiotics, Free AHF+ probiotics and, encapsulated AHF significantly reduced the DSS-induced elevation of serum TNF-α levels ($P<0.05$). Neither DSS administration nor supplementary diets showed a change in serum IL-1β levels.

### 4.2.7 Supplementary diets reduced the epithelial injury caused by DSS

H&E staining was performed to identify the structural changes in mice's colon tissues. Histopathology scoring of the colonic tissues was carried out considering the edema, presence of ulcers, crypt loss, neutrophil infiltration, and hyperplasia. Control mouse colon sections showed an intact epithelium, well-defined crypt length, no edema or neutrophil infiltration in mucosa and submucosa, and no ulcers or erosions. In contrast, colon tissue from treated mice showed increasingly severe inflammatory lesions extensively throughout the mucosa. Compared to the healthy control group (Figure 19-A), the disease model group (Figure 19-B) showed a significant increase in histology score ($P<0.05$). All groups treated with DSS showed an increase in histology scores than in the healthy control group. However, the group that received encapsulated anthocyanin displayed a significant increase in histology score ($P<0.05$). Among the dietary supplementary groups, the free AHF + probiotics group (Figure 19-E) showed the lowest histology score ($6.2 \pm 3.3$). Besides the encapsulated AHF diet, other dietary supplementations restored the colonic epithelial structure which was damaged by DSS administration.

### 4.2.8 Histology score correlated with clinical signs and serum IL-6 protein expression

To confirm the histology results, linear regression analysis of histology score versus colon length (cm), colon weight (g), DAI, IL-6 (pg/mL), IL-1β (pg/mL), and, TNF-α (pg/mL) was performed (Figure 20-A, B, C, D, E, and F, respectively). Colon length was inversely correlated with histology score with the Pearson correlation coefficient; $r^2 = 0.921$ ($P<0.05$). As the histology score increases, colon length is decreased. Colon weight was also inversely correlated with the histology score ($r^2 = 0.712$). The correlation was

significant at $\alpha = 0.05$ level. The DAI was positively correlated with the histology score; as DAI increases so did the histology score ($r^2 = 0.862$, $P<0.05$). Similarly, serum IL-6 protein expression was also positively correlated with histology score producing the $r^2$ of 0.625 ($P<0.05$). However, serum IL-1β and TNF-α were not correlated with histology scores.

### 4.2.9 Dietary supplementations failed to restore fecal microbiota diversity in the DSS-induced colitis model

The species richness and evenness of fecal microbiota of the DSS-induced colitis model were analyzed using 16S rRNA sequencing technology. The evenness of the microbiota was assessed in terms of Pielou's evenness (Figure 21-A). The evenness of the fecal microbiota was reduced upon DSS administration. There was a significant reduction of microbial evenness in the DSS alone group and dietary groups of free AHF, free AHF+ probiotics, encapsulated AHF, and encapsulated AHF+ probiotics compared to the healthy control group ($P<0.05$). Faith phylogenic diversity was higher in the control group than in other treatment groups and was significantly different from all other groups ($P<0.05$), except the probiotics group (Figure 21-B). The administration of DSS significantly reduced the observed feature score in mice's fecal microbiome (Figure 21-C). However, diets of probiotics and encapsulated AHF+ probiotics were able to restore the DSS-induced decline. When considering the alpha diversity in terms of Shannon index measures, the DSS alone, free AHF, encapsulated AHF and, encapsulated AHF+ probiotics groups showed a significant reduction than the control group (Figure 21-D). However, the Shannon index of the control group and probiotics and free AHF + probiotics groups were not different

**Table 2:** UPLC-ESI-MS results for selected anthocyanin in AHF microparticles and freeze-dried AHF powder. Values are given as mg/g of powder.

| Type of anthocyanin | WM: AHF 1:1 | WM: AHF 1:1.5 | WM: AHF 1:2 | WM: AHF 1:3 | Freeze-dried AHF powder |
|---|---|---|---|---|---|
| **Cyanidin-3-rutinoside** | 1.2±0.06[a] | 1.3±0.02[a] | 2.5±0.16[a] | 16.7±0.22[c] | 19.2±1.08[c] |
| **Cyanidin-3-glucoside** | 17.0±1.23[a] | 18.9±0.59[a] | 38.7±0.84[b] | 277.9±10.86[c] | 281.5±16.82[c] |
| **Cyanidin-3,5-diglucoside** | 1.2±0.09[a] | 1.6±0.05[a] | 3.3±0.05[a] | 23.7±1.36[c] | 27.2±1.45[c] |
| **Peonidin-3-glucoside** | 0.8±0.04[a] | 0.7±0.05[a] | 2.5±.0.04[a] | 29.4±0.43[c] | 26.2±1.90[c] |

Anthocyanin-rich haskap fraction (AHF) microparticles were produced using four different WM:AHF ratios as 1:1, 1:1.5, 1:2, and 1:3. HPLC/MS analysis of different types of anthocyanins per gram of AHF microparticles and freeze-dried AHF powder were presented. The results represent triplicates. One Way Analysis of Variance was performed ($p < 0.001$) with Bonferroni pairwise comparison (at $\alpha = 0.05$) for mean separation. Results which share the same superscript letter within the rows are not significantly different. *Abbreviations: WM; wall material*

**Table 3:** Physical properties of microparticles prepared using anthocyanin-rich haskap fraction (AHF)

| Wall material: AHF ratio | Moisture % | aW | Solubility% | Bulk density ($g/cm^{-3}$) | Hygroscopicity (g/100g) | Particle size (µm) | | |
|---|---|---|---|---|---|---|---|---|
| | | | | | | $D_{10}$ | $D_{50}$ | $D_{90}$ |
| **1:1** | $7.3\pm0.07^{b}$ | $0.6\pm0.00^{a}$ | $95.8.08^{b}$ | $0.3\pm0.01^{b}$ | $57.6\pm0.26^{a}$ | 57.5 | 281 | 2711 |
| **1:1.5** | $6.9\pm0.07^{c}$ | $0.6\pm0.00^{a}$ | $97.9\pm0.61^{a}$ | $0.2\pm0.01^{a}$ | $57.3\pm0.08^{a}$ | 47.8 | 188 | 830 |
| **1:2** | $7.5\pm0.07^{b}$ | $0.6\pm0.00^{a}$ | $93.9\pm0.09^{c}$ | $0.2\pm0.01^{a}$ | $57.5\pm0.00^{a}$ | 37.5 | 138 | 445 |
| **1:3** | $8.4\pm0.00^{a}$ | $0.6\pm0.00^{a}$ | $95.6\pm0.13^{b}$ | $0.2\pm0.01^{a}$ | $57.8\pm0.06^{a}$ | 53.5 | 186 | 965 |

Wall materials (WM) of the microparticles consisted of maltodextrin and inulin in 3:1 ratio. Anthocyanin-rich haskap fraction (AHF) microparticles were produced using four different WM:AHF ratios as 1:1, 1:1.5, 1:2, and 1:3. The results represent triplicates. One Way Analysis of Variance was performed ($p < 0.05$) with Bonferroni pairwise comparison (at $\alpha = 0.05$) for mean separation. Results which share the same superscript letter within the columns are not significantly different. *Abbreviations: $D_{10}$= particle diameter corresponding to 10% of the cumulative distribution, $D_{50}$= particle diameter corresponding to 50% of the cumulative distribution and, $D_{90}$= particle diameter corresponding to 90% of the cumulative distribution.*

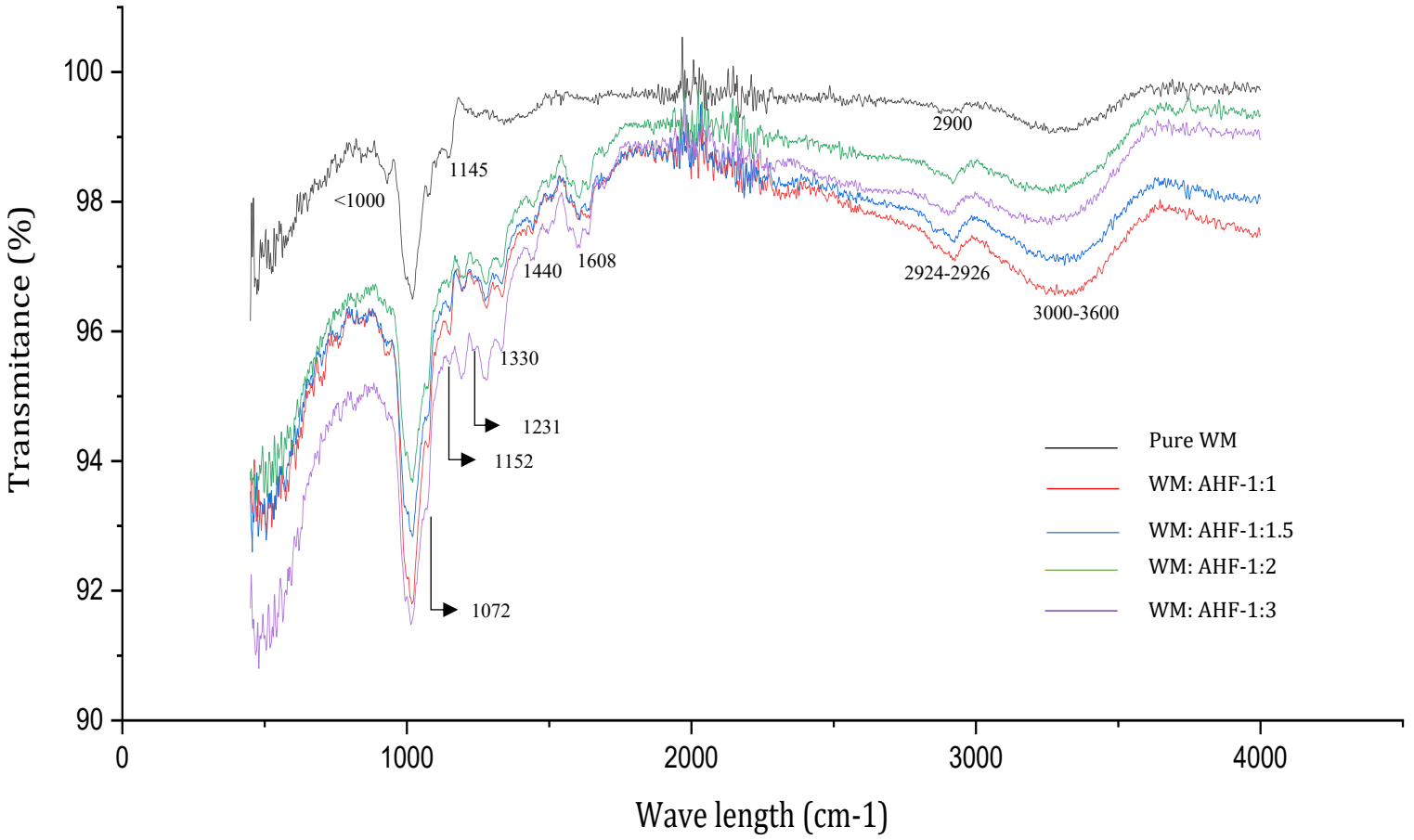


**Figure 10: FT-IR spectrum generated for freeze-dried microparticles containing wall material alone and various amounts of anthocyanin-rich haskap fraction (AHF).** WM alone (black color spectrum), WM: AHF (1:1; red color spectrum, 1:1.5; blue color spectrum, 1:2; green color spectrum, and 1:3; purple color spectrum) were presented. Wall materials contained maltodextrin and inulin in a ratio of 3:1.

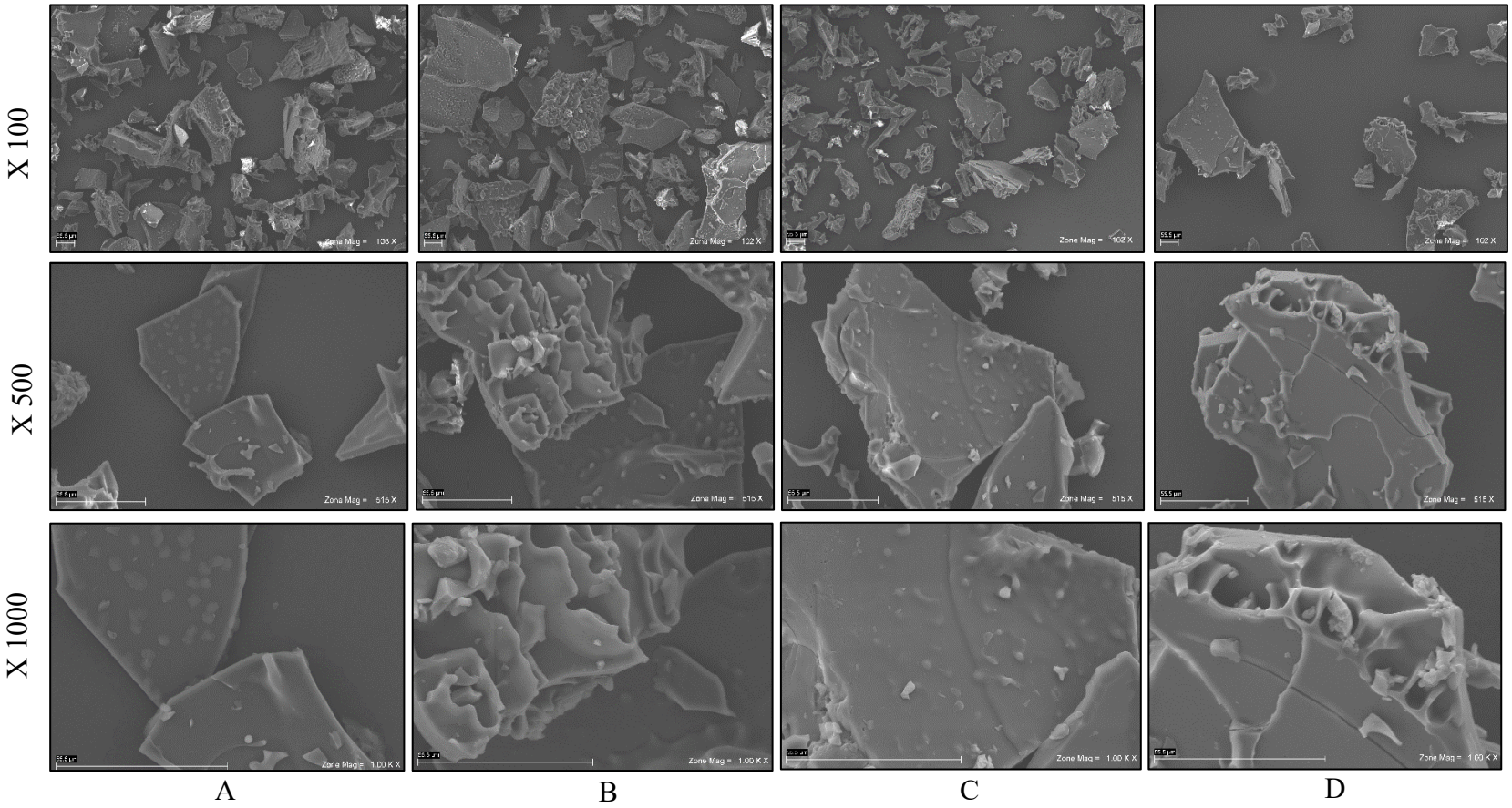


**Figure 11: Scanning electron microscopic (SEM) images of freeze-dried haskap berry anthocyanin-rich fraction incorporated microparticles in three different magnifications (×100, ×500 and ×1000).** Wall materials were consisted of maltodextrin and inulin in a ratio of 3:1 and, four different wall material: anthocyanin ratios A) 1:1, B) 1:1.5, C) 1:2, and D) 1:3 was used in microparticle production.

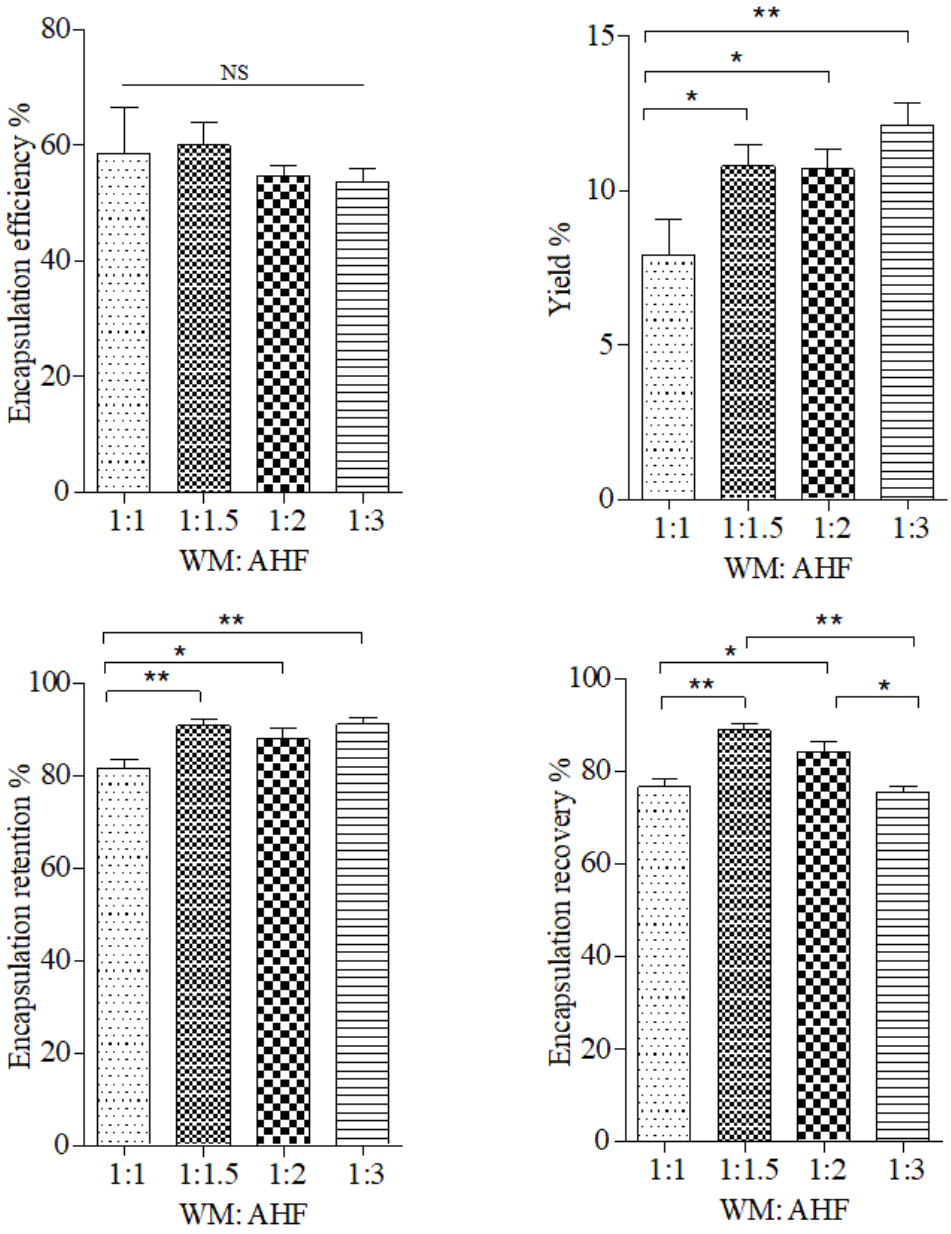


**Figure 12: Graphical representation of encapsulation efficiency (A), encapsulation yield (B), encapsulation retention (C), and encapsulation recovery (D) of anthocyanin microparticles**. Wall material (WM) to anthocyanin rich haskap fraction (AHF) ratio was used as 1:1, 1;1.5, 1:2, and 1:3. WM: AHF, 1:1.5 ratio was selected as the optimum ratio to produce anthocyanin microparticles in maltodextrin and inulin (3:1) matrix The results represent for replicates. One Way Analysis of Variance was performed ($p < 0.05$) with Tukey's multiple mean comparisons (at $\alpha = 0.05$) for mean separation. * Indicates that differences among the compared groups were significant at $\alpha = 0.05$. NS indicates the groups which are not significant at $\alpha = 0.05$.

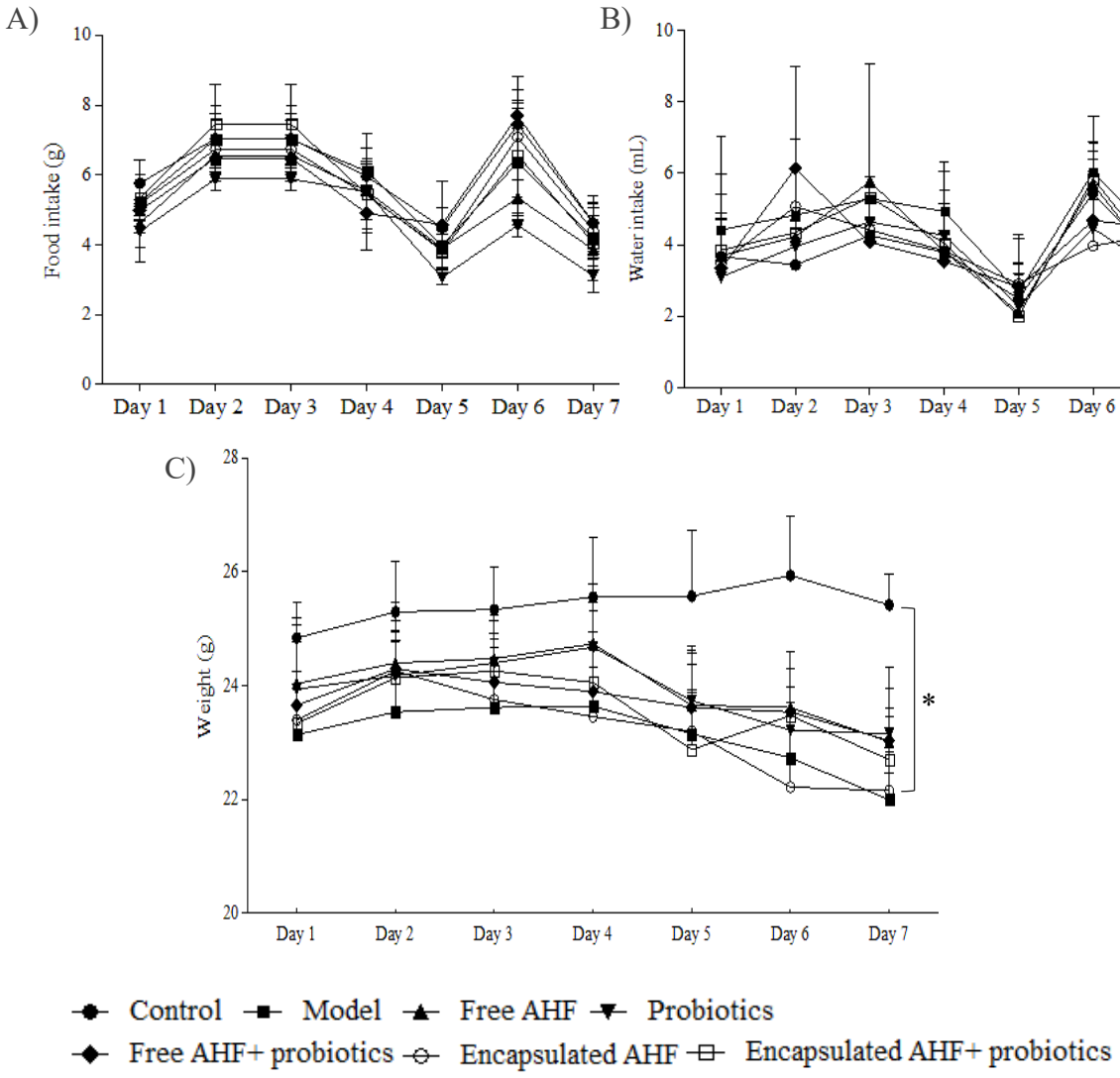


**Figure 13: Assessment of A) food (g) B) water (mL) intake and C) weight (g) of Balb/c male mice receiving different dietary supplementations during the 3% DSS administration period.** Dietary supplementary groups (n=5) were, control: regular chow, no DSS; model: regular chow, DSS; Free AHF: regular chow with non-encapsulated anthocyanin rich haskap fraction (6.2 mg C3GE/mouse/day), DSS; Probiotics: 11 strain probiotics powder ($1\times10^9$ CFU/mouse/day), DSS; Free AHF+ probiotics: regular chow with non-encapsulated anthocyanin-rich haskap fraction (6.2 mg C3GE/mouse/day), 11 strain probiotics powder ($1\times10^9$ CFU/mouse/day), DSS; Encapsulated AHF: regular chow with encapsulated anthocyanin-rich haskap fraction (6.2 mg C3GE/mouse/day), DSS; Encapsulated anthocyanin rich haskap fraction + probiotics: regular chow with encapsulated anthocyanin-rich haskap fraction (6.2 mg C3GE/mouse/day), 11 strain probiotics powder ($1\times10^9$ CFU/mouse/day) DSS. Two Way Analysis of Variance was performed ($p < 0.05$) with Tukey's multiple mean comparisons (at $\alpha = 0.05$) for mean separation. * Indicates that differences among the compared groups were significant at $\alpha=0.05$. Abbreviations: DSS = dextran sulfate sodium, AHF= anthocyanin-rich haskap fraction

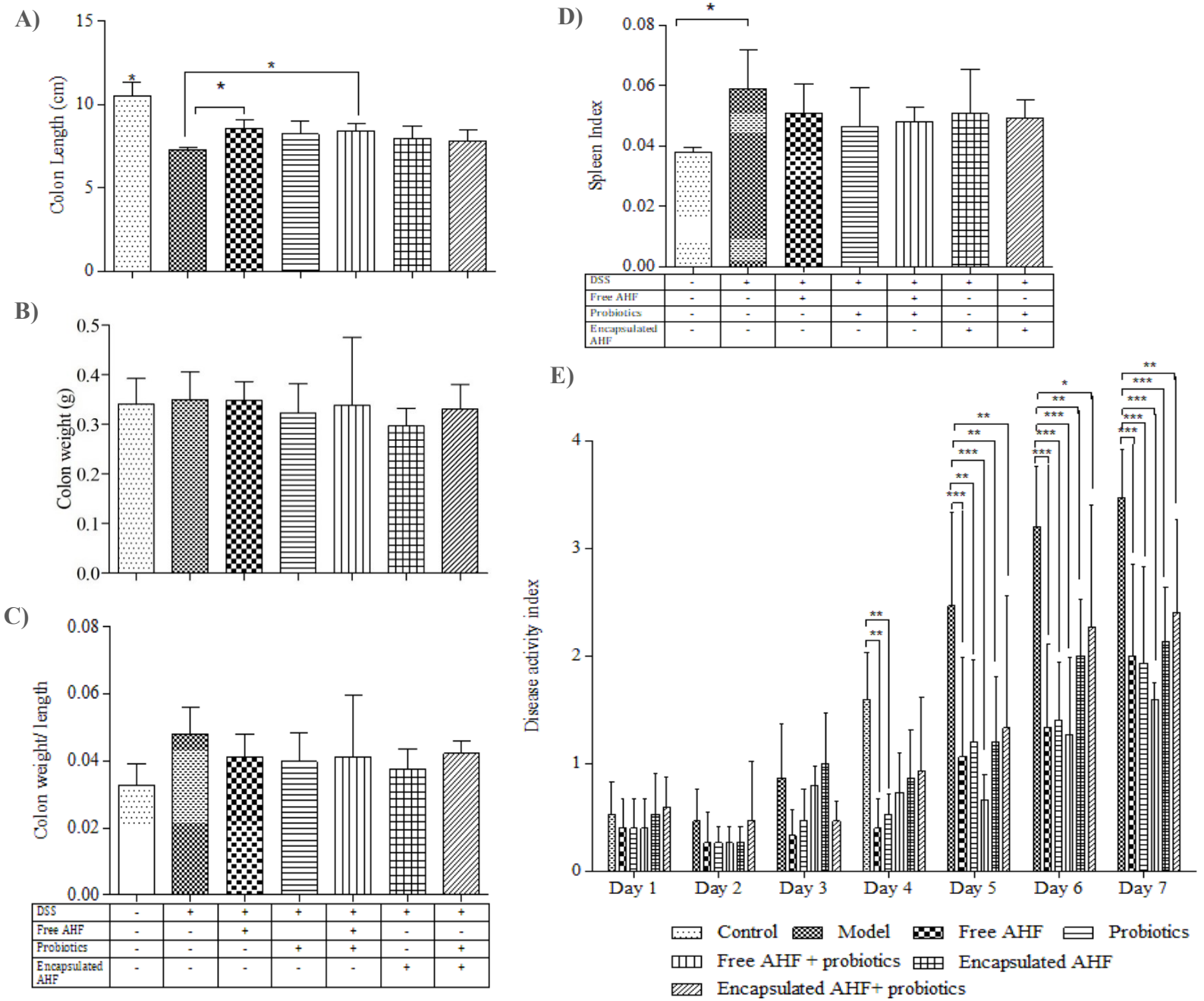
A)
Colon Length (cm)
15
10
5
0
B)
Colon weight (g)
0.5
0.4
0.3
0.2
0.1
0.0
C)
Colon weight/ length
0.08
0.06
0.04
0.02
0.00
DSS - + + + + + +
Free AHF - - + + - -
Probiotics - - - + + - +
Encapsulated AHF - - - - - + +
D)
Spleen Index
0.08
0.06
0.04
0.02
0.00
DSS - + + + + + +
Free AHF - - + + - -
Probiotics - - - + + - +
Encapsulated AHF - - - - - + +
E)
Disease activity index
4
3
2
1
0
Day 1
Day 2
Day 3
Day 4
Day 5
Day 6
Day 7
Control
Model
Free AHF
Probiotics
Free AHF + probiotics
Encapsulated AHF
Encapsulated AHF+ probiotics

**Figure 14: Clinical data assessment of Balb/c mice of 3% DSS-induced acute colitis model under dietary interventions of haskap and probiotics.** Clinical assessment was based on 4 different measurements including, A) Colon length of the mice measured at the day of sacrifice, B) Colon weight of the mice weighted at the day of sacrifice, C) Colon weight to length ratio, and D) Spleen index value calculated by dividing spleen weight by overall body weight E) Disease activity index measured by getting the average score of weight loss%, stool consistency and presence of occult blood during DSS administration. Dietary supplementary groups included control: regular chow, no DSS; model: regular chow, DSS; Free AHF: regular chow with non-encapsulated anthocyanin-rich haskap fraction (6.2 mg C3GE/mouse/day), DSS; Probiotics: 11 strain probiotics powder ($1\times10^9$ CFU/mouse/day), DSS; Free AHE+ probiotics: regular chow with non-encapsulated anthocyanin-rich haskap extract (6.2 mg C3GE/mouse/day), 11 strain probiotics powder ($1\times10^9$ CFU/mouse/day), DSS; Encapsulated AHF: regular chow with encapsulated anthocyanin-rich haskap fraction (6.2 mg C3GE/mouse/day), DSS; Encapsulated anthocyanin-rich haskap fraction + probiotics: regular chow with encapsulated anthocyanin-rich haskap fraction (6.2 mg C3GE/mouse/day), 11 strain probiotics powder ($1\times10^9$ CFU/mouse/day, DSS, at which n=5 in each. One Way Analysis of Variance was performed ($p < 0.05$) with Bonferroni pairwise comparison (at $\alpha = 0.05$) for mean separation. * Indicates that differences among the compared groups were significant at $\alpha=0.05$. Abbreviations: DSS= dextran sulfate sodium, AHF= anthocyanin-rich haskap fraction

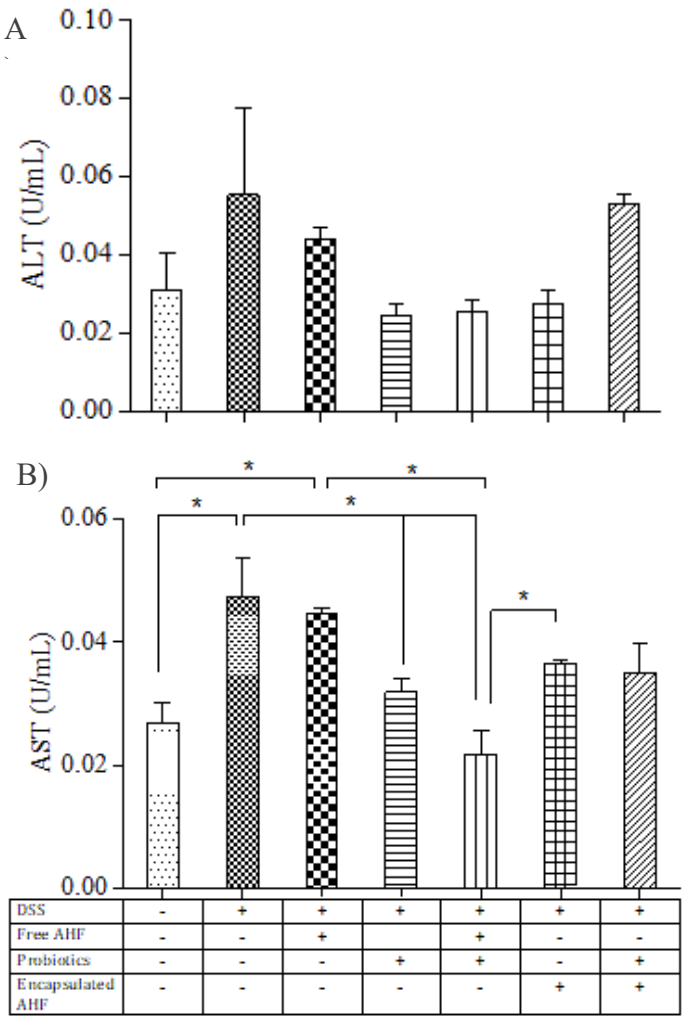


**Figure 15: Assessment of liver toxicity of Balb/c mice in 3% DSS-induced acute colitis model under several dietary interventions.** Liver toxicity was expressed in terms of A) alanine aminotransferase (ALT) and B) aspartate aminotransferase (AST) in mice serum (U/mL). Dietary supplementary groups included control: regular chow, no DSS; model: regular chow, DSS; Free AHF: regular chow with non-encapsulated anthocyanin-rich haskap fraction (6.2 mg/mouse/day), DSS; Probiotics: 11 strain probiotics powder ($1\times10^9$ CFU/mouse/day), DSS; Free AHF+ probiotics: regular chow with non-encapsulated anthocyanin-rich haskap fraction (6.2 mg/mouse/day), 11 strain probiotics powder ($1\times10^9$ CFU/mouse/day), DSS; Encapsulated AHF: regular chow with encapsulated anthocyanin (6.2 mg/mouse/day), DSS; Encapsulated anthocyanin-rich haskap fraction + probiotics: regular chow with encapsulated anthocyanin-rich haskap fraction (6.2 mg/mouse/day), 11 strain probiotics powder ($1\times10^9$ CFU/mouse/day, DSS, at which n=5 in each. One Way Analysis of Variance was performed ($p < 0.05$) with Tukey's multiple mean comparisons (at $\alpha = 0.05$) for mean separation. * Indicates that differences among the compared groups were significant at $\alpha = 0.05$. Abbreviations: DSS= dextran sulfate sodium, AHF= anthocyanin-rich haskap fraction

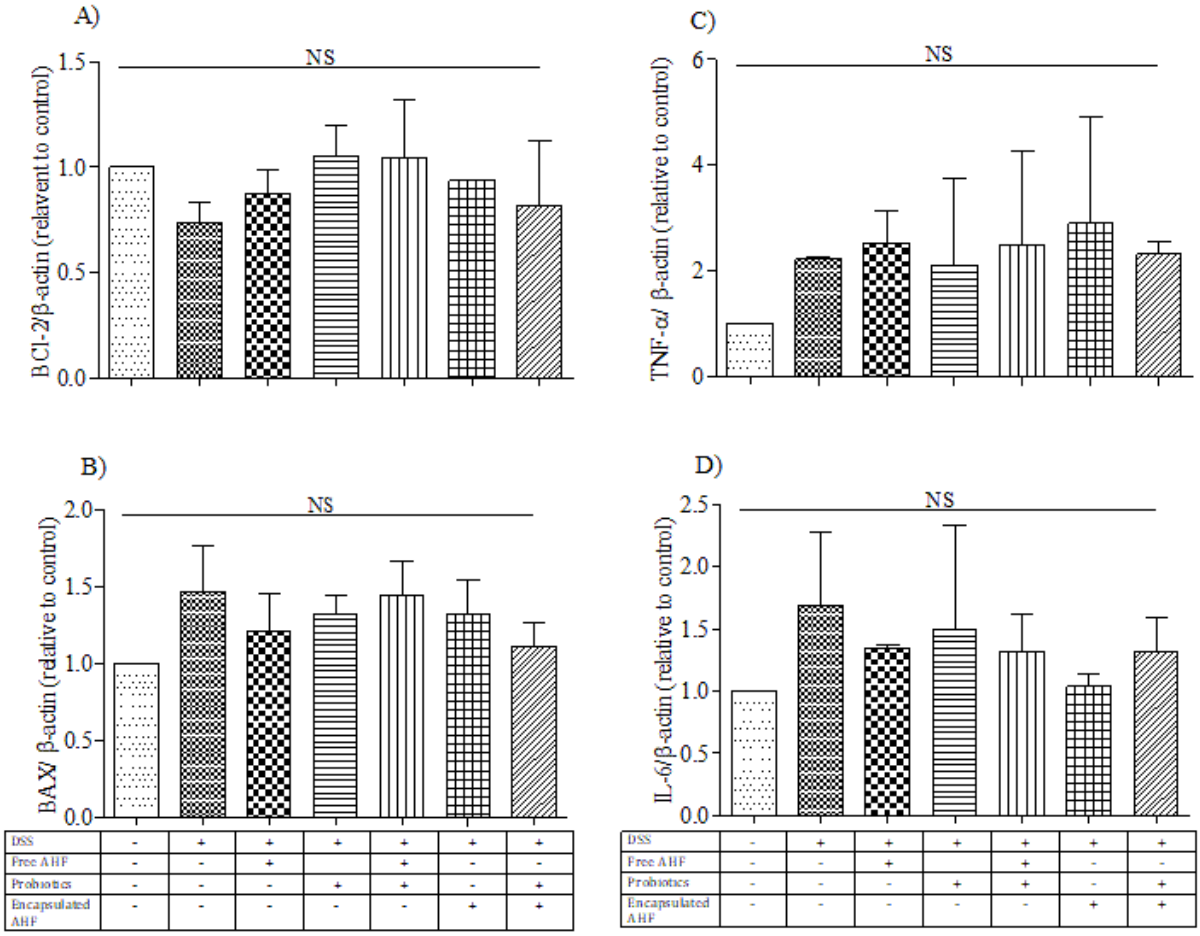
A)
BCl-2/β-actin (relavent to control)
NS
C)
TNF-α/ β-actin (relative to control)
NS
B)
BAX/ β-actin (relative to control)
NS
D)
IL-6/β-actin (relative to control)
NS
DSS
Free AHF
Probiotics
Encapsulated AHF

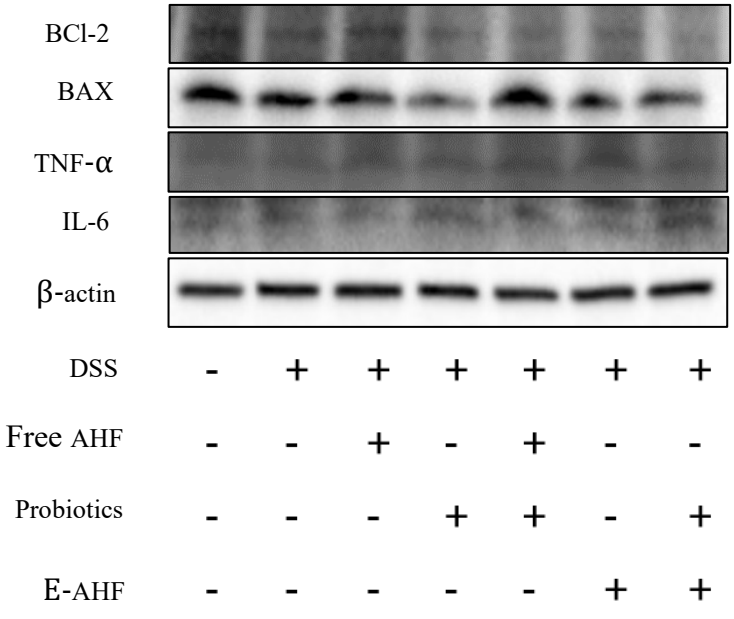
BCl-2
BAX
TNF-α
IL-6
β-actin
DSS - + + + + + +
Free AHF - - + - + - -
Probiotics - - - + + - +
E-AHF - - - - - + +

**Figure 16: Expression of BAX (A), BCl-2 (B), and inflammatory cytokines, TNF-α (C) and IL-6 (D) in Balb/c mice colon tissues.** Protein expression was determined using western blot analysis and images were analyzed using Image lab version 6.0.1 software. Results were normalized using the β-actin level and finally expressed as the relative protein levels compared to the control. At least three western blotting experiments were performed, and the results were expressed with means ± standard deviations. One Way Analysis of Variance was performed ($p < 0.05$) with Tukey's multiple mean comparisons (at $\alpha = 0.05$) for mean separation. NS indicates the groups which are not significant at $\alpha = 0.05$. Abbreviations: Free AHF= non-encapsulated anthocyanin-rich haskap fraction, E-AHF = encapsulated anthocyanin. BCL-2= B cell lymphoma 2, BAX= Bcl-2-associated X protein

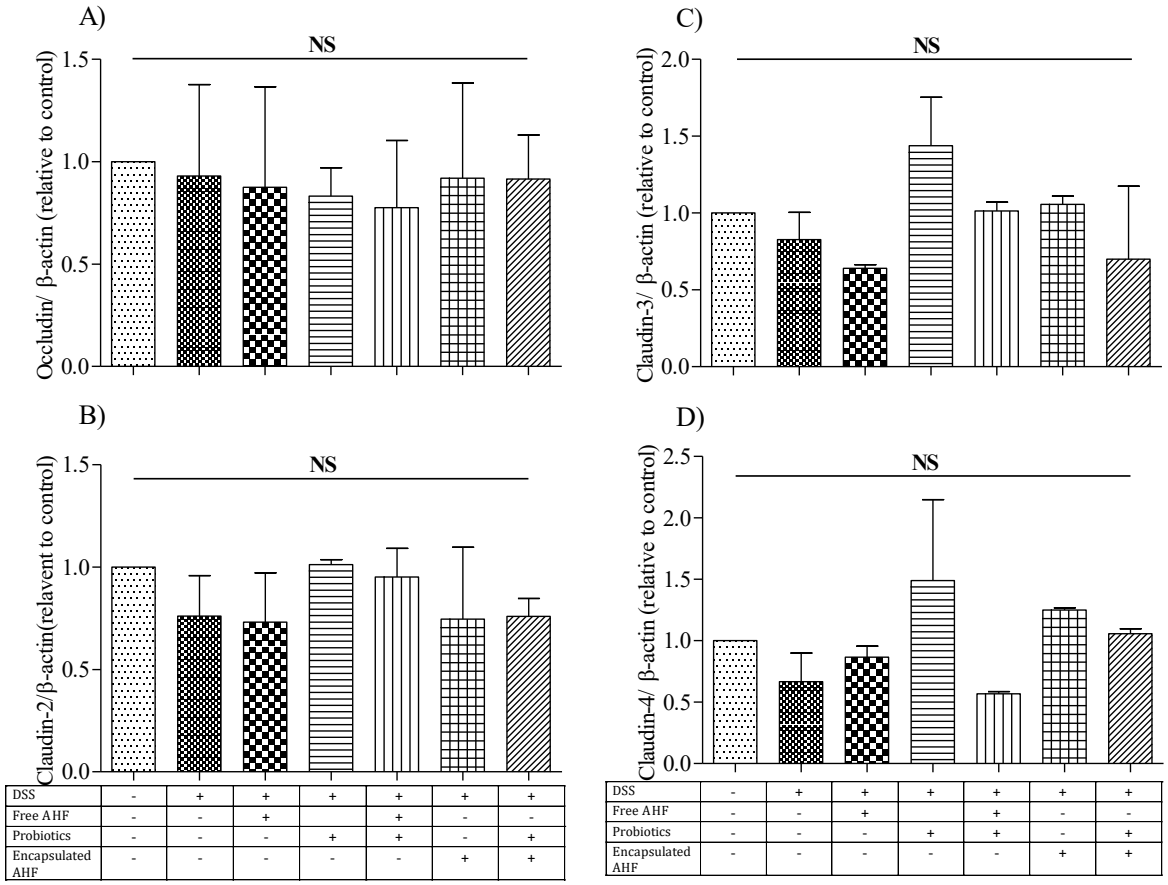
A)
NS
Occludin/ β-actin (relative to control)
1.5
1.0
0.5
0.0
C)
NS
Claudin-3/ β-actin (relative to control)
2.0
1.5
1.0
0.5
0.0
B)
NS
Claudin-2/β-actin(relavent to control)
1.5
1.0
0.5
0.0
D)
NS
Claudin-4/ β-actin (relative to control)
2.5
2.0
1.5
1.0
0.5
0.0
DSS - + + + + + +
Free AHF - - + + - -
Probiotics - - - + + - +
Encapsulated AHF - - - - - + +
DSS - + + + + + +
Free AHF - - + + - -
Probiotics - - - + + - +
Encapsulated AHF - - - - - + +

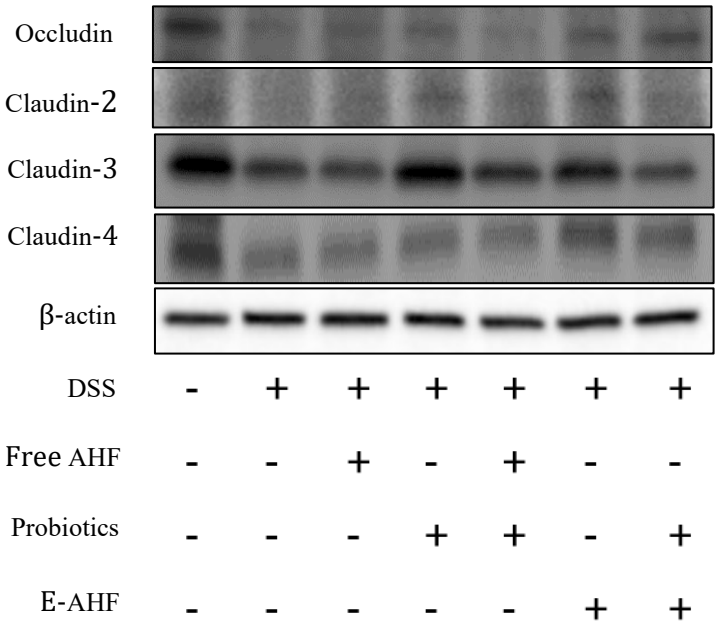
Occludin
Claudin-2
Claudin-3
Claudin-4
β-actin
DSS - + + + + + +
Free AHF - - + - + - -
Probiotics - - - + + - +
E-AHF - - - - - + +

**Figure 17: Effect of dietary supplementations on the expression of tight junction proteins in Balb/c mouse colon tissues in 3% DSS-induced acute colitis model**. A) Occludin, B) Claudin-2, C) claudin-3, and D) claudin-4 Protein expression was determined using western blot analysis and images were analyzed using Image lab version 6.0.1 software. Results were normalized using the β-actin level and finally expressed as the relative protein levels compared to the control. At least three western blotting experiments were performed, and the results were expressed with means ± standard deviations. One Way Analysis of Variance was performed ($p < 0.05$) with Tukey's multiple mean comparisons (at $\alpha = 0.05$) for mean separation. NS indicates the groups which are not significant at $\alpha = 0.05$. Abbreviations: Free AHF= non-encapsulated anthocyanin-rich haskap fraction, E-AHF = encapsulated anthocyanin-rich haskap fraction

\

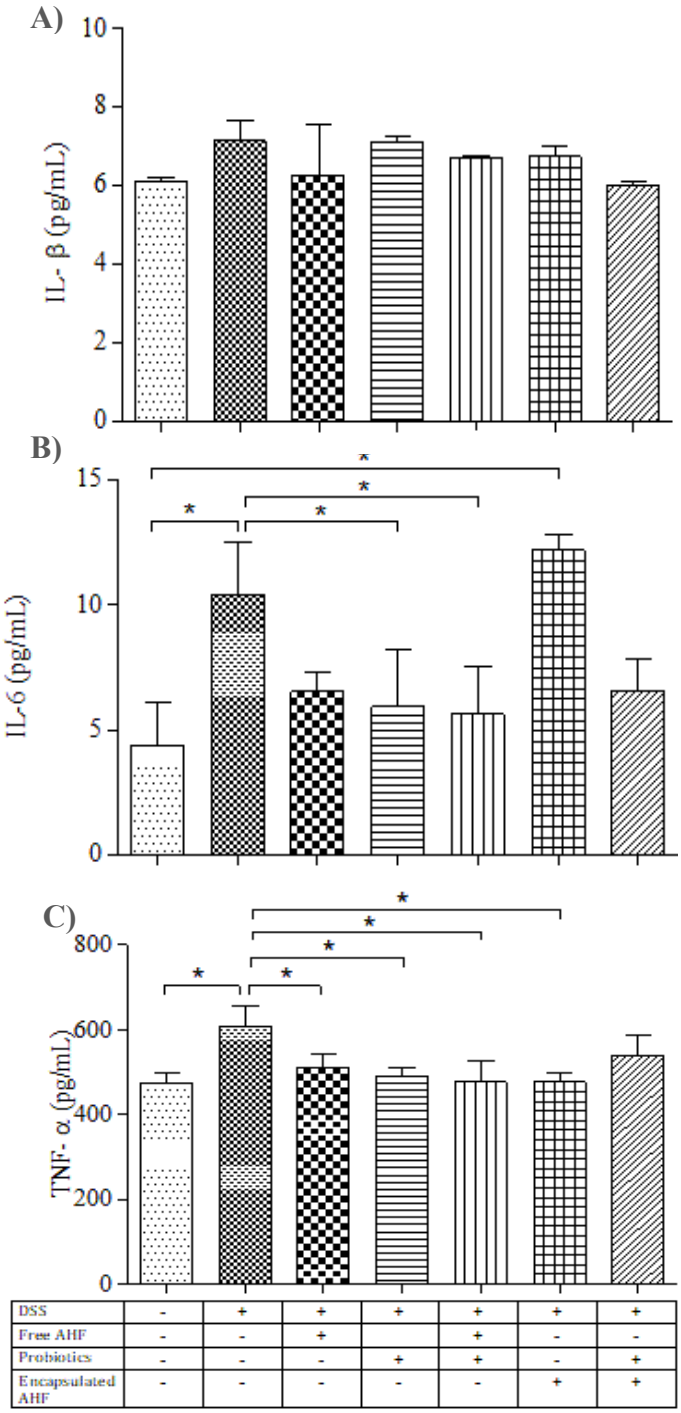


**Figure 18: Effect of dietary supplementations on the expression of pro-inflammatory markers in Balb/C mouse serum. A) IL-1β, B) IL-6, and C) TNF-α.** Expression of pro-inflammatory markers analyzed by ELISA in triplicates and the results were expressed with means ± standard deviations. One Way Analysis of Variance was performed ($p < 0.05$) with Bonferroni pairwise comparison (at $\alpha = 0.05$) for mean separation. * Indicates that differences among the compared groups were significant at $\alpha = 0.05$.

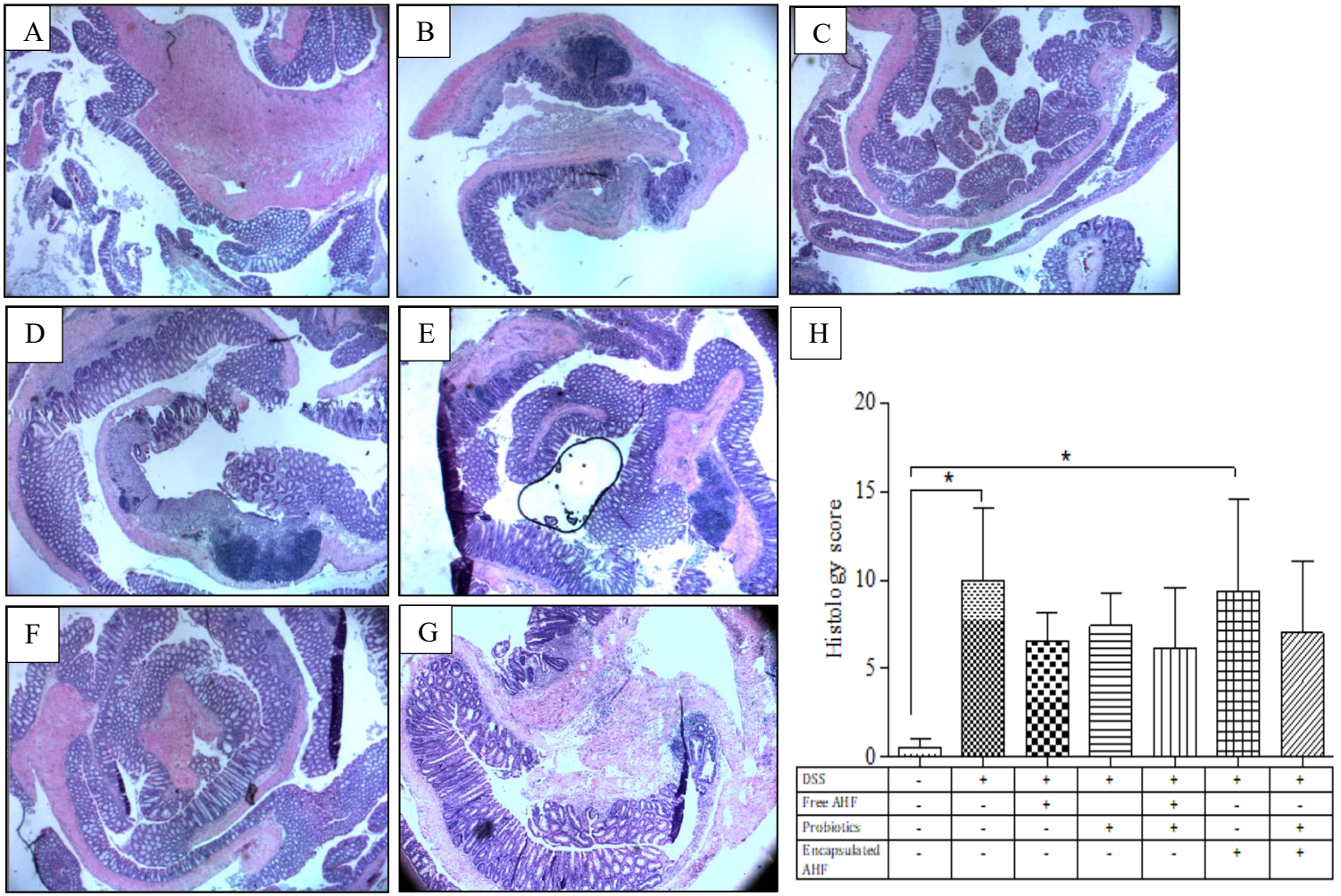
A
B
C
D
E
F
G
H
Histology score
20
15
10
5
0
*
*
DSS - + + + + + +
Free AHF - - + + - -
Probiotics - - - + + - +
Encapsulated AHF - - - - - + +

**Figure 19: Histological examination of the disease severity of colon of mice colon Swiss rolls representing different dietary supplementary groups under 200x.** A) Control: regular chow, no DSS; B) model: regular chow, DSS; C) Free AHF: regular chow with non-encapsulated anthocyanin-rich haskap fraction (6.2 mg C3GE/mouse/day), DSS; D) Probiotics: 11 strain probiotics powder ($1\times10^9$ CFU/mouse/day), DSS; E) Free AHF+ probiotics: regular chow with non-encapsulated anthocyanin-rich haskap fraction (6.2 mg C3GE/mouse/day), 11 strain probiotics powder ($1\times10^9$ CFU/mouse/day), DSS; F) Encapsulated ACN: regular chow with encapsulated anthocyanin-rich haskap fraction (6.2 mg C3GE/mouse/day), DSS; G) Encapsulated anthocyanin + probiotics: regular chow with encapsulated anthocyanin-rich haskap fraction (6.2 mg C3GE/mouse/day), 11 strain probiotics powder ($1\times10^9$ CFU/mouse/day, DSS. Histology score (H) was calculated by combining the scores given for (a) leukocyte infiltration, (b) crypt damage, (c) ulceration, (d) edema, and (e) crypt hyperplasia. Kruskal-Wallis test was performed ($p < 0.05$) with Dunn's multiple comparisons (at $\alpha = 0.05$) for mean separation. * Indicates that differences among the compared groups were significant at $\alpha = 0.05$.

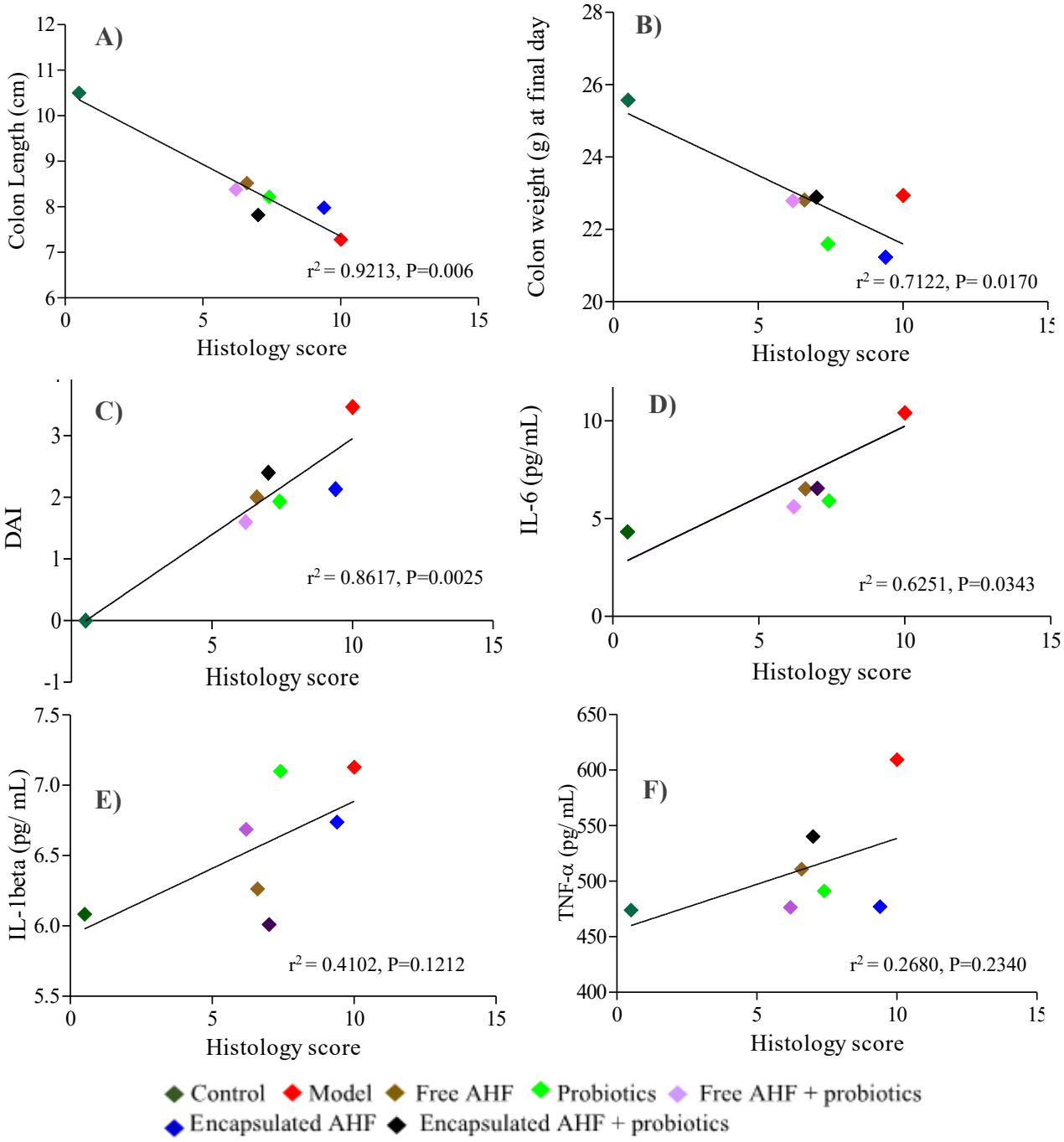


**Figure 20: Linear regression analysis of histology score vs A) colon length, B) colon weight (g) at final day, C) Disease activity Index (DAI) score, D) IL-6 (pg/mL) in serum, E) Il-1β (pg/mL) in serum and, F) TNF-α (pg/mL) in serum.** DAI measured by getting the average score of weight loss%, stool consistency and presence of occult blood during DSS administration. $r^2$= Pearson correlation coefficient.

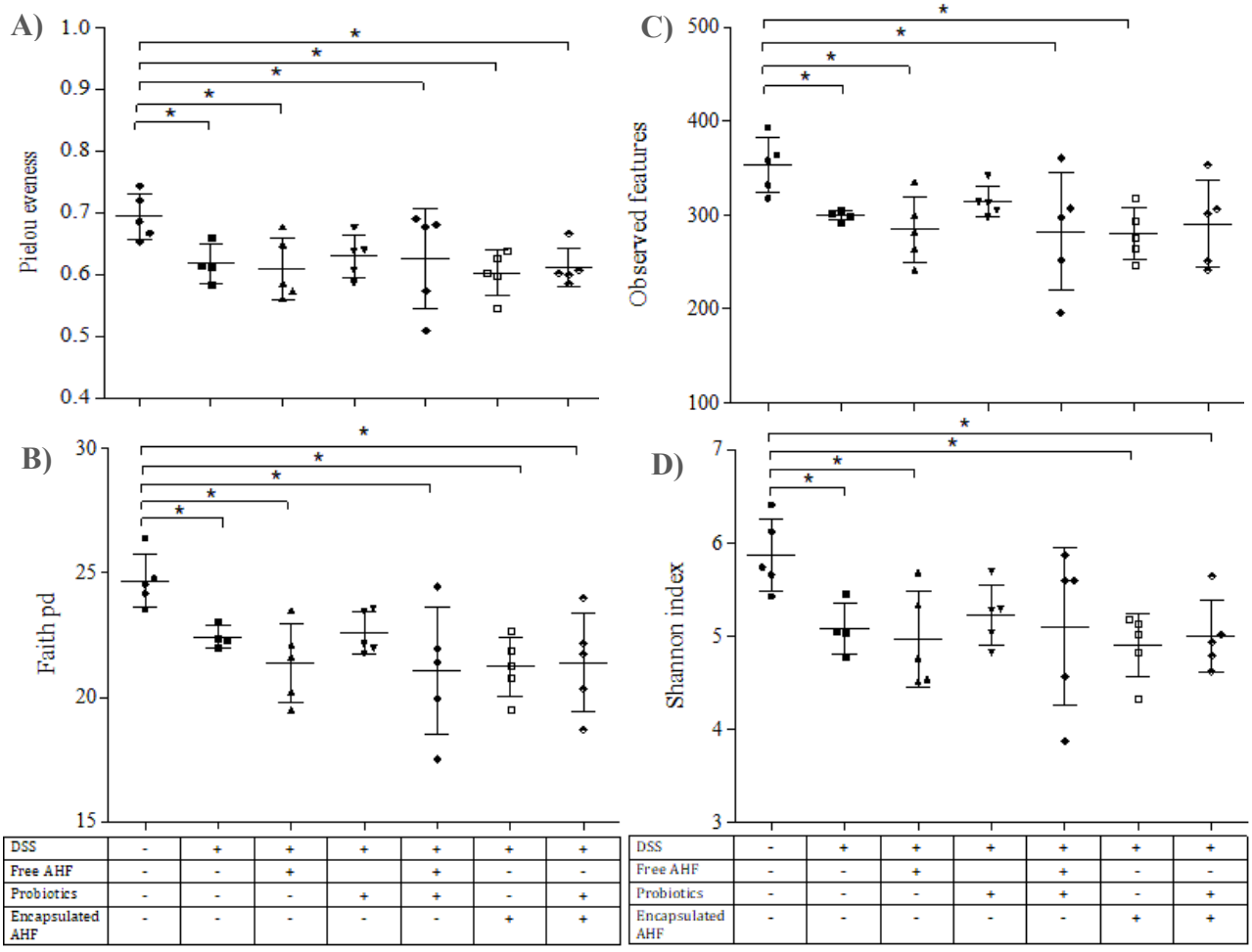


**Figure 21: Effect of dietary supplementations on the fecal microbiome in Balb/c mice of DSS-induced colitis.** A) Pieloue evenness, B) Faith pd, C) observed features and D) Shannon index. All parameters are displayed as a vertical scatter plot for each dietary supplementation which includes control: regular chow, no DSS; model: regular chow, DSS; Free AHF: regular chow with non-encapsulated anthocyanin-rich haskap fraction (6.2 mg C3GE/mouse/day), DSS; Probiotics: 11 strain probiotics powder ($1\times10^9$ CFU/mouse/day), DSS; Free AHF+ probiotics: regular chow with non-encapsulated anthocyanin-rich haskap fraction (6.2 mg C3GE/mouse/day), 11 strain probiotics powder ($1\times10^9$ CFU/mouse/day), DSS; Encapsulated AHF: regular chow with encapsulated anthocyanin-rich haskap fraction (6.2 mg C3GE/mouse/day), DSS; Encapsulated anthocyanin + probiotics: regular chow with encapsulated anthocyanin-rich haskap fraction (6.2 mg C3GE/mouse/day), 11 strain probiotics powder ($1\times10^9$ CFU/mouse/day, DSS. One Way Analysis of Variance was performed ($p < 0.05$) with Bonferroni's multiple comparison test (at $\alpha = 0.05$) for mean separation. * Indicates that differences among the compared groups were significant at $\alpha = 0.05$.

# CHAPTER 05: DISCUSSION

Polyphenols, a group of phytochemicals found abundantly in plants, have become an emerging food bioactive of interest in functional foods and nutraceuticals in recent decades. A growing body of research findings indicates that regular consumption of polyphenols primarily through fruits and vegetables plays a vital role in the prevention of chronic diseases including cancer, cardiovascular disease, neurodegenerative disorders, diabetes, and obesity (Cory et al., 2018). One class of polyphenols, named flavonoids is widely recognized for possessing anti-cancer and anti-inflammatory properties (Rupasinghe et al., 2014). Anthocyanin comes under the group of flavonoids, which are found in a 'natural' abundance in berries that are reported to attenuate inflammation and cancer associated with the gastrointestinal tract (Dharmawansa et al., 2020). In addition, the health-promoting effects attributed to anthocyanins were shown to be associated with gut microbiota modulation in terms of facilitating probiotic bacterial growth (Tian et al., 2019). However, the significantly low bioavailability of anthocyanin in the human body has led to exploring novel technologies such as microencapsulation in the stabilization, protection, and enhanced intestinal absorption of anthocyanin aiming to increase its stability, bioavailability and efficacy. The focus of the current study was to explore the potential of microencapsulated or non-encapsulated anthocyanin-rich haskap berry fraction (AHF) alone or in combination with probiotics in attenuating the severity of DSS-induced acute colitis in Balb/c mice.

Haskap berry is a type of berry that has gained significant attention for its medicinal and therapeutic properties. The anti-inflammatory and anti-cancer properties of haskap berries are largely attributed to their non-nutritive components which consist of

anthocyanins and other polyphenols. About 79%-92% of haskap anthocyanins consist of cyanidin-3-*O*-glucoside (C3G) (Rupasinghe et al., 2018). C3G also has tremendous advantages in protecting gut health, including repairing the intestinal mucosal barrier and relieving inflammation via modulating the level of colitis-related indicators and signaling pathways. In addition, C3G can be passed through the small intestine and bio-transformed into metabolites such as protocatechuic acid and phloroglucinaldehyde via colonic microbiota (Olivas-Aguirre et al., 2016). In the present study, haskap anthocyanin was extracted using 80% ethanol solution, which has been identified as one of the best extraction solvents for the haskap berries and is more efficient in the extraction of bioactives than methanol (Myjavcová et al., 2010). Besides, ethanol is less toxic and can be effectively used in food systems (Celli et al., 2015). The addition of formic acid in low concentrations assisted the extraction procedure of anthocyanins by damaging cellular membranes and facilitating anthocyanin release from cells (Z. Li et al., 2010). Ultrasound-assisted extraction (UAE) was used to improve the preservation of anthocyanins. Ultrasound frequencies above 20 kHz produce sound waves in water which create cavitation bubbles near the sample tissues. Once the bubbles enlarge to their maximum capacity, they undergo blasting and release a massive amount of energy. It destroys the cell walls and improves the mass transport of the anthocyanins from the plant cell walls to the solvent (Tena & Asuero, 2022). In the anthocyanin extraction process, a large number of impurities such as soluble sugars are also extracted. To obtain anthocyanin with high stability, strong physiological activity and high quality, crude anthocyanin extracts were separated and purified using column chromatography (Tan et al., 2022).

Microencapsulation is an emerging technology that serves as a tool to protect sensitive and active compounds by providing them with a protective wall and producing capsules with diameters ranging from 1 μm to 1,000 μm (M. N. Singh et al., 2010). In contrast to the above explanation, some researchers classified particle size as macro (>5,000 μm), micro (1–5,000 μm), and nano (<1 μm) (Jafari et al., 2008). Microencapsulation of anthocyanins has become a satisfactory solution for its low bioavailability and highly susceptible nature of degradation. Instead of using a single WM, the use of WM combinations leads to higher encapsulation efficiencies as a single WM does not possess all the required characteristics (Gharsallaoui et al., 2007). In the present study, a combination of maltodextrin (MD) and inulin (IN) have been utilized as WMs in the microencapsulation of AHF. Polysaccharides such as MD have been used commonly in the microencapsulation of anthocyanin for their high holding capacity, low viscosity, and excellent solubility (Pieczykolan & Kurek, 2019). However, to obtain microcapsules with improved mechanical stability and tailored microstructure, maltodextrin is commonly used in combination with other biomaterials (M. N. Singh et al., 2010). Evidence showed that anthocyanin has been successfully encapsulated in MD + Gum Arabic matrix (Khazaei et al., 2014), MD + whey protein or soy protein (Moser et al., 2017), MD + pectin or soy protein isolates (Pereira Souza et al., 2017) and in MD + IN as well (Nguyen et al., 2022). However, as maltodextrin is a digestible polymer encapsulated bioactive compounds may be released during digestion and get destroyed due to harsh gastric conditions (González et al., 2020).

IN, a slightly branched fructooligosaccharide, is composed of β-(2-1) linked fructose units, which are resistant to getting digested in the human small intestine and pass to the large

intestine. It is moderately water-soluble and highly indigestible by humans due to the presence of β-(2-1) glycosidic linkage (González et al., 2020). Once reaches the colon inulin gets digested by colonic microbiota (Tadesse Teferra, 2019). The colonic microbiota breakdown IN into short-chain fatty acids (SCFA) such as propionic acid and butyric acid which has a protective effect against colon cancer. Besides, IN facilitates the growth of probiotics as well. These modulatory effects aid in the prevention of mucosal inflammation (Akram et al., 2019). IN is widely used in the pharmaceutical industry as an excipient or stabilizer and is known to have utility as a slow-release drug delivery medium (Barclay et al., 2010). Further, anthocyanin was found to be more stable in IN matrix and no effect of the dextrose equivalent of MD was detected (Bakowska-Barczak & Kolodziejczyk, 2011). Therefore, MD and IN were selected as the WMs in AHF encapsulation. The most common methods of encapsulation of anthocyanin are spray-drying and freeze-drying. However, a comparison of the encapsulation efficiencies of various methods showed that the best performance was obtained for the freeze-drying method (Sharif et al., 2020). It is based on dehydration by sublimation of a frozen product and, during this procedure, the core materials and matrix solutions are homogenized and then lyophilized, resulting in a dry material (Yamashita et al., 2017). Moreover, as freeze-drying occurs in minus temperatures bioactive properties of anthocyanins are very well preserved (Wilkowska et al., 2016).

The anthocyanin profiling in microparticles and freeze-dried AHF powder was analyzed by HPLC-ESI-MS technology. The results confirmed that the major anthocyanin compound found in tested samples was C3G. Other identified anthocyanins were cyanidin-3-rutinoside, cyanidin-3,5-diglucoside and peonidin-3-glucoside. C3G content was significantly higher in the microparticles and AHF powder and accounted for 80% of the

total anthocyanin content. It was aligned with the previous findings of 76% (Rupasinghe et al., 2015) and 82-91% (Khattab et al., 2016). When the amount of AHF was increased, the total anthocyanin content in the microparticles was increased. In contrast, Mazuco et al., (2018) reported an increase in anthocyanin content with an increase in the wall material proportion. This might be due to the matrix differences of the wall materials used.

The moisture content of microparticles is an indicator of particle stability. The higher the moisture content higher the instability of the particles as they tend to agglomerate. Moreover, it is related to drying efficiency, powder flowability, stickiness, and storage stability (Akhavan Mahdavi et al., 2016). The moisture content of AHF microparticles was observed within the range of 6.9-8.4%. The results are consistent with reported moisture content ranging from 4.89% to 9.03% observed in red raspberry anthocyanin microparticles produced using soy protein isolates and Gum Arabic matrix (Mansour et al., 2020). Microencapsulation of anthocyanin-rich black soybean coat extract by spray drying using maltodextrin, gum Arabic and skimmed milk powder was also reported with similar moisture contents of 5.2-6.7%. However, chokeberry anthocyanin encapsulated in MD+IN by spray drying showed far less amount of moisture % (1.7%) than observed in the current study (Pieczykolan & Kurek, 2019). Higher moisture content observed in AHF microparticles could be due to rapid freezing during the freezing process at temperatures lower than −40 °C. This could reduce the pore diameter at the surface of microcapsules which may hinder mass transfer and act as a barrier against sublimation, resulting in increased moisture retention (Kuck & Noreña, 2016). Anthocyanin microparticles produce from freeze-drying, usually have higher $a_W$ contents than the spray-dried particles (Fredes et al., 2018). The $a_W$ of the microparticles was not significantly

different according to the WM:AHF ratio. However, the recorded $a_W$ level (0.6) was higher than in previous studies which utilized MD as a wall material constituent. To further elaborate, MD incorporated blackberry powder resulted in 0.11-0.15 range of $a_W$ (Oro et al., 2021) whereas, anthocyanin in elderberry pulp resulted in 0.12-0.20 $a_W$ content after encapsulated with MD using freeze-drying (Baeza et al., 2021). The $a_W$ values obtained, concurred with that provided by Yamashita et al. (2017) for anthocyanin-rich blackberry extract (0.51-0.53 $a_W$), and Rocha-Parra et al. (2016) observed in freeze-dried red wine (0.58 $a_W$). Microencapsulated AHF can be considered relatively stable against microbial growth, and hydrolytic and enzymatic reactions because an aw <0.6 is considered to be microbiologically stable (Quek et al., 2007). The solubility of all samples was between 93.9-97.9%. Solubility (wettability, dispersibility) as the ability of powders to form a solution in water is an important physicochemical property that influences the functional characteristics of powders intended to use in nutraceutical or pharmaceutical industries. Kuck & Noreña (2016), found solubility which ranged from 85.96% to 88% for microencapsulated grape skin phenolic extract using gum Arabic, polydextrose, and partially hydrolyzed guar gum as encapsulating agents. The kind of wall material used had no significant effect on the solubility of the powders. Supporting the previous claim, Pieczykolan & Kurek., (2019) also reported no difference in solubilities of chokeberry anthocyanin encapsulated in guar gum, gum arabic, pectin, beta-glucan and inulin. On the other hand, considerably lower solubilities (59.9–59.1%) were also reported with Maqui juice microparticles prepared by freeze-drying using MD blended with soy protein isolate (Fredes et al., 2018). Hygroscopicity is the ability of solids to adsorb water onto their surfaces microscopically (Lau, 2001). There was no significant difference in the

hygroscopicity of AHF microparticles (57.3-57.8 g/100 g of powder). Higher hygroscopicity could be associated with the number of hydrophilic groups present in the structure of MD and IN. Moreover, the use of other WMs together with MD increases the hygroscopicity of the powder in relation to the use of MD alone (Mohd Nawi et al., 2015). Microencapsulated AHF was found with a broader range of particle sizes ($D_{10}$= 57.5 µm, $D_{90}$= 2711.0 µm). The highest particle size was observed with the least amount of AHF incorporated (WM: AHF, 1:1). As evident, the bulk density of the particles was proportional to the particle size. The particle diameter of spray dried powders can be ranged between 1-15 µm whereas freeze-dried products can reach 300 µm (Che Man et al., 1999). However, the particle size of the present study was exceeded 300 µm and it might be due to the difference in the strength of the manual force used in particle grinding (Kuck & Noreña, 2016). The same phenomenon has been suggested by Fang & Bhandari, 2010, explaining that the encapsulation method as well as the grinding process directly affects both the shape and size of powders.

The FTIR analysis reveals the information useful in predicting the chemical bonding and interactions in AHF microparticles. The functional groups of the compounds are identified as they absorb radiation in a characteristic frequency of the infrared spectrum (Laila et al., 2019). The main infrared regions of MD are located at wavelengths less than 1,000 $cm^{-1}$ corresponding with C-O stretching vibrations of an anhydrous glucose ring. The band located around 1,000 $cm^{-1}$ belonged to the vibration of the C-C pyranoid ring of the glucose monomers, the vibration of the C-O-C glycosidic bond, and the stretching of the C-OH side group in MD (Kutzli et al., 2018). The characteristic vibrations at 800-1,200 $cm^{-1}$ are the fingerprint region of the carbohydrate's representative with C-C, C-O and, C-

O-C stretching vibrations of fructo-furanose rings in IN (Akram & Garud, 2020). The broadband at 3,000-3,600 $cm^{-1}$ was assigned with O-H vibration groups in both MD and IN molecules and the band at 2,933 $cm^{-1}$ was due to C-H stretching vibrations in carbohydrates (Petkova et al., 2022). The WM+AHF spectrums showed multiple bands around 1,150 $cm^{-1}$ -1,400 $cm^{-1}$ which are attributed to the C-O stretching and C-O-H bending vibrations of phenols including the $CH_2$ bending by the peak at 1,152 $cm^{-1}$ and starching of pyran rings typical to flavonoids producing the peak at 1,231 $cm^{-1}$ (Swer et al., 2018). The bands appearing between 1,300 $cm^{-1}$ and 1,380 $cm^{-1}$ are assigned to C-O angular deformations of phenols (Pereira et al., 2015). The clear increase of the band intensities in the region of 1,500 $cm^{-1}$- 1,700 $cm^{-1}$ shows that anthocyanin is incorporated in microparticles since the modified region is typical of C-C stretching from aromatic rings, as well as changes in the 750 $cm^{-1}$-1,000 $cm^{-1}$ region, indicating the presence of aromatic rings with ortho substitution (Pereira et al., 2015). In addition, bands corresponding to symmetric and asymmetric C-H vibrations were observed in the range of 2,924 $cm^{-1}$ to 2,926 $cm^{-1}$ modified region. An increase in the depth of the broader bands produced at 3,000 $cm^{-1}$-3,600 $cm^{-1}$ is associated with the stretching vibration of O-H bonds in anthocyanins (H. R. da Silva et al., 2019).

With respect to the particle morphology, freeze-dried microparticles exhibited broken glass structures without having a uniform surface, which are characteristics of microparticles produced by this drying method (Kuck & Noreña, 2016). The particles were in irregular shapes of various sizes as observed by other authors (Oro et al., 2021; Yamashita et al., 2017). Furthermore, the heterogeneous surface of microparticles was observed with multi-cavities and flake-like structures which agreed with the observations

of Stoll et al., (2016) and, Yamashita et al., (2017). A possible explanation for this phenomenon is the rapid sublimation of frozen water from the coating matrix, resulting in the formation of cavities where there were ice crystals before (Smrdel et al., 2008).

The encapsulation parameters such as encapsulation efficiency, yield, retention, and recovery are used to determine whether the core material is successfully encapsulated. All AHF microparticles showed comparable high encapsulation efficiencies (53.68% to 59.9%) with no statistical difference which suggests the compatibility of the MD+IN matrix in the encapsulation of AHF. As previously found, the use of maltodextrin alone in encapsulating Roselle calyxes anthocyanin exhibited an efficiency of 33.3% (Nafiunisa et al., 2017). Therefore, encapsulating efficiency was observed to be improved with the use of a combination of wall materials. As an example, Yu & Lv. (2019) reported the higher encapsulation efficiency (72%) of freeze-dried rose anthocyanin in maltodextrin and gum arabic mixture. Higher encapsulating efficiencies might be attributed to the hydrogen bonding and/or electrostatic interactions that occur between maltodextrin/inulin and anthocyanins (Vergara et al., 2020). Further, it was found that freeze drying is more effective than spray drying in terms of encapsulating efficiency. Contradictory to that, encapsulation of anthocyanin from *hibiscus sabdariffa. l* using maltodextrin and gum arabic by spray drying technology was reported to have higher encapsulation efficiencies (Idham et al., 2012). The encapsulating efficiency also depends on the type and concentration of the wall materials and the number of loaded anthocyanins (Sharif et al., 2020). However, as found in the present study, encapsulation efficiency was independent of the amount of AHF powder in the matrix mixture. Opposing our findings, Akhavan Mahdavi et al., (2016), indicated that the encapsulation efficiency of barberry extract

microparticles encapsulated with maltodextrin, gum arabic and gelatin was largely dependent on the core/wall ratio. According to the results, encapsulating yield was increased with increasing the AHF amount in encapsulating mixture. The possible explanation might be that when the amount of anthocyanin is in excess, more of the powder is loaded inside the encapsulating matrix. With comparing to previous findings, the yield values (maximum yield = 12.2%) observed in the current study were relatively low. Microencapsulation of maqui juice anthocyanin by spray drying resulted in a yield of 73.4%, which was not statistically different from that of the freeze-drying method (Fredes et al., 2018). The anthocyanin retention in the encapsulated microparticles (maximum retention= 81.6%) was also increased with the amount of AHF powder in the mixing matrix. In contrast to that, phenolics extracted from rambutan peel were reported to have higher encapsulation retention when encapsulating agent concentration increased from 10% to 13% (Boyano-Orozco et al., 2020). Similar retention efficiency has previously been reported for the spray-drying of grape skin extract (99.58%) with the use of 10% gum arabic over 5% partially hydrolyzed guar gum and polydextrose (Kuck & Noreña, 2016). In this context, encapsulating yield and encapsulating retention are strongly dependable on the amounts of core and wall materials. Yu & L. (2019), who attempted to microencapsulate rose residue anthocyanins, showed that the anthocyanin retention was 91.44% for freeze-drying and 75.85% for spray drying. The anthocyanin recovery is the parameter that demonstrates the effect of the freeze-drying process on anthocyanin content (or stability during freeze-drying). With respect to the anthocyanin recovery of the AHF micro-particles, the results were independent of the AHF amount used in the encapsulating matrix. In the present study, maximum anthocyanin recovery of 90% was observed which

is in agreement with other studies where obtaining anthocyanin microparticles by spray drying with maltodextrin for maqui juice reported recovery of 99.8% (Fredes et al., 2018), for pomegranate extract and juice recovery of 97% and 100% (Robert et al., 2010) and for bayberry extract recovery of 94% (Z. Fang & Bhandari, 2011).

The DSS model of mice was used to investigate the effectiveness of AHF and probiotics on the prevention of acute colitis, as the DSS-induced colitis model produces symptoms comparable to those of human UC such as body weight loss, diarrhea, bloody feces, shortening of the colon and mucosal ulceration (Perše & Cerar, 2012). The oral administration of DSS is regarded as a simple, economical and effective method in mice (Xu et al., 2020). Therefore, colitis was induced in mice by adding DSS to drinking water. Even though the exact mechanism is yet to be understood, DSS-induced inflammation is associated with the disruption of colonic epithelial monolayer lining by loosening the epithelial tight junctions, leading to the invasion of gut microbiota and their derivatives into the colonic mucosa (Xu et al., 2020). The damage is thought to cause by the negatively charged sulfate groups in DSS (Kim et al., 2021). Depending on the concentration, duration, and frequency of DSS administration acute or chronic conditions can be developed (Perše & Cerar, 2012). According to previous studies, a fixed dose of 3% of DSS given for 7 days was effective in recapitulating the loss of barrier function present in clinical colitis (Cochran et al., 2020). The molecular weight of the DSS, mice strain, gender of the animal, and microbiological factors (gut microbiome) of the animal are also responsible for the differential susceptibilities and responsiveness of the DSS (Bramhall et al., 2015). As reported by Eichele & Kharbanda. (2017) molecular weight of 40-50 kDa of DSS is suitable for producing acute colitis in animals, as larger molecules (≥ 500 kDa) fail

to penetrate colonic tissues well and smaller molecules (5-40 kDa) have inadequate tissue penetration and produce mild disease. Therefore, in the present study, DSS with a molecular weight range of 36 kDa-50 kDa was selected to observe better resemblance features of human colitis (Monk et al., 2016). Considering the differences in mouse strains, C3H/HeJ, C57BL/6 and Balb/C mice are more genetically susceptible to DSS-induced colitis (Eichele & Kharbanda, 2017). The role of the gender of animals in inflammatory models is well established (Fish, 2008). The male mice are observed with more pronouncing symptoms of colitis than the female in the DSS model (Mähler et al., 1998; Perše & Cerar, 2012). In regard to external factors, the stress triggered by transportation, movement and housing can also cause differences in DSS susceptibility. Hence a minimum of 48-72 hrs acclimatization period is recommended for the rodents used in laboratory experiments (Montonye et al., 2018). The DSS-induced colitis model is reported with at least 1 week of acclimatization period (Hamilton et al., 2011; Khan et al., 2022). As to investigate the preventive potential of AHF and probiotics, mice were started to be fed with the supplementary diets 5 days prior to DSS administration and continued till the day they sacrificed.

Appetite, water/food consumption, and body weight loss are often considered to be revealing clinical signs in diseased animals. The appearance of clinical signs of DSS-induced colitis usually takes place on days 3-4 of DSS exposure and gradually increased in severity over time (Anderson et al., 2019). Upon DSS administration, loss of appetite indicated by the reduction in water and food intake was observed. The reduction was initiated by day 3 and showed non-pattern fluctuation. Similar results were observed by Anderson et al. (2019) in the mice treated with Azithromycin and in which the colitis was

induced using 3.5% of DSS. However, differences in DSS susceptibility do not correlate with differences in the consumption of DSS-supplemented water (Mähler et al., 1998). The mice in the healthy or control group showed an increase in their body weight whereas all DSS groups reported weight reduction during the DSS to introduce period initiated at day 4. Moreover, DSS causes dose- and time-dependent body weight loss (Kim et al., 2021). The body weight of animals used in experiments is a simple parameter which is easy to access objectively and can provide information about disease severity and decision about humane endpoints (Talbot et al., 2020). Many animal experiments, scientists, and local authorities define a weight loss threshold of 20% or more as severe suffering and thereby as a potential parameter for humane endpoint decisions and the same criteria were used in the present study (Talbot et al., 2020). How DSS is responsible for weight reduction might be attributed to loss of appetite and water intake.

The colon weight, colon length and colon weight-to-length ratio are gross biomarkers of colonic inflammation (Charpentier et al., 2012). As per our results, the normal length of the colon was shortened by DSS treatment, however free AHF and free AHF + probiotics treatments significantly inhibited the changing of colon length in DSS-treated mice. The effect of DSS on colon length is well documented (Jeon et al., 2021; Scarano et al., 2018; J. Zhao et al., 2013). Confirming our findings, plant bioactive-rich lingonberry fruit ethanol extract (Jeon et al., 2021), sesamol extract (B. Zhao et al., 2020), maqui berry extract (G. Zhou et al., 2019) and probiotics supplementations (Y. Zhang et al., 2018) improved the DSS-induced colon shortening. In the present study, colon weight was not found to differ among the experimental groups. However, evidence has been made earlier to show the effect of DSS on weight reduction in mice colon (Kwon et al., 2021).

The ratio between the weight (g) and the length (cm) of the colon, an indirect indicator of edema and inflammation, increased in all DSS-treated groups. Similar findings were reported by Kwon et al., (2021). The colon weight-to-length ratio was increased in a DSS dose-dependent manner producing the highest ratio in 3% DSS-treated C57BL/6 N mice. The DSS causes an increase in spleen weight which generally correlates with the severity of inflammation (Chassaing et al., 2014). The main reason behind the spleen enlargement likely attributes to an inflammation-driven increase in the immune cell count in terms of neutrophils and lymphocytes in the spleen (Liverani et al., 2014). As per the current results, the spleen index of the experimental model group was significantly increased than that of the control group and AHF and probiotics dietary supplementations were able to reduce the spleen index values. Zuo et al., (2021) made similar observations, as luteolin decreased the elevated spleen index values in C57BL/6 mice where the colitis was induced using 3% of DSS.

The DAI was used to determine the severity of colitis. Consistent with previous studies, mice exposed to DSS developed body weight loss, watery diarrhea, and bloody stools (Yan et al., 2009). The current study demonstrated the successful induction of acute colitis upon the intake of 3% DSS in drinking for 7 days, which was recognized by the appearance of colitis and clinical signs and symptoms including weight reduction, changes in stool features, rectal bleeding, and an increase of DAI. The highest DAI values were observed with the experimental model group along with no mortality among the experimental groups. The supplementation of AHF and probiotics improved the DAI, which could be due to their effects on the inflammatory process, mucosal damage, and epithelial integrity. The DSS-induced colitis leads to a disturbance in epithelial barrier

integrity, resulting in an increased influx of gut microbiota into the intestinal wall, further accelerating the inflammatory process (Perše & Cerar, 2012). Colitis severity was mitigated by all dietary supplementations starting from day 5, providing evidence for inflammation preventive potential of AHF and probiotics by reducing the weight loss, increasing stool consistency, and modulating the barrier integrity. Similar observations were made by Zhang. (2012), in C57BL/6 male mice fed with cooked common beans whereas the colitis severity dropped down starting from day 4. Further, dietary supplementation of soybeans Bowman-Birk inhibitor concentrate reduced the severity of DSS-colitis by suppressing inflammation in the colon and improving the recovery following DSS induction (Ware et al., 1999). In support of the findings, supplementation of cranberry bean diets prior to DSS exposure reduced the DAI scoring in C57BL/6 mice (Monk et al., 2016). Administration of lingonberry fruit ethanol extract also reduced the DAI score in Balb/c mice in a dose-dependent manner (Jeon et al., 2021). They also used 3% DSS to induce colitis conditions. Despite their health benefits, high dose of plant exacts can be harmful to the liver and kidneys (Al-Nuaimi, 2018). Anthocyanin toxicity has not been shown as the currently available toxicologic database is inadequate to establish a numerically acceptable daily intake for anthocyanins (T. C. Wallace & Giusti, 2015). However, DSS-induced inflammation can cause acute liver damage, which reflects via increased levels of biochemical parameters such as plasma levels of ALT and AST enzymes (Kwon et al., 2021; Zhan et al., 2022). Similar results were obtained in the present study. The serum levels of ALT were elevated in the groups treated with DSS and supplemented with free AHF, encapsulated AHF+ probiotics and in DSS alone group while showing no significant difference from the control group suggesting that DSS was not an

effective influencer in acute liver injury. Similarly, some murine studies have shown that DSS alone is not influencing serum ALT and AST levels; however, DSS with alcohol (Shao Tuo et al., 2017) and high-fat high carbohydrate diets (M.-Y. Wang et al., 2022) were effective. In the present study, a significantly higher level of AST was found in the experimental model group and supplementation of probiotics and AHF+ probiotics significantly reduced the increase in serum AST levels. However, free AHF was not effective in reducing the AST levels. In contrast to our findings, anthocyanin extracted from black chokeberry showed a reduction in plasma ALT/AST levels in adult male Kunming mice in a dose-dependent manner after feeding for 8 weeks (Wei et al., 2017). On the other hand, administration of high doses of probiotics ($1\times10^{10}$ CFU) to healthy and to Balb/c mice treated with 2, 4, 6-trinitrobenzene sulfonic acid (TNBS) to induce acute colitis, found with no toxicity (Daniel et al., 2006). Confirming that, $1\times10^{11}$ CFU dose of lactic acid bacteria (LAB) strains, *Lactobacillus rhamnoses, Lb. acidophilus* and *Bifidobacterium lactis* were also not associated with any toxic effect in Blab/c mice (J. S. Zhou et al., 2000). Therefore, it can be confirmed that the amounts of anthocyanin (6.2 mg C3GE/mouse/day) and probiotics ($1\times10^{9}$ CFU), used in the present study were within safe limits for consumption. Moreover, as encapsulated AHF groups also showed no difference in ALT and AST levels compared to the control, it can be suggested that maltodextrin and inulin are safe core materials.

The most prominent function of B-cell lymphoma 2 (BCL-2) family proteins is regulating the initiation of the intrinsic (mitochondrial) apoptotic pathway by controlling the permeabilization of the mitochondrial outer membrane (Youle & Strasser, 2008). This family of proteins includes anti-apoptotic proteins such as BCL-2 and pro-apoptotic pore-

formers such as Bcl-2 associated X (BAX) as well (Kale et al., 2017). The imbalance between Bcl-2 and BAX may cause cell apoptosis (Fu et al., 2022). However, there are controversial findings on BCL-2 and BAX expressions in DSS-treated murine models. For example, the administration of 4 % DSS for 7 days caused an increase in BCL-2 and BAX levels in the colon epithelial cells of Sprague-Dawley rats (Vetuschi et al., 2002). In contrast to that, as reported by Yang et al., (2017), the C57BL/6 mice exposed to 3% DSS for 7 days showed increased levels of BAX and decreased levels of BCL-2 in colon tissues. Similarly, 2.5 % of DSS given for 7 days, increased the BAX protein expression and decreased the BCL-2 protein expressions in C57BL/6 mice (Fu et al., 2022). However, DSS-induced colitis had no significant effect on BAX and BCL-2 changes and that may be the reason why supplementary diets failed to improve those changes significantly. In contradiction to that, DSS-treated C57BL/6 mice fed with apple peel polyphenols significantly reduced the colonic tissue expression of BAX and improved the BCL-2 (Yeganeh et al., 2018). Moreover, high hydrostatic pressure-treated cyanidin-3-glucoside and blueberry pectin complexes were found to be restoring the DSS effect on BAX and BCL-2 proteins expressions in Balb/c mice (Tan et al., 2022).

Cytokines are important mediators of inflammation and elevated levels of pro-inflammatory cytokines such as TNF-α, IL-6 and IL-1β are observed in patients with UC and also in DSS-induced colitis models (Li et al., 2018). They are mainly secreted by macrophages and neutrophils which penetrate the colon and are destined to regulate the inflammatory response (Li et al., 2019). In particular, TNF-α plays an essential part in suppressing tumours and viruses. However, when TNF-α is overexpressed, a continuous inflammatory reaction occurs (Naito et al., 2004). There is growing evidence that the pro-

inflammatory cytokines IL-6 and IL-1β play a crucial part in the uncontrolled colitis process (Atreya & Neurath, 2005; Coccia et al., 2012). The increased level of IL-6 leads to overexpression of signal transducer and activator of transcription 3 (STAT3) pathway, which in turn causes induction of anti-apoptotic genes such as B-cell lymphoma-extra large (Bcl-xl) (Atreya & Neurath, 2005). As literature suggested, high levels of IL-1β secretion by colon lamina propria monocytes were observed in patients with active IBD and high levels of IL-1β were associated with active lesions which facilitated the localized inflammation (Coccia et al., 2012). Thus, modulators of these inflammatory cytokines may provide important clues to the treatment of colitis. In the present study, serum levels of TNF-α and IL-6 cytokines were significantly increased in the experimental model group in comparison with the control group, with no detectable change in serum IL-1β and colonic expressions of TNF-α and IL-6 expressions. However, AHF and/or probiotics diets were potent in downregulating the serum TNF-α and IL-6 cytokine expressions. Consistent with our findings, DSS administration had no significant change in the colonic TNF-α expression of male Wistar rats when compared to the control; however, it was reduced by grape pomace extract which contains high amounts of anthocyanins, hydroxycinnamic acids, flavanols and flavonol glucosides (Boussenna et al., 2016). These findings indicate the complexity of the regulation of TNF-α in murine models. As reported in other studies, diets of anthocyanin-rich powders such as Goji berry (Y. Kang et al., 2017), Maqui berry (Zhou et al., 2019), Aronia berry (S. Kang et al., 2017)and probiotics such as *Lactobacillus acidophilus* (Hu et al., 2020), were potent in reversing DSS-induced cytokine up-regulation. Feeding of black rice anthocyanin extracts along with rosmarinic acid in a dose of 0.5 mg/mouse/day to 1.0 mg/mouse/day was effective in reducing the DSS-induced

elevation of serum TNF-α and IL-1β cytokine expression in C57BL/6 mice (L. Zhao et al., 2018). Further, the doses of 1.0 mg/mouse/day and 2 mg/mouse/day of black rice anthocyanin and rosmarinic acid reduced the serum IL-6 levels. To elaborate further, oral administration of crude anthocyanin extracts of Aronia berry (2 mg/mouse/day) reduced the serum levels of TNF-α and IL-6 levels in C57BL/6 mice (S. H. Kang et al., 2017). Previously reported studies have used crude extracts of anthocyanin which consisted of many other polyphenol fractions and not solely anthocyanin. Therefore, solely the anthocyanin-rich fractions may not be effective as same as the whole berry powder in the prevention of DSS-induced acute colitis. Moreover, the amount of anthocyanin and the mode of anthocyanin administration also influence its effectiveness in attenuation of colitis. As an example, vacuum-dried ethanol extraction of mulberry anthocyanin in a dose of 4 mg/mouse/day (was more effective than 2 mg/mouse/day) administered via oral gavage for 14 days reduced the severity of DSS-induced colitis in C57BL/6 mice in the terms of reversing the colonic levels of cytokines; TNF-α, IL-6 and IL-1β (Mo et al., 2022). Moreover, oral gavage allows for more precise volume and dose delivery and faster peak absorption of unstable or unpalatable compounds, as compared with delivery in feed (Gad, 2006). In agreement with these findings, intraperitoneal injection of C3G, in a dose of 1 ug/mouse for every two days, a total of three times also improved the DSS-induced cytokine expressions in C57BL/6 mice (Xia et al., 2019). The oral administration of blueberry anthocyanin (40 mg/kg) dissolved in 100 μL of physiological saline also inhibited the TNBS-induced experimental colitis in C57BL/6 mice (Yu et al., 2011). Taken together, these findings confirmed that the composition, dose, and mode of the delivery method of anthocyanin is crucial for its pronounced anti-inflammatory effects and further

optimizations are needed. Moreover, gut microbiota affects host immune response and can induce an imbalance in cytokine levels in which the TNF-α production capacity appears to be more strongly influenced by the microbiome, whereas other cytokines such as IL-1β and IL-6 exhibit fewer, but more specific, associations with the gut microbiota (Schirmer et al., 2016). Consistent with that, the mice with intact gut microbiota and gut microbiota ablated mice (using antibiotics) showed differences in colonic cytokine levels upon DSS administration followed by purple/red fleshed potato supplementary diets (Wang, 2019). The colonic TNF-α levels were not altered in intact gut microbiome mice and no effect of potato diets was observed, whereas, TNF-α levels were drastically increased with DSS administration in gut microbiota ablated mice and red fleshed potato diets down-regulated the expression. In contrast to that, purple or red potato supplementations ameliorated DSS-induced up-regulation of colonic IL-6 and IL-1β levels in mice with the intact gut microbiome, but not in gut microbiota ablated mice (Li et al., 2021).

The colon epithelium maintains its selective permeabilities by limiting the passage of pathogenic bacteria and/or their toxic metabolites, chemical toxins, and antigens and permitting the absorption of nutrients, electrolytes and water (Groschwitz & Hogan, 2009). The TJs, typically located at the apical side, play a vital role in contributing to the sealing of paracellular spaces of epithelium and consist of at least 40 different proteins including claudins and occludin (Kosińska & Andlauer, 2013). However, there are inconsistencies in the reported literature on DSS-induced TJ expression. The colitis induced by 2.5% DSS in Balb/c mice down-regulated the colonic occludin and claudin-4 expressions; with inducing no change in claudin-2 and claudin-3 expressions (Mennigen et al., 2009). Similar results were observed by Mo et al. (2022) for occludin, whereas the claudin-3 was down-regulated

in C57BL/6J mice. In contrast, another study claimed to observe increased levels of claudin-2, occludin and decreased levels of claudin-3 in 2.5% of DSS-treated C57BL/6J mice (Bibi et al., 2018). In a study that investigated on anti-inflammatory effect of Goji berry, the administration of 3% DSS on C57BL/6 mice resulted in increased levels of colonic claudin-2 expression (Y. Kang et al., 2017). Partially agree with the above findings, a study conducted by Čužić et al. (2021) indicated a higher elevation in claudin-4 and reduction in claudin-2 and claudin-3 expressions in C57BL mice colonic tissues once administered with 3% DSS. Taking it together, it is clearly visible that DSS-induced changes in TJ expression are varied upon the dose of DSS and even in the same mouse strain. To date, the exact mechanism by which DSS causes colitis and loss in TJ proteins is poorly identified. Considering the functionality of claudins, claudin-2 is recognized as a pore-forming protein whereas claudin-3 and claudin-4 are involved in the pore-sealing process (Khan & Asif, 2015). In this context, overexpression of claudin-2 should result in increasing intercellular permeability and leakiness while overexpression of claudin-3 and 4 enhances the paracellular barrier and reduces intercellular permeability. In agreement with that, colon biopsies taken from active UC patients exhibited, a significant downregulation of pore-sealing claudin-4, upregulation of pore-forming claudin-2 (Das et al., 2012; Oshima et al., 2008), and no change in claudin-3 expressions (Oshima et al., 2008). In addition to that, an analysis of colonic biopsies of UC patients revealed over-expression levels of occludin in the active colitis stage (Yamamoto-Furusho et al., 2012). The dysfunction of TJ proteins, therefore, can cause colitis by weakening the intercellular adhesion and by promoting intestinal permeability for pathogenic bacteria (Oh-oka et al., 2014). Thus, to investigate the effect of AHF and probiotics on DSS-induced epithelial TJ

protein expressions, mice colon tissues were analyzed using western blot analysis. As observed DSS or supplementary diets were failed to induce significant difference in occludin and claudin-2, 3 and 4 expressions. Conversely, Bibi et al. (2018), evaluated the intestinal barrier protective activity of anthocyanins from red raspberries and reported that the red raspberries supplementation observably suppressed the elevation of claudin-2 protein and enhanced the expression of claudin-3 and occludin under DSS treatment. Similarly, in a recent study, oral gavage of mulberry anthocyanin (4 mg/mouse for 14 days) reversed the DSS-induced down-regulation of the expression of occludin and claudin-3 in mice colon tissues (Mo et al., 2022). Further, the dose of 2 mg/mouse was not effective in restoring the changes. The VSL#3 (15 mg) containing 2.7 billion freeze-dried bacteria (*Streptococcus thermophilus, Bifidobacterium longum, B. breve, B. infantis, Lactobacillus acidophilus, L. plantarum, L. casei, L. bulgaricus*) and corn starch administered via gastric tube improved the DSS-induced reduction in occludin and claudin-4 but not the claudin-2 and claudin-3 expressions (Mennigen et al., 2009). Once the DSS treatment is stopped, colons can be regenerated as inflammation resolution/epithelial repair occurred (Vidal-Lletjós et al., 2019). Hence, DSS-induced colonic epithelial changes are restored. In the present study, mice were sacrificed on the 6th day DSS was arrested. As the literature suggested, the maximum severity of DSS-induced colitis was observed 2 days after the DSS termination and colon inflammation was still evident 5 days after DSS consumption arrest (Vidal-Lletjós et al., 2019). However, as such, any effect of DSS on TJs could not be due to the ongoing colonic regeneration that occurred after the end of DSS.

The DSS-induced colitis also changed the morphological structure of the colon tissue which was evident by the histopathological observations. Results of H&E staining

of colon tissue revealed that the epithelial cells of the control group were normal as expected. The crypt structure was regular and with no spaces, damages, or hyperplasia. Further, a control group of mice colon tissues were found with no ulcers/inflammatory lesions, submucosal edema, or leukocyte infiltration. However, the colonic tissues of mice in the experimental model group, which significantly differed from the control group, showed the typical architecture of severe inflammation, which was indicated by massive loss of crypts, crypt hyperplasia, large inflammatory lesions/ulcers in the submucosa, lack of surface epithelium, obvious leukocyte infiltration and submucosal edema. Similar tissue architectures were reported for DSS-induced colonic destruction (Bibi et al., 2018; S. H. Kang et al., 2017; Mo et al., 2022; Zhou et al., 2019). As expected, the diets of free AHF and free AHF + probiotics mitigated the severity of inflammation in DSS-treated mice. Similarly, mulberry anthocyanin extracts (Mo et al., 2022), purple carrot (Kim et al., 2018), black rice anthocyanin (L. Zhao et al., 2018) and *L. plantarum* AR113 alleviated the histological symptoms of inflammation of colon in DSS-induced mice. Moreover, the histology score of the present study was negatively correlated with colon length and colon weight, indicating that mice fed with free AHF + probiotics and free AHF tended to have higher colon length and lower histology score or lower disease severity with respect to the experimental model. On the other hand, the same feeding groups exhibited the least DAI and histology score with respect to other dietary groups and the experimental model group. As indicated, colonic cytokine levels (IL-6, TNF-α and, IL-1β) were increased with histology score providing a moderately positive relationship. The levels of cytokines, in all dietary supplementary groups, tended to have less disease severity than that of the experimental model.

The mice's fecal microbial composition was analyzed using 16S rRNA sequencing technology followed by calculations of four major ecological parameters, including Pielou's evenness (to show how evenly the individuals in the community are distributed over different operational taxonomic units), faith phylogenetic diversity (pd, the abundance of microbial population and includes the abundance of rare species), observed features (richness of the microbial community) and Shannon index (the combined parameter of richness and evenness) as to explore the alpha diversity (Rodríguez-Nogales et al., 2017; Wu et al., 2020). The higher the alpha diversity index, the more complex the diversity of the sample (Wu et al., 2020). The results of the present study showed that the treatment with 3% DSS resulted in a decrease in the species' alpha diversity. However, faith pd, observed features and Shannon index values of mice fed with a probiotics diet appeared similar to that of the control group, whereas free AHF + probiotics and probiotics groups resembled Pielou's evenness in the control group. In agreement with the findings of the present study, previous studies also demonstrated the effect of probiotics on restoring microbial alpha diversity. The diet of *L. fermentum* successfully improved the microbial richness, evenness, and diversity in 3% DSS-treated male C57BL/6J mice (Rodríguez-Nogales et al., 2017). In another study that examined the effect of polyphenol-rich grapes, Azoxymethane + DSS treatment significantly reduced the gut microbial richness and evenness as indicated by the Shannon index and 10% grape polyphenols improved the Shannon index and Pielou's evenness of male Balb/c mice but failed to improve the observed features and faith PD indexes (Wu et al., 2020). As per the results obtained in the present study, encapsulated AHF was not efficient as free AHF in the prevention of DSS-induced colitis. As reported by Miles et al. (2017), the DSS-induced disease severity was

worsened by adding inulin (200 g/kg of diet) to a compositionally defined diet in C57BL/6 mice. The mice fed with diets of inulin exhibited greater splenomegaly which is associated with severe systematic inflammation, obvious gross rectal bleeding and severe gut inflammation as observed in the histopathologic analysis. However, the exact mechanism by which inulin elevates the DSS-induced inflammation is unknown. Seven days of pre-treatment with inulin also failed to improve the DSS (3%)-induced colitis in C57Bl/6 mice (Nadolski et al., 2020). As reported, inulin pre-treated, DSS-exposed mice were positive for blood in the stool a day sooner than mice given DSS only and the disease activity index, colon length, colon weight and histological score were similar in inulin-treated mice and non-inulin-treated colitis mice. Contrarily, there are supportive studies on the anti-inflammatory effects of inulin as well. The Swiss albino mice received 2.5% of DSS and 1% (w/v) inulin in their drinking water for 7 days and showed improved DSS-induced colitis symptoms by reducing the NO production (Ryma et al., 2014). In the current findings, the inulin-induced elevation of colitis was not observed. Therefore, the role of inulin in DSS-induced colitis is yet to be explored. The reason for not observing a significant impact of dietary supplementation could be due to the smaller sample size used; however, the number of animals used in the study was selected adhering to the 3R rule; replacement, reduction and refinement. Further, the mouse models even differed from one another in their responses to inflammatory conditions and recovery status (Akhtar, 2015). Taking together, free AHF and free AHF + probiotics diets mitigated the severity of DSS-induced acute colitis in Balb/C mice as demonstrated by improving the colon length, reducing the DAI and, downregulating the TNF-α and IL-6 expressions. The AHF is rich in C3G, which has has intensively been studied for its anti-inflammatory properties. In

general, C3G metabolizes in the stomach followed by hydrolyzation happens in the small intestine, specifically in the ileum (Cheng et al., 2021). The phenolic acid metabolites produced during this process are mainly protocatechuate (PCA) and phloroglucinaldehyde (PGA). Under the regulation of gut microbiota, PCA and PGA further metabolized into microbial metabolites such as vanillic acid and ferulic acid (Cheng et al., 2021). Even more than 20 kinds of C3G metabolites have been identified, mainly PCA, vanillic acid and ferulic acid and their derivatives are considered the potential bioactive metabolites against inflammation (Amin et al., 2015). As well, PCA has been reported to inhibit the production of inflammatory mediators, such as IL-6, TNF-α, IL-1β, and prostaglandin E2 (PGE2), potentially by suppressing the activation of NF-κB and extracellular signal-regulated kinase (ERK) in murine BV2 microglia cells and colitis-model mice (Tan et al., 2019). The vanillic acid can also inhibit the production of pro-inflammatory cytokines such as TNF-α, IL-6, IL-1β, and IL-33 by down-regulating caspase-1 and NF-κB pathways (Calixto-Campos et al., 2015). In addition to that, a clinical study revealed that ferulic acid administration ameliorated inflammation, concomitantly reduced plasma TNF-α and IL-6, and increased IL-10 levels in human subjects (Katcher et al., 2008). The anti-inflammatory effects of probiotics have been also explored. The exact mechanism of how probiotics exert anti-inflammation is yet to be understood. However, as reported in many studies, probiotics are potent in reducing inflammation by producing the immunoregulatory factors, that directly suppress the pro-inflammatory cytokines, by promoting the proliferation of regulatory T lymphocytes, resulting in cell contact-dependent immunoregulation and the secretion of anti-inflammatory cytokines and also by modulating gut microbiota (Versalovic et al., 2008). As demonstrated in the present study, the combination of free

AHF and probiotics improved the DSS-induced colitis more than the probiotic alone group. In addition to that, microencapsulated AHF was not effective in reducing the colitis severity in experimental mice. However, the underlying mechanism of the free AHF and free AHF + probiotics in the prevention of DSS-induced colitis is yet to be understood.

# CHAPTER 06: CONCLUSION

## 6.1 Research Summary

Despite the advanced medical treatments, ulcerative colitis or the chronic inflammatory disease affecting the colon is rising worldwide. The pathogenesis is multifactorial, involving genetic predisposition, epithelial barrier defects, dysregulated immune responses, and environmental factors (Ungaro et al., 2017). The colonic inflammatory condition is a major risk factor for colitis-associated colon cancer (CAC). Therefore, by regulating colonic inflammation, the prevalence of CAC can be controlled. There is an increasing interest in anti-cancer and anti-inflammatory polyphenols derived from plant-food due to their known safety. However, their low bioavailability in human body, makes it difficult to utilize them as functional foods or nutraceuticals. In order to facilitate bioavailability and target delivery, phytochemicals can be encapsulated with non-digestible polymers. Upon reaching the colon, via the action of gut microbiota, the encapsulated matrix will be disintegrated, and active compounds are released to be absorbed. Based on this phenomenon, the present study used maltodextrin and inulin (wall materials, 3:1 ratio) to encapsulate the anthocyanin-rich fraction extracted from haskap berry (AHF). The wall materials to AHF ratio was selected as 1:1.5 after considering a few analysis parameters, such as having a lower moisture %, higher solubility, average particle size, higher encapsulation efficiency, encapsulation recovery and encapsulation retention. The AHF microparticles were observed with broken glass structures with sharp edges and inconsistent shapes. The cyanidin-3-rutionoside, cyanidin-3-glucoside, cyanidin-3,5-diglucoside and peonidin-3glucoside were the main anthocyanins found in AHF microparticles. Assessment of the preventive potential of free and encapsulated AHF

microparticles with or without combining with probiotics, the DSS-induced acute colitis model was used. The mice received 3% of DSS in drinking water for seven days and were given supplementary diets throughout the experimental period. The mice fed on free AHF and free AHF+ probiotics were observed with significantly longer colons than the experimental model group. Moreover, supplementation of free AHF and free AHF + probiotics mitigated the severity of DSS-induced colitis in terms of producing the least DAI index which was calculated using body weight loss, stool consistency and occult blood. In addition to that, the same supplementary diets of free AHF and free AHF + probiotics were able to reduce the serum levels of pro-inflammatory cytokines TNF-α and IL-1β. Specifically, mice fed on probiotics alone showed with a trend of improvement in TJ protein expression in colonic tissues which was analyzed using western blotting. The supplementary diets were potent in attenuating the DSS-induced histopathological changes in mice colon tissues. The colonic ulceration, neutrophil infiltration, crypt damage, crypt loss, crypt hyperplasia and edema were lessened in mice fed with free AHF and free AHF + probiotics diets. Interestingly, the diets of AHF and AHF + probiotics improved the alpha-diversity index of mice fecal microbiota as well. However, encapsulated AHF microparticles were not effective in attenuating the DSS-induced colonic inflammation as hypothesized. Taken together, considering the in vivo findings of this study, it can be concluded that free AHF and free AHF + probiotics attenuate the DSS-induced colitis in mice, thus need further investigations.

## 6.2 Future recommendations

The current study targeted to investigate the free and encapsulated AHF microparticles and probiotics in the prevention of DSS-induced acute colitis. It was found that AHF microparticles produced, using maltodextrin and inulin as wall materials were not effective as free AHF in DSS-induced colitis prevention. As reported in the latest studies, inulin might have caused the facilitation of colitis in the mice fed with AHF microparticles. Hence, there is a need to re-evaluate the anti-inflammatory potential of AHF microparticles which can be produced with alternative wall materials such as chitosan, pectin, and guar gum. The dextrose equivalent of maltodextrin also needs to be taken into consideration. The in vitro simulatory gastrointestinal digestion can be performed to investigate the in vitro bio-accessibility of the AHF microparticles which can be used to measure the amount of bioactive materials that reach the colon. Further studies should be included to investigate the anti-inflammatory properties of the synbiotic mixture (free AHF + probiotics) in in vitro models. Considering the in vivo experiment, providing supplementary diets by oral gavage would have produced more pronounced effects. The immunohistochemistry analysis of tight junction proteins, anti- and pro-apoptotic proteins and colonic cytokine would help to confirm the results of western blot analysis. When proceeding with the fecal microbiome analysis, analyzing the fecal microbiome before the DSS administration would provide more insights into how the microflora was altered. In addition to that, sacrificing the mice need to be done soon after the DSS is terminated.

# REFERENCES


Abascal, K., Ganora, L., & Yarnell, E. (2005). The effect of freeze-drying and its implications for botanical medicine: a review. *Phytotherapy Research*, *19*(8), 655–660. https://doi.org/10.1002/PTR.1651

Adachi, T., Eguchi, S., & Muto, Y. (2022). Pathophysiology and pathology of acute cholecystitis: A secondary publication of the Japanese version from 1992. *Journal of Hepato-Biliary-Pancreatic Sciences*, *29*(2), 212–216. https://doi.org/10.1002/JHBP.912

Afonso, P. V, Janka-Junttila, M., Lee, Y. J., Mccann, C. P., Oliver, C. M., Aamer, K. A., Losert, W., Cicerone, M. T., & Parent, C. A. (2012). Article LTB 4 is a signal-relay molecule during neutrophil chemotaxis. *Developmental Cell*, *22*, 1079–1091. https://doi.org/10.1016/j.devcel.2012.02.003

Akdeniz, B., Sumnu, G., & Sahin, S. (2017). The effects of maltodextrin and gum Arabic on encapsulation of onion skin phenolic compounds. *Chemical Engineering Transactions*, *57*, 1891–1896. https://doi.org/10.3303/CET1757316

Akhavan Mahdavi, S., Jafari, S. M., Assadpoor, E., & Dehnad, D. (2016). Microencapsulation optimization of natural anthocyanins with maltodextrin, gum Arabic and gelatin. *International Journal of Biological Macromolecules*, *85*, 379–385. https://doi.org/10.1016/j.ijbiomac.2016.01.011

Akram, W., & Garud, N. (2020). Optimization of inulin production process parameters using response surface methodology. *Future Journal of Pharmaceutical Sciences 2020 6:1*, *6*(1), 1–9. https://doi.org/10.1186/S43094-020-00087-1

Akram, W., Garud, N., & Joshi, R. (2019). Role of inulin as prebiotics on inflammatory bowel disease. *Drug Discoveries & Therapeutics*, *13*(1), 1–8. https://doi.org/10.5582/DDT.2019.01000

Al-Nuaimi, A. A. H. D. (2018). Extracts of plants used as traditional medicines have toxic effect on the liver and kidney. *MOJ Anatomy & Physiology*, *5*(2). https://doi.org/10.15406/mojap.2018.05.00161

Amir Mortazavian, Seyed Hadi Razavi, Mohammad Reza Ehsani, S. S. (2007). Principles and methods of microencapsulation of probiotic microorganisms. *Iranian Journal of Biotechnology*, *5*(1), 1–18. http://www.ijbiotech.com/article_7032.html

Anderson, S. J., Lockhart, J. S., Estaki, M., Quin, C., Hirota, S. A., Alston, L., Buret, A. G., Hancock, T. M., Petri, B., Gibson, D. L., & Morck, D. W. (2019). Effects of azithromycin on behavior, pathologic signs, and changes in cytokines, chemokines, and neutrophil migration in C57BL/6 mice exposed to dextran sulfate sodium. *Comparative Medicine*, *69*(1), 4. https://doi.org/10.30802/AALAS-CM-18-000001

Antigo, J. L. D., Silva, J. M. da, Bergamasco, R. de C., & Madrona, G. S. (2020). Microencapsulation of beet dye (Beta vulgaris L.) using maltodextrin and xanthan gum as encapsulant agents and application in yogurt. *Research, Society and Development*, *9*(12), e14091210896–e14091210896. https://doi.org/10.33448/RSD-V9I12.10896

Antoniou, E., Margonis, G. A., Angelou, A., Pikouli, A., Argiri, P., Karavokyros, I., Papalois, A., & Pikoulis, E. (2016). The TNBS-induced colitis animal model: An overview. *Annals of Medicine and Surgery,* 11, 9–15. https://doi.org/10.1016/j.amsu.2016.07.019

AOAC International. (2006). AOAC Official Method 2005.02 Total monomeric anthocyanin pigment content of fruit juices, beverages, natural colorants, and wines pH differential method. *Official Methods of Analysis of AOAC International* 37–39. https://www.researchgate.net/publication/260264533

Arend, W. P., Palmer, G., & Gabay, C. (2008). IL-1, IL-18, and IL-33 families of cytokines. *Immunological Reviews*, *223*(1), 20–38. https://doi.org/10.1111/J.1600-065X.2008.00624.X

Arulselvan, P., Fard, M. T., Tan, W. S., Gothai, S., Fakurazi, S., Norhaizan, M. E., & Kumar, S. S. (2016). Role of antioxidants and natural products ininflammation. *Oxidative Medicine and Cellular Longevity*, 2016. https://doi.org/10.1155/2016/5276130

Azimi, T., Nasiri, M. J., Chirani, A. S., Pouriran, R., & Dabiri, H. (2018). The role of bacteria in the inflammatory bowel disease development: a narrative review. *APMIS : Acta Pathologica, Microbiologica, et Immunologica Scandinavica*, *126*(4), 275–283. https://doi.org/10.1111/APM.12814

Baeza, R., Sánchez, V., Salierno, G., Molinari, F., López, P., & Chirife, J. (2021). Storage stability of anthocyanins in freeze-dried elderberry pulp using low proportions of encapsulating agents. *Food Science and Technology International*, *27*(2), 135–144. https://doi.org/10.1177/1082013220937867

Bai, A. P., & Ouyang, Q. (2006). Probiotics and inflammatory bowel diseases. In *Postgraduate Medical Journal* 82(968), 376–382. https://doi.org/10.1136/pgmj.2005.040899

Bakowska-Barczak, A. M., & Kolodziejczyk, P. P. (2011). Black currant polyphenols: Their storage stability and microencapsulation. *Industrial Crops and Products*, *34*(2), 1301–1309. https://doi.org/10.1016/J.INDCROP.2010.10.002

Bannenberg, G. L., Chiang, N., Ariel, A., Arita, M., Tjonahen, E., Gotlinger, K. H., Hong, S., & Serhan, C. N. (2005). Molecular circuits of resolution: formation and actions of resolvins and protectins. *Journal of Immunology, 174*(7), 4345–4355. https://doi.org/10.4049/JIMMUNOL.174.7.4345

Barclay, T., Ginic-Markovic, M., Cooper, P., & Petrovsky, N. (2010). Inulin - A versatile polysaccharide with multiple pharmaceutical and food chemical uses. *Journal of Excipients and Food Chemicals*, *1*(3), 27–50. https://jefc.scholasticahq.com/article/1132-inulin-a-versatile-polysaccharide-with-multiple-pharmaceutical-and-food-chemical-uses

Barros, V. J. da S., Severo, J. S., Mendes, P. H. M., da Silva, A. C. A., de Oliveira, K. B. V., Parente, J. M. L., Lima, M. M., Neto, E. M. M., Aguiar dos Santos, A., & Tolentino, M. (2021). Effect of dietary interventions on inflammatory biomarkers of inflammatory bowel diseases: A systematic review of clinical trials. In *Nutrition*, 91–92. https://doi.org/10.1016/j.nut.2021.111457

Basar, A. O., Prieto, C., & Lagarón, J. M. (2021). Novel encapsulation of bioactives: use of electrohydrodynamic processing and applications. Importance & applications of nanotechnology. In importance & applications of nanotechnology (Vol. 6). http://meddocsonline.org

Bell, L., & Williams, C. M. (2018). A pilot dose–response study of the acute effects of haskap berry extract (Lonicera caerulea L.) on cognition, mood, and blood pressure in older adults. *European Journal of Nutrition*, *58*, 3325–3334. https://doi.org/10.1007/s00394-018-1877-9

Benly, P. (2015). Role of histamine in acute inflammation. *Journal of Pharmaceutical Sciences and Research*, *7*(6), 373–376.

Bermudez-Brito, M., Plaza-Díaz, J., Muñoz-Quezada, S., Gómez-Llorente, C., & Gil, A. (2012). *Annals of Nutrition and Metabolism*, *61*(2), 160–174. https://doi.org/10.1159/000342079

Beyak, M., & Vanner, S. (1995). Histamine H1 and H3 vasodilator mechanisms in the guinea pig ileum. *Gastroenterology*, *108*(3), 712–718. https://doi.org/10.1016/0016-5085(95)90443-3

Biton, I. E., Stettner, N., Brener, O., Erez, A., Harmelin, A., & Garbow, J. R. (2018). Assessing mucosal inflammation in a DSS-Induced colitis mouse model by MR colonography. *Tomography (Ann Arbor, Mich.)*, *4*(1), 4–13. https://doi.org/10.18383/j.tom.2017.00021

Blasco, N. S., Latorre, V. L., Gasca, T. R., & Arenas, A. F. (2022). Gastritis. *Medicine (Spain)*, *13*(2), 74–81. https://doi.org/10.1016/j.med.2020.01.012

Boismenu, R., & Chen, Y. (2000). Insights from mouse models of colitis. *Journal of Leukocyte Biology*, *67*(3), 267–278. https://doi.org/10.1002/JLB.67.3.267

Bors, B. (2009). Breeding of lonicera caerulea l. For saskatchewan and Canada. *Proceedings of the 1st Virtual International Scientific Conference on Lonicera Caerulea L.; Saskatoon, SK, Canada*, 88–98. https://www.eutopiamall.com/images/MD/1566827/BREEDING OF LONICERA CAERULEA L_.pdf

Boyano-Orozco, L., Gallardo-Velázquez, T., Meza-Márquez, O. G., & Osorio-Revilla, G. (2020). Microencapsulation of rambutan peel extract by spray drying. *Foods*, *9*(7). https://doi.org/10.3390/foods9070899

Braga, A. R. C., Mesquita, L. M. de S., Martins, P. L. G., Habu, S., & de Rosso, V. V. (2018). Lactobacillus fermentation of jussara pulp leads to the enzymatic conversion of anthocyanins increasing antioxidant activity. *Journal of Food Composition and Analysis*, *69*, 162–170. https://doi.org/10.1016/J.JFCA.2017.12.030

Bramhall, M., Florez-Vargas, O., Stevens, R., Brass, A., & Cruickshank, S. (2015). Quality of methods reporting in animal models of colitis. *Inflammatory Bowel Diseases*, *21*(6), 1248–1259. https://doi.org/10.1097/MIB.0000000000000369

Brenna, Ø., Furnes, M. W., Drozdov, I., van Beelen Granlund, A., Flatberg, A., Sandvik, A. K., Zwiggelaar, R. T. M., Mårvik, R., Nordrum, I. S., Kidd, M., & Gustafsson, B. I. (2013). Relevance of TNBS-Colitis in rats: A methodological study with endoscopic, historical and transcripttomic characterization and correlation to IBD. *PLoS ONE*, *8*(1). https://doi.org/10.1371/journal.pone.0054543

Brennan, J. J., & Gilmore, T. D. (2018). Evolutionary origins of Toll-like reeceptor signaling. *Molecular Biology and Evolution*, *35*(7), 1576–1587. https://doi.org/10.1093/MOLBEV/MSY050

Brock, C., Nielsen, L. M., Lelic, D., & Drewes, A. M. (2013). Pathophysiology of chronic pancreatitis. *World Journal of Gastroenterology : WJG*, *19*(42), 7231. https://doi.org/10.3748/WJG.V19.I42.7231

Caporaso, J. G., Kuczynski, J., Stombaugh, J., Bittinger, K., Bushman, F. D., Costello, E. K., Fierer, N., Pẽa, A. G., Goodrich, J. K., Gordon, J. I., Huttley, G. A., Kelley, S. T., Knights, D., Koenig, J. E., Ley, R. E., Lozupone, C. A., McDonald, D., Muegge, B. D., Pirrung, M., … Knight, R. (2010). QIIME allows analysis of high-throughput community sequencing data. *Nature Methods*, *7*(5), 335. https://doi.org/10.1038/NMETH.F.303

Caroline Ferrari, C., Pimentel Marconi Germer, S., Dutra Alvim, I., & Maurício de Aguirre, J. (2013). Storage stability of spray-dried blackberry powder produced with maltodextrin or gum arabic. *Drying Technology*, *31*(4), 470–478. https://doi.org/10.1080/07373937.2012.742103

Carpena, M., Garcia-Oliveira, P., Lourenço-Lopes, C., Pereira, A. G., Fraga-Corral, M., Prieto, M. A., & Simal-Gandara, J. (2021). Freeze-drying encapsulation as a mechanism of choice in oils: methods and mechanism. *Basic Protocols in Encapsulation of Food Ingredients*, 91–101. Humana, New York, NY. https://doi.org/10.1007/978-1-0716-1649-9_9

Castaneda, D., Gonzalez, A. J., Alomari, M., Tandon, K., & Zervos, X. B. (2021). From hepatitis A to E: A critical review of viral hepatitis. *World Journal of Gastroenterology*, *27*(16), 1691. https://doi.org/10.3748/WJG.V27.I16.1691

Celli, G. B., Ghanem, A., & Brooks, M. S. L. (2014). Haskap Berries (Lonicera caerulea L.)-a critical review of antioxidant capacity and health-related studies for potential value-added products. *Food and Bioprocess Technology*, *7*(6), 1541–1554. https://doi.org/10.1007/S11947-014-1301-2/TABLES/5

Celli, G. B., Ghanem, A., & Brooks, M. S. L. (2015). Optimization of ultrasound-assisted extraction of anthocyanins from haskap berries (Lonicera caerulea L.) using Response Surface Methodology. *Ultrasonics Sonochemistry*, *27*, 449–455. https://doi.org/10.1016/j.ultsonch.2015.06.014

Chai, J., Jiang, P., Wang, P., Jiang, Y., Li, D., Bao, W., Liu, B., Liu, B., Zhao, L., Norde, W., Yuan, Q., Ren, F., & Li, Y. (2018). The intelligent delivery systems for bioactive compounds in foods: Physicochemical and physiological conditions, absorption mechanisms, obstacles and responsive strategies. *Trends in Food Science and Technology*, 78, 144–154. https://doi.org/10.1016/j.tifs.2018.06.003

Charpentier, C., Marion-Letellier, R., Savoye, G., Nicol, L., Mulder, P., Aziz, M., Vera, P., Déchelotte, P., & Savoye-Collet, C. (2012). Magnetic resonance colonography in rats with TNBS-induced colitis: A feasibility and validation study. *Inflammatory Bowel Diseases*, *18*(10), 1940–1949. https://doi.org/10.1002/ibd.22897

Chassaing, B., Aitken, J. D., Malleshappa, M., & Vijay-Kumar, M. (2014). Dextran sulfate sodium (DSS)-induced colitis in mice. *Current Protocols in Immunology*, *104*. https://doi.org/10.1002/0471142735.im1525s104

Che Man, Y. B., Irwandi, J., & Abdullah, W. J. W. (1999). Effect of different types of maltodextrin and drying methods on physico-chemical and sensory properties of encapsulated durian flavour. *Journal of the Science of Food and Agriculture*, *79*(8), 1075–1080. https://doi.org/10.1002/(SICI)1097-0010(199906)79:8<1075::AID-JSFA329>3.0.CO;2-Q

Chen, K., Pittman, R. N., & Popel, A. S. (2008). Nitric Oxide in the vasculature: Where does it come from and where does it go? A Quantitative Perspective. *Antioxidants & Redox Signaling*, *10*(7), 1185. https://doi.org/10.1089/ARS.2007.1959

Chen, L., Deng, H., Cui, H., Fang, J., Zuo, Z., Deng, J., Li, Y., Wang, X., & Zhao, L. (2018). Inflammatory responses and inflammation-associated diseases in organs. *Oncotarget*, *9*(6), 7204. https://doi.org/10.18632/ONCOTARGET.23208

Chen, L. L., Wang, X. H., Cui, Y., Lian, G. H., Zhang, J., Ouyang, C. H., & Lu, F. G. (2009). Therapeutic effects of four strains of probiotics on experimental colitis in mice. *World Journal of Gastroenterology, 15*(3), 321. https://doi.org/10.3748/WJG.15.321

Chen, L., Lv, F., & Pei, L. (2014). Annexin 1: A glucocorticoid-inducible protein that modulates inflammatory pain. *European Journal of Pain*, *18*(3), 338–347. https://doi.org/10.1002/J.1532-2149.2013.00373.X

Chen, Y., Li, Q., Zhao, T., Zhang, Z., Mao, G., Feng, W., Wu, X., & Yang, L. (2017). Biotransformation and metabolism of three mulberry anthocyanin monomers by rat gut microflora. *Food Chemistry*, *237*, 887–894. https://doi.org/10.1016/j.foodchem.2017.06.054

Cheng, Z., Lin, J., Gao, N., Sun, X., Meng, X., Liu, R., Liu, Y., Wang, W., Li, B., & Wang, Y. (2020). Blueberry malvidin-3-galactoside modulated gut microbial dysbiosis and microbial TCA cycle KEGG pathway disrupted in a liver cancer model induced by HepG2 cells. *Food Science and Human Wellness*, *9*(3), 245–255. https://doi.org/10.1016/J.FSHW.2020.04.006

Choy, M. C., Visvanathan, K., & De Cruz, P. (2017). An overview of the innate and adaptive immune system in inflammatory bowel disease. *Inflammatory Bowel Diseases*, *23*(1), 2–13. https://doi.org/10.1097/MIB.0000000000000955

Clemente, J. C., Ursell, L. K., Parfrey, L. W., & Knight, R. (2012). The impact of the gut microbiota on human health: an integrative view. *Cell*, *148*(6), 1258–1270. https://doi.org/10.1016/J.CELL.2012.01.035

Cochran, K. E., Lamson, N. G., & Whitehead, K. A. (2020). Expanding the utility of the dextran sulfate sodium (DSS) mouse model to induce a clinically relevant loss of intestinal barrier function. *2020*(3). https://doi.org/10.7717/peerj.8681

Comeau, A. M., Douglas, G. M., & Langille, M. G. I. (2017). Microbiome helper: a custom and streamlined workflow for microbiome research. *MSystems*, *2*(1). https://doi.org/10.1128/msystems.00127-16

Cory, H., Passarelli, S., Szeto, J., Tamez, M., & Mattei, J. (2018). The role of polyphenols in human health and food systems: A mini-review. *Frontiers in Nutrition*, 5, 87. https://doi.org/10.3389/fnut.2018.00087

Costello, M. E., Ciccia, F., Willner, D., Warrington, N., Robinson, P. C., Gardiner, B., Marshall, M., Kenna, T. J., Triolo, G., & Brown, M. A. (2015). Brief report: Intestinal dysbiosis in ankylosing spondylitis. *Arthritis and Rheumatology*, *67*(3), 686–691. https://doi.org/10.1002/ART.38967/ABSTRACT

Coussens, L. M., & Werb, Z. (2002). Inflammation and cancer. *Nature*, *420*(6917), 860. https://doi.org/10.1038/NATURE01322

Craddock, J. C., Neale, E. P., Peoples, G. E., & Probst, Y. C. (2019). Vegetarian-based dietary patterns and their relation with inflammatory and immune biomarkers: A systematic review and meta-analysis. *Advances in Nutrition*, 10(3), 433–451.

Cremonini, E., Daveri, E., Mastaloudis, A., Adamo, A. M., Mills, D., Kalanetra, K., Hester, S. N., Wood, S. M., Fraga, C. G., & Oteiza, P. I. (2019). Anthocyanins protect the gastrointestinal tract from high fat diet-induced alterations in redox signaling, barrier integrity and dysbiosis. *Redox Biology*, *26*. 101269. https://doi.org/10.1016/j.redox.2019.101269

Cristofori, F., Dargenio, V. N., Dargenio, C., Miniello, V. L., Barone, M., & Francavilla, R. (2021). Anti-inflammatory and immunomodulatory effects of probiotics in gut inflammation: A door to the body. *Frontiers in Immunology*, *12*. 578386 https://doi.org/10.3389/fimmu.2021.578386

Czank, C., Cassidy, A., Zhang, Q., Morrison, D. J., Preston, T., Kroon, P. A., Botting, N. P., & Kay, C. D. (2013). Human metabolism and elimination of the anthocyanin, cyanidin-3-glucoside: a (13)C-tracer study. *The American Journal of Clinical Nutrition*, *97*(5), 995–1003. https://doi.org/10.3945/AJCN.112.049247

Daniel, C., Poiret, S., Goudercourt, D., Dennin, V., Leyer, G., & Pot, B. (2006). Selecting lactic acid bacteria for their safety and functionality by use of a mouse colitis model. *Applied and Environmental Microbiology*, *72*(9), 5799–5805. https://doi.org/10.1128/AEM.00109-06

de Vos, P., Faas, M. M., Spasojevic, M., & Sikkema, J. (2010). Encapsulation for preservation of functionality and targeted delivery of bioactive food components. *International Dairy Journal*, *20*(4), 292–302. https://doi.org/10.1016/J.IDAIRYJ.2009.11.008

Dharmawansa, K. V. S., Hoskin, D. W., & Rupasinghe, H. P. V (2020). Chemopreventive effect of dietary anthocyanins against gastrointestinal cancers: A review of recent advances and perspectives. *International Journal of Molecular Sciences* 21(18), 1–36. https://doi.org/10.3390/ijms21186555

Domitrovic, R. (2011). The molecular basis for the pharmacological activity of anthocyans. *Current Medicinal Chemistry*, *18*(29), 4454–4469. https://doi.org/10.2174/092986711797287601

Duan, L., Rao, X., & Sigdel, K. R. (2019). Regulation of inflammation in autoimmune disease. *Journal of Immunology Research*, *2019*. https://doi.org/10.1155/2019/7403796

Eichele, D. D., & Kharbanda, K. K. (2017a). Dextran sodium sulfate colitis murine model: An indispensable tool for advancing our understanding of inflammatory bowel diseases pathogenesis. In *World Journal of Gastroenterology* , 23(33), 6016–6029. https://doi.org/10.3748/wjg.v23.i33.6016

Eichele, D. D., & Kharbanda, K. K. (2017b). Dextran sodium sulfate colitis murine model: An indispensable tool for advancing our understanding of inflammatory bowel diseases pathogenesis. *World Journal of Gastroenterology*, *23*(33), 6016. https://doi.org/10.3748/WJG.V23.I33.6016

Elfar, M., Gaber, L. W., Sabek, O., Fischer, C. P., & Gaber, A. O. (2007). The inflammatory cascade in acute pancreatitis: relevance to clinical disease. *The Surgical Clinics of North America*, *87*(6), 1325–1340. https://doi.org/10.1016/J.SUC.2007.09.002

Ellulu, M. S., Patimah, I., Khaza'ai, H., Rahmat, A., & Abed, Y. (2017). Obesity and inflammation: the linking mechanism and the complications. *Archives of Medical Science : AMS*, *13*(4), 851. https://doi.org/10.5114/AOMS.2016.58928

Fang, J. (2014). Bioavailability of anthocyanins. *Drug Metabolism Reviews*, *46*(4), 508–520. https://doi.org/10.3109/03602532.2014.978080

Fang, Z., & Bhandari, B. (2010). Encapsulation of polyphenols – a review. *Trends in Food Science & Technology*, *21*(10), 510–523. https://doi.org/10.1016/J.TIFS.2010.08.003

Fang, Z., & Bhandari, B. (2011). Effect of spray drying and storage on the stability of bayberry polyphenols. *Food Chemistry*, *129*(3), 1139–1147. https://doi.org/10.1016/J.FOODCHEM.2011.05.093

Feehan, K. T., & Gilroy, D. W. (2019). Is resolution the end of inflammation? *Trends in Molecular Medicine* 25(3), 198–214. https://doi.org/10.1016/j.molmed.2019.01.006

Feghali, C. A., & Wright, T. M. (1997). Cytokines in acute and chronic inflammation. *Frontiers in bioscience : a journal and virtual library*, 2. https://doi.org/10.2741/a171

Felgines, C., Talavéra, S., Texier, O., Besson, C., Fogliano, V., Lamaison, J.-L., Fauci, L. la, Galvano, G., Rémésy, C., & Galvano, F. (2006). Absorption and metabolism of red orange juice anthocyanins in rats. *The British Journal of Nutrition*, *95*(5), 898–904. https://doi.org/10.1079/BJN20061728

Felgines, C., Texier, O., Besson, C., Vitaglione, P., Lamaison, J. L., Fogliano, V., Scalbert, A., Vanella, L., & Galvano, F. (2008). Influence of glucose on cyanidin 3-glucoside absorption in rats. *Molecular Nutrition & Food Research*, *52*(8), 959–964. https://doi.org/10.1002/MNFR.200700377

Fernandes, I., Faria, A., de Freitas, V., Calhau, C., & Mateus, N. (2015). Multiple-approach studies to assess anthocyanin bioavailability. *Phytochemistry Reviews 2015 14:6*, *14*(6), 899–919. https://doi.org/10.1007/S11101-015-9415-3

Ferrari, D., Speciale, A., Cristani, M., Fratantonio, D., Molonia, M. S., Ranaldi, G., Saija, A., & Cimino, F. (2016). Cyanidin-3-O-glucoside inhibits NF-kB signalling in intestinal epithelial cells exposed to TNF-α and exerts protective effects via Nrf2 pathway activation. *Toxicology Letters*, *264*, 51–58. https://doi.org/10.1016/j.toxlet.2016.10.014

Fidan-Yardimci, M., Akay, S., Sharifi, F., Sevimli-Gur, C., Ongen, G., & Yesil-Celiktas, O. (2019). A novel niosome formulation for encapsulation of anthocyanins and modelling intestinal transport. *Food Chemistry*, *293*, 57–65. https://doi.org/10.1016/j.foodchem.2019.04.086

Fish, E. N. (2008). The X-files in immunity: sex-based differences predispose immune responses. *Nature Reviews. Immunology*, *8*(9), 737–744. https://doi.org/10.1038/NRI2394

Fraga, C. G., Croft, K. D., Kennedy, D. O., & Tomás-Barberán, F. A. (2019). The effects of polyphenols and other bioactives on human health. *Food & Function*, *10*(2), 514–528. https://doi.org/10.1039/C8FO01997E

Fredes, C., Becerra, C., Parada, J., & Robert, P. (2018). The microencapsulation of maqui (Aristotelia chilensis (Mol.) Stuntz) juice by spray-drying and freeze-drying produces powders with similar anthocyanin stability and bioaccessibility. *Molecules*, *23*(5), 1227. https://doi.org/10.3390/molecules23051227

Garrood, T., Lee, L., & Pitzalis, C. (2006). Molecular mechanisms of cell recruitment to inflammatory sites: general and tissue-specific pathways. *Rheumatology*, *45*(3), 250–260. https://doi.org/10.1093/RHEUMATOLOGY/KEI207

Gbassi, G. K., & Vandamme, T. (2012). Probiotic encapsulation technology: from microencapsulation to release into the gut. *Pharmaceutics*, *4*(1), 149. https://doi.org/10.3390/PHARMACEUTICS4010149

Gharsallaoui, A., Roudaut, G., Chambin, O., Voilley, A., & Saurel, R. (2007). Applications of spray-drying in microencapsulation of food ingredients: An overview. *Food Research International*, *40*(9), 1107–1121. https://doi.org/10.1016/J.FOODRES.2007.07.004

Ghattamaneni, N. K., Sharma, A., Panchal, S. K., & Brown, L. (2020). Pelargonidin 3-glucoside-enriched strawberry attenuates symptoms of DSS-induced inflammatory bowel disease and diet-induced metabolic syndrome in rats. *European Journal of Nutrition*, *59*(7), 2905–2918. https://doi.org/10.1007/S00394-019-02130-1

Giusti, M. M., & Wrolstad, R. E. (2003). Acylated anthocyanins from edible sources and their applications in food systems. *Biochemical Engineering Journal*, *14*(3), 217–225. https://doi.org/10.1016/S1369-703X(02)00221-8

Golia, E., Limongelli, G., Natale, F., Fimiani, F., Maddaloni, V., Pariggiano, I., Bianchi, R., Crisci, M., D'Acierno, L., Giordano, R., Di Palma, G., Conte, M., Golino, P., Russo, M. G., Calabrò, R., & Calabrò, P. (2014). Inflammation and cardiovascular disease: From pathogenesis to therapeutic target. In *Current Atherosclerosis Reports*, 16(9), 435. https://doi.org/10.1007/s11883-014-0435-z

González, E., Gómez-Caravaca, A. M., Giménez, B., Cebrián, R., Maqueda, M., Parada, J., Martínez-Férez, A., Segura-Carretero, A., & Robert, P. (2020). Role of maltodextrin and inulin as encapsulating agents on the protection of oleuropein during in vitro gastrointestinal digestion. *Food Chemistry*, *310*(Apr), 125976. https://doi.org/10.1016/j.foodchem.2019.125976

Gouvêa, A. C. M. S., de Araujo, M. C. P., Schulz, D. F., Pacheco, S., Godoy, R. L. de O., & Cabral, L. M. C. (2012). Anthocyanins standards (cyanidin-3-O-glucoside and cyanidin-3-O-rutinoside) isolation from freeze-dried açaí (Euterpe oleraceae Mart.) by HPLC." Food Science and Technology, *32*(1), 43–46. https://doi.org/10.1590/S0101-20612012005000001

Goyal, N., Rana, A., Ahlawat, A., Bijjem, K. R. V., & Kumar, P. (2014). Animal models of inflammatory bowel disease: A review. *Inflammopharmacology*, 22(4), 219–233. https://doi.org/10.1007/s10787-014-0207-y

Gul, O., & Atalar, I. (2019). Different stress tolerance of spray and freeze dried Lactobacillus casei Shirota microcapsules with different encapsulating agents. *Food Science and Biotechnology*, *28*(3), 807. https://doi.org/10.1007/S10068-018-0507-X

Guo, H., Callaway, J. B., & Ting, J. P.-Y. (2015). Inflammasomes: mechanism of action, role in disease, and therapeutics. *Nature Medicine 2015 21:7*, *21*(7), 677–687. https://doi.org/10.1038/nm.3893

Gyires, K., Toth, E., & Zadori, S. (2014). Gut inflammation: current update on pathophysiology, molecular mechanism and pharmacological treatment modalities. *Current Pharmaceutical Design*, *20*(7), 1063–1081. https://doi.org/10.2174/13816128113199990417

Haffner, F. B., Diab, R., Pasc, A., Haffner, F. B., Diab, R., & Pasc, A. (2016). Encapsulation of probiotics: insights into academic and industrial approaches. *AIMS Materials Science 2016 1:114*, *3*(1), 114–136. https://doi.org/10.3934/MATERSCI.2016.1.114

Hamilton, M. J., Sinnamon, M. J., Lyng, G. D., Glickman, J. N., Wang, X., Xing, W., Krilise, S. A., Blumberg, R. S., Adachi, R., Lee, D. M., & Stevens, R. L. (2011). Essential role for mast cell tryptase in acute experimental colitis. *Proceedings of the National Academy of Sciences of the United States of America*, *108*(1), 290–295. https://doi.org/10.1073/PNAS.1005758108/SUPPL_FILE/SM05.MOV

Hannoodee, S., & Nasuruddin, D. N. (2020). Acute inflammatory response. *Nature*, *206*(4979), 20. https://www.ncbi.nlm.nih.gov/books/NBK556083/

Hanske, L., Engst, W., Loh, G., Sczesny, S., Blaut, M., & Braune, A. (2013). Contribution of gut bacteria to the metabolism of cyanidin 3-glucoside in human microbiota-associated rats. *British Journal of Nutrition*, *109*(8), 1433–1441. https://doi.org/10.1017/S0007114512003376

Hansson, G. K., Robertson, A. K. L., & Söderberg-Nauclér, C. (2006). Inflammation and atherosclerosis. In *Annual Review of Pathology*, 1, 297–329. https://doi.org/10.1146/annurev.pathol.1.110304.100100

Hasturk, H., Kantarci, A., & Van Dyke, T. E. (2012). Oral inflammatory diseases and systemic inflammation: Role of the macrophage. *Frontiers in Immunology*, 3 (May), https://doi.org/10.3389/fimmu.2012.00118

He, J., & Monica Giusti, M. (2010). Anthocyanins: natural colorants with health-promoting properties. *Annual Review of Food Science and Technology*, *1*(1), 163–187. https://doi.org/10.1146/ANNUREV.FOOD.080708.100754

Headland, S. E., & Norling, L. V. (2015). The resolution of inflammation: Principles and challenges. *Seminars in Immunology*, *27*(3), 149–160. https://doi.org/10.1016/J.SMIM.2015.03.014

Hidalgo, M., Oruna-Concha, M. J., Kolida, S., Walton, G. E., Kallithraka, S., Spencer, J. P. E., Gibson, G. R., & De Pascual-Teresa, S. (2012). Metabolism of anthocyanins by human gut microflora and their influence on gut bacterial growth. *Journal of Agricultural and Food Chemistry*, *60*(15), 3882–3890. https://doi.org/10.1021/JF3002153

Holdsworth, S. R., & Can, P. Y. (2015). Cytokines: Names and numbers you should care about. *Clinical Journal of the American Society of Nephrology : CJASN*, *10*(12), 2243. https://doi.org/10.2215/CJN.07590714

Ibrahim Silva, P., Stringheta, P. C., Teofílo, R. F., & De Oliveira, I. R. N. (2013). Parameter optimization for spray-drying microencapsulation of jaboticaba (Myrciaria jaboticaba) peel extracts using simultaneous analysis of responses. *Journal of Food Engineering*, *117*(4), 538–544. https://doi.org/10.1016/J.JFOODENG.2012.08.039

Idham, Z., Muhamad, I. I., & Sarmidi, M. R. (2012). Degradation kinetics and color stability of spray-dried encapsulated anthocyanins from hibiscus sabdariffa l. *Journal of Food Process Engineering*, *35*(4), 522–542. https://doi.org/10.1111/J.1745-4530.2010.00605.X

Jackman, R. L., Yada, R. Y., Tung, M. A., & Speers, R. A. (1987). Anthocyanins as food colorants- A review. *Journal of Food Biochemistry*, *11*(3), 201–247. https://doi.org/10.1111/J.1745-4514.1987.TB00123.X

Jafari, S. M., Assadpoor, E., He, Y., & Bhandari, B. (2008). Encapsulation efficiency of food flavours and oils during spray drying. *Http://Dx.Doi.Org/10.1080/07373930802135972*, *26*(7), 816–835. https://doi.org/10.1080/07373930802135972

Jamwal, S., & Kumar, P. (2017). Animal models of inflammatory bowel disease. *Animal Models for the Study of Human Disease: Second Edition*, 467–477. https://doi.org/10.1016/B978-0-12-809468-6.00019-X

Jeon, Y. D., Lee, J. H., Kang, S. H., Myung, H., & Jin, J. S. (2021). Lingonberry fruit ethanol extract ameliorates dss-induced ulcerative colitis in vivo and in vitro. *Applied Sciences (Switzerland)*, *11*(17). https://doi.org/10.3390/app11177955

Jucker, M., Abts, H., Li, W., Schindler, R., Merz, H., Gunther, A., Von Kalle, C., Schaadt, M., Diamantstein, T., Feller, A. C., Krueger, G. R. F., Diehl, V., Blankenstein, T., & Tesch, H. (1991). Expression of interleukin-6 and interleukin-6 receptor in Hodgkin's disease. *Blood*, *77*(11), 2413–2418. https://doi.org/10.1182/BLOOD.V77.11.2413.2413

Kandasamy, S., & Naveen, R. (2022a). A review on the encapsulation of bioactive components using spray-drying and freeze-drying techniques. In Journal of Food Process Engineering (Vol. 45, Issue 8). https://doi.org/10.1111/jfpe.14059

Kandasamy, S., & Naveen, R. (2022b). A review on the encapsulation of bioactive components using spray-drying and freeze-drying techniques. In Journal of Food Process Engineering (Vol. 45, Issue 8, p. 14059). John Wiley & Sons, Ltd. https://doi.org/10.1111/jfpe.14059

Kang, S., Jeon, Y. D., Moon, K. H., Lee, J. H., Kim, D. G., Kim, W., Myung, H., Kim, J. S., Kim, H. J., Bang, K. S., & Jin, J. S. (2017). Aronia berry extract ameliorates the severity of dextran sodium sulfate-induced ulcerative colitis in mice. *Journal of Medicinal Food*, *20*(7), 667–675. https://doi.org/10.1089/jmf.2016.3822

Kang, Y., Xue, Y., Du, M., & Zhu, M. J. (2017). Preventive effects of Goji berry on dextran-sulfate-sodium-induced colitis in mice. *The Journal of Nutritional Biochemistry*, *40*, 70–76. https://doi.org/10.1016/J.JNUTBIO.2016.10.009

Karabucak, B., Walsch, H., Jou, Y. T., Simchon, S., & Kim, S. (2005). The Role of endothelial nitric oxide in the substance P induced vasodilation in bovine dental pulp. *Journal of Endodontics*, *31*(10), 733–736. https://doi.org/10.1097/01.DON.0000157988.13010.25

Kelly, M. P. (2003). Colitis. In *Colitis*. StatPearls Publishing. https://doi.org/10.4324/9780203392706

Keppler, K., & Humpf, H. U. (2005). Metabolism of anthocyanins and their phenolic degradation products by the intestinal microflora. *Bioorganic & Medicinal Chemistry*, *13*(17), 5195–5205. https://doi.org/10.1016/J.BMC.2005.05.003

Keshteli, A. H., Madsen, K. L., & Dieleman, L. A. (2019). Diet in the pathogenesis and management of ulcerative colitis; A review of randomized controlled dietary interventions. *Nutrients*, 11(7), 1498. https://doi.org/10.3390/nu11071498

Khan, I., Bai, Y., Ullah, N., Liu, G., Rajoka, M. S. R., & Zhang, C. (2022). Differential susceptibility of the gut microbiota to DSS treatment interferes in the conserved microbiome association in mouse models of colitis and is related to the initial gut microbiota difference. *Advanced Gut & Microbiome Research*, *2022*, 1–20. https://doi.org/10.1155/2022/7813278

Khattab, R., Brooks, M. S. L., & Ghanem, A. (2016). Phenolic analyses of haskap berries (Lonicera caerulea L.): Spectrophotometry versus high performance liquid chromatography. *International journal of food properties*, *19*(8), 1708–1725. https://doi.org/10.1080/10942912.2015.1084316

Khazaei, M. K., Jafari, S. M., Ghorbani, M., & Kakhki, H. A. (2014). Application of maltodextrin and gum Arabic in microencapsulation of saffron petal's anthocyanins and evaluating their storage stability and color. *Carbohydrate Polymers*, *105*(1), 57–62. https://doi.org/10.1016/J.CARBPOL.2014.01.042

Kim, S. H., Kwon, D., Son, S. W., Jeong, T. Bin, Lee, S., Kwak, J.-H., Cho, J.-Y., Hwang, D. Y., Seo, M.-S., Kim, K. S., & Jung, Y.-S. (2021). Inflammatory responses of C57BL/6NKorl mice to dextran sulfate sodium-induced colitis: comparison between three C57BL/6 N sub-strains. *Laboratory Animal Research 2021 37:1*, *37*(1), 1–7. https://doi.org/10.1186/S42826-021-00084-2

King, T. C. (2007). Inflammation, inflammatory mediators, and immune-mediated disease. In *Elsevier's Integrated Pathology*, *chapter 2*, 21–57. Elsevier. https://doi.org/10.1016/B978-0-323-04328-1.50008-5

Kitajima, S., Takuma, S., & Morimoto, M. (2000). Histological analysis of murine colitis induced by dextran sulfate sodium of different molecular weights. *Experimental Animals*, *49*(1), 9–15. https://doi.org/10.1538/EXPANIM.49.9

Kobayashi, N., Karisola, P., Peña-Cruz, V., Dorfman, D. M., Jinushi, M., Umetsu, S. E., Butte, M. J., Nagumo, H., Chernova, I., Zhu, B., Sharpe, A. H., Ito, S., Dranoff, G., Kaplan, G. G., Casasnovas, J. M., Umetsu, D. T., DeKruyff, R. H., & Freeman, G. J. (2007). TIM-1 and TIM-4 glycoproteins bind phosphatidylserine and mediate uptake of apoptotic cells. *Immunity*, *27*(6), 927–940. https://doi.org/10.1016/J.IMMUNI.2007.11.011

Kösling, S. (2008). Oral cavity, inflammatory diseases. In *Encyclopedia of Diagnostic Imaging*, 1415–1418. Springer, Berlin, Heidelberg. https://doi.org/10.1007/978-3-540-35280-8_1799

Kotas, M. E., & Medzhitov, R. (2015). Homeostasis, inflammation, and disease susceptibility. *Cell*, *160*(5), 816–827. https://doi.org/10.1016/J.CELL.2015.02.010

Kourtzelis, I., Li, X., Mitroulis, I., Grosser, D., Kajikawa, T., Wang, B., Grzybek, M., von Renesse, J., Czogalla, A., Troullinaki, M., Ferreira, A., Doreth, C., Ruppova, K., Chen, L. S., Hosur, K., Lim, J. H., Chung, K. J., Grossklaus, S., Tausche, A. K., … Chavakis, T. (2018). DEL-1 promotes macrophage efferocytosis and clearance of inflammation. *Nature Immunology, 20*(1), 40–49. https://doi.org/10.1038/s41590-018-0249-1

Krasaekoopt, W. (2013). Microencapsulation of probiotics in hydrocolloid gel matrices: A review. In *Agro Food Industry Hi-Tech*, 24(2), 76–83. https://repository.au.edu/handle/6623004553/20710

Kuck, L. S., & Noreña, C. P. Z. (2016). Microencapsulation of grape (Vitis labrusca var. Bordo) skin phenolic extract using gum Arabic, polydextrose, and partially hydrolyzed guar gum as encapsulating agents. *Food Chemistry*, *194*, 569–576. https://doi.org/10.1016/j.foodchem.2015.08.066

Kutzli, I., Gibis, M., Baier, S. K., & Weiss, J. (2018). Fabrication and characterization of food-grade fibers from mixtures of maltodextrin and whey protein isolate using needleless electrospinning. *Journal of Applied Polymer Science*, *135*(22), 46328. https://doi.org/10.1002/APP.46328

Kwon, J., Lee, C., Heo, S., Kim, B., & Hyun, C. K. (2021). DSS-induced colitis is associated with adipose tissue dysfunction and disrupted hepatic lipid metabolism leading to hepatosteatosis and dyslipidemia in mice. *Scientific Reports*, *11*(1), 1–16. https://doi.org/10.1038/s41598-021-84761-1

Lacerda, E. C. Q., Calado, V. M. D. A., Monteiro, M., Finotelli, P. V., Torres, A. G., & Perrone, D. (2016). Starch, inulin and maltodextrin as encapsulating agents affect the quality and stability of jussara pulp microparticles. *Carbohydrate Polymers*, *151*, 500–510. https://doi.org/10.1016/j.carbpol.2016.05.093

Lacy, P., & Stow, J. L. (2011). Cytokine release from innate immune cells: association with diverse membrane trafficking pathways. *Blood*, *118*(1), 9–18. https://doi.org/10.1182/BLOOD-2010-08-265892

Laila, U., Rochmadi, & Pudjiraharti, S. (2019). Microencapsulation of purple-fleshed sweet potato anthocyanins with Chitosan-sodium tripolyphosphate by using emulsification-crosslinking technique. *Journal of Mathematical and Fundamental Sciences*, *51*(1), 29–46. https://doi.org/10.5614/j.math.fund.sci.2019.51.1.3

Laokuldilok, T., & Kanha, N. (2017). Microencapsulation of black glutinous rice anthocyanins using maltodextrins produced from broken rice fraction as wall material by spray drying and freeze drying. Journal of Food Processing and Preservation, 41(1), e12877. https://doi.org/10.1111/JFPP.12877

Lau, E. (2001). Preformulation Studies. *Separation Science and Technology*, *3*(C), 173–233. https://doi.org/10.1016/S0149-6395(01)80007-6

Lee, S. G., Brownmiller, C. R., Lee, S. O., & Kang, H. W. (2020). Anti-inflammatory and antioxidant effects of anthocyanins of trifolium pratense (red clover) in lipopolysaccharide-stimulated raw-267.4 macrophages. *Nutrients*, *12*(4). https://doi.org/10.3390/nu12041089

Leonardis, F., De Angelis, V., Frisardi, F., Pietrafitta, C., Riva, I., Valetti, T. M., Broletti, V., Marchesi, G., Menato, L., Nani, R., Marson, F., Fabbris, M., Cabrini, L., Colombo, S., Zangrillo, A., Coniglio, C., Gordini, G., Stalteri, L., Giuliani, G., … La Manna, G. (2018). Effect of hemoadsorption for cytokine removal in pneumococcal and meningococcal sepsis. *Case Reports in Critical Care*, *2018*, 1–7. https://doi.org/10.1155/2018/1205613

Lescheid, D. W. (2014). Probiotics as regulators of inflammation: A review. *Functional Foods in Health and Disease*, *4*(7), 299–311. https://doi.org/10.31989/FFHD.V4I7.2

Levy, M., Kolodziejczyk, A. A., Thaiss, C. A., & Elinav, E. (2017). Dysbiosis and the immune system. *Nature Reviews Immunology 2017 17:4*, *17*(4), 219–232. https://doi.org/10.1038/nri.2017.7

Li, D., Wang, P., Luo, Y., Zhao, M., & Chen, F. (2017). Health benefits of anthocyanins and molecular mechanisms: Update from recent decade. *Critical Reviews in Food Science and Nutrition*, *57*(8), 1729–1741. https://doi.org/10.1080/10408398.2015.1030064

Li, J. J., & Zreiqat, H. (2019). Tissue response to biomaterials. In *Encyclopedia of Biomedical Engineering*, 1–3, 270–277. Elsevier. https://doi.org/10.1016/B978-0-12-801238-3.99880-5

Li, J., & Kirsner, R. S. (2005). Wound healing. In *Surgery of the Skin*, 97–115. Mosby. https://doi.org/10.1016/B978-0-323-02752-6.50012-2

Li Jeon, N., Baskaran, H., Dertinger, S. K. W., Whitesides, G. M., De Water, L. Van, & Toner, M. (2002). Neutrophil chemotaxis in linear and complex gradients of interleukin-8 formed in a microfabricated device. *Nature Biotechnology, 20*(8), 826–830. https://doi.org/10.1038/nbt712

Li, L., Wang, L., Wu, Z., Yao, L., Wu, Y., Huang, L., Liu, K., Zhou, X., & Gou, D. (2014). Anthocyanin-rich fractions from red raspberries attenuate inflammation in both RAW264.7 macrophages and a mouse model of colitis. *Scientific Reports*, *4*(29), 6234. https://doi.org/10.1038/srep06234

Li, S., Wu, B., Fu, W., & Reddivari, L. (2019). The anti-inflammatory effects of dietary anthocyanins against ulcerative colitis. In *International Journal of Molecular Sciences*, https://doi.org/10.3390/ijms20102588

Li, Z., Pan, Q., Cui, X., & Duan, C. (2010). Optimization on anthocyanins extraction from wine grape skins using orthogonal test design. *Food Science and Biotechnology*, *19*(4), 1047–1053. https://doi.org/10.1007/S10068-010-0147-2

Limtrakul, P., Yodkeeree, S., Pitchakarn, P., & Punfa, W. (2015). Suppression of inflammatory responses by black rice extract in RAW 264.7 macrophage cells via downregulation of NF-kB and AP-1 signaling pathways. *Asian Pacific Journal of Cancer Prevention : APJCP*, *16*(10), 4277–4283. https://doi.org/10.7314/APJCP.2015.16.10.4277

Lisovsky, M. (2020). Inflammatory conditions of the esophagus: an update. *Annals of the New York Academy of Sciences*, *1481*(1), 5–10. https://doi.org/10.1111/NYAS.14450

Liu, F., Wang, T. T. Y., Tang, Q., Xue, C., Li, R. W., & Wu, V. C. H. (2019). Malvidin 3-glucoside modulated gut microbial dysbiosis and global metabolome disrupted in a murine Ccolitis model induced by dextran sulfate sodium. *Molecular Nutrition and Food Research*, *63*(21). https://doi.org/10.1002/mnfr.201900455

Liu, Y., Alookaran, J. J., & Rhoads, J. M. (2018). Probiotics in autoimmune and inflammatory disorders. *Nutrients* (https://doi.org/10.3390/nu10101537

Liu, Y., Zhang, D., Wu, Y., Wang, D., Wei, Y., Wu, J., & Ji, B. (2014). Stability and absorption of anthocyanins from blueberries subjected to a simulated digestion process. *International Journal of Food Sciences and Nutrition*, *65*(4), 440–448. https://doi.org/10.3109/09637486.2013.869798

Liverani, E., Rico, M. C., Yaratha, L., Tsygankov, A. Y., Kilpatrick, L. E., & Kunapuli, S. P. (2014). LPS-induced systemic inflammation is more severe in P2Y12 null mice. *Journal of Leukocyte Biology*, *95*(2), 313. https://doi.org/10.1189/JLB.1012518

Lobito, A. A., Gabriel, T. L., Medema, J. P., & Kimberley, F. C. (2011). Disease causing mutations in the TNF and TNFR superfamilies: Focus on molecular mechanisms driving disease. *Trends in Molecular Medicine*, *17*(9), 494–505. https://doi.org/10.1016/J.MOLMED.2011.05.006

Lopes, T. J., Coutinho, M. R., & Novy Quadri, M. G. (2019). Use of maltodextrin and gum arabic for encapsulation of red cabbage anthocyanins. *Brazilian Journal of Food Research*, *10*(4), 18. https://doi.org/10.3895/REBRAPA.V10N4.11043

Low, D., Nguyen, D. D., & Mizoguchi, E. (2013). Animal models of ulcerative colitis and their application in drug research. *Drug Design, Development and Therapy*, https://doi.org/10.2147/DDDT.S40107

Luo, R., Zhang, J., Zhang, X., Zhou, Z., Zhang, W., Zhu, Z., Liu, H., Wang, L., Zhong, Z., Fu, H., Jing, B., & Peng, G. (2020). Bacillus subtilis HH2 ameliorates TNBS-induced colitis by modulating gut microbiota composition and improving intestinal barrier function in rabbit model. *Journal of Functional Foods*, *74*, 104167. https://doi.org/10.1016/j.jff.2020.104167

Mahdavi-Roshan, M., Salari, A., Kheirkhah, J., & Ghorbani, Z. (2022). The effects of probiotics on inflammation, endothelial dysfunction, and atherosclerosis progression: A mechanistic overview. *Heart, Lung and Circulation*, *31*(5), 45–71. https://doi.org/10.1016/J.HLC.2021.09.006

Mähler, M., Bristol, I. J., Leiter, E. H., Workman, A. E., Birkenmeier, E. H., Elson, C. O., & Sundberg, J. P. (1998). Differential susceptibility of inbred mouse strains to dextran sulfate sodium-induced colitis. *American Journal of Physiology - Gastrointestinal and Liver Physiology*, *274*(337-3). https://doi.org/10.1152/ajpgi.1998.274.3.g544

Maleki, S. J., Crespo, J. F., & Cabanillas, B. (2019). Anti-inflammatory effects of flavonoids. In *Food Chemistry*, 299, Elsevier Ltd. https://doi.org/10.1016/j.foodchem.2019.125124

Mansour, M., Salah, M., & Xu, X. (2020). Effect of microencapsulation using soy protein isolate and gum arabic as wall material on red raspberry anthocyanin stability, characterization, and simulated gastrointestinal conditions. *Ultrasonics Sonochemistry*, *63*, 104927. https://doi.org/10.1016/j.ultsonch.2019.104927

Mariggiò, M. A., Minunno, V., Riccardi, S., Santacroce, R., De Rinaldis, P., & Fumarulo, R. (2008). Sulfide Enhancement of Pmn Apoptosis. *Immunopharmacology and Immunotoxicology, 20*(3), 399–408. https://doi.org/10.3109/08923979809034822

Martino, J. V., Van Limbergen, J., & Cahill, L. E. (2017). The role of carrageenan and carboxymethylcellulose in the development of intestinal inflammation. *Frontiers in Pediatrics*, 5, 96. https://doi.org/10.3389/fped.2017.00096

Mattila-Sandholm, T., Myllärinen, P., Crittenden, R., Mogensen, G., Fondén, R., & Saarela, M. (2002). Technological challenges for future probiotic foods. *International Dairy Journal*, *12*(2–3), 173–182. https://doi.org/10.1016/S0958-6946(01)00099-1

Mazuco, R. A., Cardoso, P. M. M., Bindaco, É. S., Scherer, R., Castilho, R. O., Faraco, A. A. G., Ruas, F. G., Oliveira, J. P., Guimarães, M. C. C., de Andrade, T. U., Lenz, D., Braga, F. C., & Endringer, D. C. (2018). Maltodextrin and gum arabic-based microencapsulation methods for anthocyanin preservation in juçara palm (Euterpe edulis Martius) fruit pulp. *Plant Foods for Human Nutrition*, *73*(3), 209–215. https://doi.org/10.1007/S11130-018-0676-Z/FIGURES/2

Medzhitov, R. (2008). Origin and physiological roles of inflammation. *Nature*, 454(7203), 428–435. https://doi.org/10.1038/nature07201

Meier, J., & Sturm, A. (2011). Current treatment of ulcerative colitis. *World Journal of Gastroenterology : WJG*, *17*(27), 3204. https://doi.org/10.3748/WJG.V17.I27.3204

Meseeha, M., & Attia, M. (2021). Proctitis and anusitis. In *StatPearls*. StatPearls Publishing. https://www.ncbi.nlm.nih.gov/books/NBK430892/

Michalska, A., Wojdyło, A., Brzezowska, J., Majerska, J., & Ciska, E. (2019). The influence of inulin on the retention of polyphenolic compounds during the drying of blackcurrant juice. *Molecules*, https://doi.org/10.3390/molecules24224167

Mitsuyama, K., Toyonaga, A., & Sata, M. (2000). Cytokine-targeted therapeutic approaches for inflammatory bowel disease. *Drugs of Today*, *36*(5), 281–293. https://doi.org/10.1358/DOT.2000.36.5.575041

Mizoguchi, E., Low, D., Ezaki, Y., & Okada, T. (2020). Recent updates on the basic mechanisms and pathogenesis of inflammatory bowel diseases in experimental animal models. *Intestinal Research*, *18*(2), 151. https://doi.org/10.5217/IR.2019.09154

Moens, L., & Tangye, S. G. (2014). Cytokine-mediated regulation of plasma cell generation: IL-21 takes center stage. *Frontiers in Immunology*, *5*(Feb), 65. https://doi.org/10.3389/FIMMU.2014.00065/BIBTEX

Mohammadalinejhad, S., & Kurek, M. A. (2021). Microencapsulation of anthocyanins—critical review of techniques and wall materials. *Applied Sciences*, 11(9), 3936. https://doi.org/10.3390/APP11093936

Mohd Nawi, N., Muhamad, I. I., & Mohd Marsin, A. (2015). The physicochemical properties of microwave-assisted encapsulated anthocyanins from Ipomoea batatas as affected by different wall materials. *Food Science and Nutrition*, *3*(2), 91–99. https://doi.org/10.1002/FSN3.132

Monk, J. M., Lepp, D., Zhang, C. P., Wu, W., Zarepoor, L., Lu, J. T., Pauls, K. P., Tsao, R., Wood, G. A., Robinson, L. E., & Power, K. A. (2016). Diets enriched with cranberry beans alter the microbiota and mitigate colitis severity and associated inflammation. *Journal of Nutritional Biochemistry*, *28*, 129–139. https://doi.org/10.1016/j.jnutbio.2015.10.014

Montonye, D. R., Ericsson, A. C., Busi, S. B., Lutz, C., Wardwell, K., & Franklin, C. L. (2018). Acclimation and institutionalization of the mouse microbiota following transportation. *Frontiers in Microbiology*, *9*(May), 1085. https://doi.org/10.3389/FMICB.2018.01085/FULL

Morais, C. A., de Rosso, V. V., Estadella, D., & Pisani, L. P. (2016). Anthocyanins as inflammatory modulators and the role of the gut microbiota. *The Journal of Nutritional Biochemistry*, *33*, 1–7. https://doi.org/10.1016/J.JNUTBIO.2015.11.008

Moser, P., Telis, V. R. N., de Andrade Neves, N., García-Romero, E., Gómez-Alonso, S., & Hermosín-Gutiérrez, I. (2017). Storage stability of phenolic compounds in powdered BRS Violeta grape juice microencapsulated with protein and maltodextrin blends. *Food Chemistry*, *214*, 308–318. https://doi.org/10.1016/J.FOODCHEM.2016.07.081

Mueller, D., Jung, K., Winter, M., Rogoll, D., Melcher, R., & Richling, E. (2017). Human intervention study to investigate the intestinal accessibility and bioavailability of anthocyanins from bilberries. *Food Chemistry*, *231*, 275–286. https://doi.org/10.1016/j.foodchem.2017.03.130

Myjavcová, R., Marhol, P., Křen, V., Šimánek, V., Ulrichová, J., Palíková, I., Papoušková, B., Lemr, K., & Bednář, P. (2010). Analysis of anthocyanin pigments in Lonicera (Caerulea) extracts using chromatographic fractionation followed by microcolumn liquid chromatography-mass spectrometry. *Journal of Chromatography A*, *1217*(51), 7932–7941. https://doi.org/10.1016/J.CHROMA.2010.05.058

Nafiunisa, A., Aryanti, N., Wardhani, D. H., & Kumoro, A. C. (2017). Microencapsulation of natural anthocyanin from purple rosella calyces by freeze drying. *Journal of Physics: Conference Series*, https://doi.org/10.1088/1742-6596/909/1/012084

Nair, A. B., & Jacob, S. (2016). A simple practice guide for dose conversion between animals and human. *Journal of Basic and Clinical Pharmacy*, *7*(2), 27. https://doi.org/10.4103/0976-0105.177703

Navaneethan, U., & Giannella, R. A. (2011). Infectious colitis. *Current Opinion in Gastroenterology*, *27*(1), 66–71. https://doi.org/10.1097/MOG.0B013E3283400755

Neurath, M. F. (2019). Resolution of inflammation: from basic concepts to clinical application. *Seminars in Immunopathology, 41*(6), 627–631. https://doi.org/10.1007/S00281-019-00771-2

Nguyen, Q.-D., Dang, T.-T., Nguyen, T.-V.-L., Nguyen, T.-T.-D., Nguyen, N.-N., Nguyen, -Duy, & Nguyen, T.-L. (2022). Microencapsulation of roselle (Hibiscus sabdariffa L.) anthocyanins: Effects of different carriers on selected physicochemical properties and antioxidant activities of spray-dried and freeze-dried powder. *International Journal of Food Properties*, *25*(1), 359–374. https://doi.org/10.1080/10942912.2022.2044846

Norkaew, O., Thitisut, P., Mahatheeranont, S., Pawin, B., Sookwong, P., Yodpitak, S., & Lungkaphin, A. (2019). Effect of wall materials on some physicochemical properties and release characteristics of encapsulated black rice anthocyanin microcapsules. *Food Chemistry*, *294*, 493–502. https://doi.org/10.1016/j.foodchem.2019.05.086

Novotny, J. A., Clevidence, B. A., & Kurilich, A. C. (2012). Anthocyanin kinetics are dependent on anthocyanin structure. `-*British Journal of Nutrition*, *107*(4), 504–509. https://doi.org/10.1017/S000711451100314X

Nunes, C., Freitas, V., Almeida, L., & Laranjinha, J. (2019). Red wine extract preserves tight junctions in intestinal epithelial cells under inflammatory conditions: implications for intestinal inflammation. *Food & Function*, *10*(3), 1364–1374. https://doi.org/10.1039/C8FO02469C

Nutrition Division. (2006). Probiotics in food Health and nutritional properties and guidelines for evaluation. *FAO Food and Nutrition Paper*, *85*, 56.

Oh, S. Y., Cho, K. A., Kang, J. L., Kim, K. H., & Woo, S. Y. (2014). Comparison of experimental mouse models of inflammatory bowel disease. *International Journal of Molecular Medicine*, *33*(2), 333–340. https://doi.org/10.3892/IJMM.2013.1569/HTML

Okayasu, I., Hatakeyama, S., Yamada, M., Ohkusa, T., Inagaki, Y., & Nakaya, R. (1990). A novel method in the induction of reliable experimental acute and chronic ulcerative colitis in mice. *Gastroenterology*, *98*(3), 694–702. https://doi.org/10.1016/0016-5085(90)90290-H

Olivas-Aguirre, F. J., Rodrigo-García, J., Martínez-Ruiz, N. D. R., Cárdenas-Robles, A. I., Mendoza-Díaz, S. O., Álvarez-Parrilla, E., González-Aguilar, G. A., De La Rosa, L. A., Ramos-Jiménez, A., & Wall-Medrano, A. (2016). Cyanidin-3-*O*-glucoside: Physical-chemistry, foodomics and health effects. *Molecules*, *21*(9), 1264. https://doi.org/10.3390/MOLECULES21091264

Opal, S. M., & DePalo, V. A. (2000). Anti-inflammatory cytokines. *Chest*, *117*(4), 1162–1172. https://doi.org/10.1378/CHEST.117.4.1162

Oro, C. E. D., Paroul, N., Mignoni, M. L., Zabot, G. L., Backes, G. T., Dallago, R. M., & Tres, M. V. (2021). Microencapsulation of Brazilian Cherokee blackberry extract by freeze-drying using maltodextrin, gum Arabic, and pectin as carrier materials, *Food Science and Technology International*. https://doi.org/10.1177/10820132211068979

Oteiza, P. I., Fraga, C. G., Mills, D. A., & Taft, D. H. (2018). Flavonoids and the gastrointestinal tract: Local and systemic effects. In *Molecular Aspects of Medicine* (Vol. 61, pp. 41–49). https://doi.org/10.1016/j.mam.2018.01.001

Passamonti, S., Vrhovsek, U., Vanzo, A., & Mattivi, F. (2003). The stomach as a site for anthocyanins absorption from food. *FEBS Letters*, *544*(1–3), 210–213. https://doi.org/10.1016/S0014-5793(03)00504-0

Peng, Y., Yan, Y., Wan, P., Chen, D., Ding, Y., Ran, L., Mi, J., Lu, L., Zhang, Z., Li, X., Zeng, X., & Cao, Y. (2019). Gut microbiota modulation and anti-inflammatory properties of anthocyanins from the fruits of Lycium ruthenicum Murray in dextran sodium sulfate-induced colitis in mice. *Free Radical Biology and Medicine*, *136*, 96–108. https://doi.org/10.1016/j.freeradbiomed.2019.04.005

Peng, Y., Yan, Y., Wan, P., Dong, W., Huang, K., Ran, L., Mi, J., Lu, L., Zeng, X., & Cao, Y. (2020). Effects of long-term intake of anthocyanins from Lycium ruthenicum Murray on the organism health and gut microbiota in vivo. *Food Research International*, https://doi.org/10.1016/j.foodres.2019.108952

Pereira Souza, A. C., Deyse Gurak, P., & Damasceno Ferreira Marczak, L. (2017). Maltodextrin, pectin and soy protein isolate as carrier agents in the encapsulation of anthocyanins-rich extract from jaboticaba pomace. *Food and Bioproducts Processing*, *102*, 186–194. https://doi.org/10.1016/j.fbp.2016.12.012

Pereira, V. A., de Arruda, I. N. Q., & Stefani, R. (2015). Active chitosan/PVA films with anthocyanins from Brassica oleraceae (Red Cabbage) as Time-Temperature Indicators for application in intelligent food packaging. *Food Hydrocolloids*, *43*, 180–188. https://doi.org/10.1016/j.foodhyd.2014.05.014

Perše, M., & Cerar, A. (2012). Dextran sodium sulphate colitis mouse model: Traps and tricks. *Journal of Biomedicine and Biotechnology*, 13. https://doi.org/10.1155/2012/718617

Petkova, N., Hambarlyiska, I., Tumbarski, Y., Vrancheva, R., Raeva, M., & Ivanov, I. (2022). Phytochemical composition and antimicrobial properties of burdock (Arctium lappa L.) roots extracts. *Biointerface Research in Applied Chemistry*, *12*(3), 2826–2842. https://doi.org/10.33263/BRIAC123.28262842

Petri, B., & Sanz, M. J. (2018). Neutrophil chemotaxis. *Cell and Tissue Research 2018 371:3*, *371*(3), 425–436. https://doi.org/10.1007/S00441-017-2776-8

Phan, M. A. T., Bucknall, M. P., & Arcot, J. (2019). Interferences of anthocyanins with the uptake of lycopene in Caco-2 cells, and their interactive effects on anti-oxidation and anti-inflammation in vitro and ex vivo. *Food Chemistry*, *276*, 402–409. https://doi.org/10.1016/j.foodchem.2018.10.012

Pieczykolan, E., & Kurek, M. A. (2019). Use of guar gum, gum arabic, pectin, beta-glucan and inulin for microencapsulation of anthocyanins from chokeberry. *International Journal of Biological Macromolecules*, *129*, 665–671. https://doi.org/10.1016/j.ijbiomac.2019.02.073

Prescott, S. L. (2013). Early-life environmental determinants of allergic diseases and the wider pandemic of inflammatory noncommunicable diseases. *Journal of Allergy and Clinical Immunology*, *131*(1), 23–30. https://doi.org/10.1016/J.JACI.2012.11.019

Pudziuvelyte, L., Marksa, M., Sosnowska, K., Winnicka, K., Morkuniene, R., & Bernatoniene, J. (2020). Freeze-drying technique for microencapsulation of elsholtzia ciliata Ethanolic extract using different coating materials. *Molecules*, https://doi.org/10.3390/molecules25092237

Qian, B., Wang, C., Zeng, Z., Ren, Y., Li, D., & Song, J. Le. (2020). Ameliorative effect of sinapic acid on dextran sodium sulfate-(DSS-) induced ulcerative colitis in kunming (km) mice. *Oxidative Medicine and Cellular Longevity*, *2020*, 13. https://doi.org/10.1155/2020/8393504

Quek, S. Y., Chok, N. K., & Swedlund, P. (2007). The physicochemical properties of spray-dried watermelon powders. *Chemical Engineering and Processing: Process Intensification*, *46*(5), 386–392. https://doi.org/10.1016/j.cep.2006.06.020

Quinn, A. C., Petros, A. J., & Vallance, P. (1995). Nitric oxide: an endogenous gas. *British Journal of Anaesthesia*, *74*(4), 443–451. https://doi.org/10.1093/BJA/74.4.443

Randhawa, P. K., Singh, K., Singh, N., & Jaggi, A. S. (2014). A review on chemical-induced inflammatory bowel disease models in rodents. *Korean Journal of Physiology & Pharmacology*, *18*(4), 279–288. https://doi.org/10.4196/KJPP.2014.18.4.279

Razgonova, M., Zakharenko, A., Pikula, K., Manakov, Y., Ercisli, S., Derbush, I., Kislin, E., Seryodkin, I., Sabitov, A., Kalenik, T., & Golokhvast, K. (2021). LC-MS/MS screening of phenolic compounds in wild and cultivated grapes vitis amurensis Rupr. *Molecules*, *26*(12). https://doi.org/10.3390/MOLECULES26123650

Rezvankhah, A., Emam-Djomeh, Z., & Askari, G. (2019). Encapsulation and delivery of bioactive compounds using spray and freeze-drying techniques: A review. *Drying Technology, 38*(1–2), 235–258. https://doi.org/10.1080/07373937.2019.1653906

Ricciotti, E., & Fitzgerald, G. A. (2011). Prostaglandins and Inflammation. *Arteriosclerosis, Thrombosis, and Vascular Biology*, *31*(5), 986. https://doi.org/10.1161/ATVBAHA.110.207449

Robert, P., & Fredes, C. (2015). The encapsulation of anthocyanins from berry-type fruits, *20*(4), 5875–5888. https://doi.org/10.3390/MOLECULES20045875

Robert, P., Gorena, T., Romero, N., Sepulveda, E., Chavez, J., & Saenz, C. (2010). Encapsulation of polyphenols and anthocyanins from pomegranate (Punica granatum) by spray drying. *International Journal of Food Science & Technology*, *45*(7), 1386–1394. https://doi.org/10.1111/J.1365-2621.2010.02270.X

Rocha-Parra, D. F., Lanari, M. C., Zamora, M. C., & Chirife, J. (2016). "Influence of storage conditions on phenolic compounds stability, antioxidant capacity and colour of freeze-dried encapsulated red wine." *LWT - Food Science and Technology*, *70*, 162–170. https://doi.org/10.1016/j.lwt.2016.02.038

Rosales, C. (2018). Neutrophil: A cell with many roles in inflammation or several cell types? *Frontiers in Physiology*, *9*(FEB), 113. https://doi.org/10.3389/FPHYS.2018.00113/BIBTEX

Rupasinghe, H. P. V., Boehm, M. M. A., Sekhon-Loodu, S., Parmar, I., Bors, B., & Jamieson, A. R. (2015). Anti-inflammatory activity of haskap cultivars is polyphenols-dependent. *Biomolecules*, *5*(2), 1079–1098. https://doi.org/10.3390/BIOM5021079

Rupasinghe, H. P.V ., Yu, L. J., Bhullar, K. S., & Bors, B. (2012). Haskap (Lonicera caerulea): A new berry crop with high antioxidant capacity. *Canadian Journal of Plant Science*, *92*(7), 1311–1317. https://doi.org/10.4141/CJPS2012-073/ASSET/IMAGES/CJPS2012-073TAB4.GIF

Rupasinghe, H. P. V., Arumuggam, N., Amararathna, M., & De Silva, A. B. K. H. (2018). The potential health benefits of haskap (Lonicera caerulea L.): Role of cyanidin-3-O-glucoside. *Journal of Functional Foods*, *44*, 24–39. https://doi.org/10.1016/J.JFF.2018.02.023

Rupasinghe, H. P. V., Nair, S. V. G., & Robinson, R. A. (2014). Chemopreventive Properties of Fruit Phenolic Compounds and Their Possible Mode of Actions, 42, 229–266. Elsevier. https://doi.org/10.1016/b978-0-444-63281-4.00008-2

Rupasinghe, H. P. V., Wang, L., Huber, G. M., & Pitts, N. L. (2008). Effect of baking on dietary fibre and phenolics of muffins incorporated with apple skin powder. *Food Chemistry*, *107*(3), 1217–1224. https://doi.org/10.1016/j.foodchem.2007.09.057

De Silva, A. K. H., & Rupasinghe, H. P. V. (2020). Polyphenols composition and anti-diabetic properties in vitro of haskap (Lonicera caerulea L.) berries in relation to cultivar and harvesting date. *Journal of Food Composition and Analysis*, 88, 103402.

Sarao, L. K., & Arora, M. (2017). Probiotics, prebiotics, and microencapsulation: A review. *Critical Reviews in Food Science and Nutrition*, *57*(2), 344–371. https://doi.org/10.1080/10408398.2014.887055

Satoh, H., Sato, F., Takami, K., & Szabo, S. (1997). New ulcerative colitis model induced by sulfhydryl blockers in rats and the effects of antiinflammatory drugs on the colitis. *Japanese Journal of Pharmacology*, *73*(4), 299–309. https://doi.org/10.1254/JJP.73.299

Scarano, A., Butelli, E., De Santis, S., Cavalcanti, E., Hill, L., De Angelis, M., Giovinazzo, G., Chieppa, M., Martin, C., & Santino, A. (2018). Combined dietary anthocyanins, flavonols, and stilbenoids alleviate inflammatory bowel disease symptoms in mice. *Frontiers in Nutrition*, *4*, 75. https://doi.org/10.3389/fnut.2017.00075

Scheiffele, F., & Fuss, I. J. (2002). Induction of TNBS colitis in mice. *Current Protocols in Immunology*, *49*(1), 1-15. https://doi.org/10.1002/0471142735.IM1519S49

Schnoor, M., Alcaide, P., Voisin, M. B., & Van Buul, J. D. (2015). Crossing the Vascular Wall: Common and Unique Mechanisms Exploited by Different leukocyte subsets during extravasation. *Mediators of Inflammation*, 2015, 23. https://doi.org/10.1155/2015/946509

Schwab, J. M., Chiang, N., Arita, M., & Serhan, C. N. (2007). Resolvin E1 and protectin D1 activate inflammation-resolution programmes. *Nature*, *447*(7146), 869–874. https://doi.org/10.1038/NATURE05877

Schwab, J. M., & Serhan, C. N. (2006). Lipoxins and new lipid mediators in the resolution of inflammation. *Current Opinion in Pharmacology*, *6*(4), 414–420. https://doi.org/10.1016/J.COPH.2006.02.006

Scott, A., Khan, K. M., Roberts, C. R., Cook, J. L., & Duronio, V. (2004). What do we mean by the term "inflammation"? A contemporary basic science update for sports medicine. In *British Journal of Sports Medicine*, 38(3), 372–380. https://doi.org/10.1136/bjsm.2004.011312

Serhan, C. N., Clish, C. B., Brannon, J., Colgan, S. P., Chiang, N., & Gronert, K. (2000). Novel functional sets of lipid-derived mediators with antiinflammatory actions generated from omega-3 fatty acids via cyclooxygenase 2-nonsteroidal antiinflammatory drugs and transcellular processing. *The Journal of Experimental Medicine*, *192*(8), 1197–1204. https://doi.org/10.1084/JEM.192.8.1197

Seyedian, S. S., Nokhostin, F., & Malamir, M. D. (2019). A review of the diagnosis, prevention, and treatment methods of inflammatory bowel disease. *Journal of Medicine and Life*, *12*(2), 113. https://doi.org/10.25122/JML-2018-0075

Shao Tuo, Craig McClain, & Feng, W. (2017). DSS-induced intestinal damage exacerbates liver injury by acute alcohol exposure in mice: Role of intestinal hypoxia-inducible factor 1α. *FASEB Journal*, *31*(1), 994.1-994.1. https://doi.org/10.1096/FASEBJ.31.1_SUPPLEMENT.994.1

Sharif, N., Khoshnoudi-Nia, S., & Jafari, S. M. (2020). Nano/microencapsulation of anthocyanins; a systematic review and meta-analysis. *Food Research International*, *132*, 109077. https://doi.org/10.1016/j.foodres.2020.109077

Sher, Y.-P., & Hung, M.-C. (2013). Blood AST, ALT and UREA/BUN Level Analysis. *BIO-PROTOCOL*, *3*(19). https://doi.org/10.21769/bioprotoc.931

Sherwood, E. R., & Toliver-Kinsky, T. (2004). Mechanisms of the inflammatory response. *Best Practice & Research Clinical Anaesthesiology*, *18*(3), 385–405. https://doi.org/10.1016/J.BPA.2003.12.002

Shori, A. B. (2017). Microencapsulation Improved Probiotics Survival During Gastric Transit. *HAYATI Journal of Biosciences*, *24*(1), 1–5. https://doi.org/10.1016/J.HJB.2016.12.008

Silva, H. R. da, Assis, D. da C. de, Prada, A. L., Silva, J. O. C., Sousa, M. B. de, Ferreira, A. M., Amado, J. R. R., Carvalho, H. de O., Santos, A. V. T. de L. T. dos, & Carvalho, J. C. T. (2019). Obtaining and characterization of anthocyanins from Euterpe oleracea (açaí) dry extract for nutraceutical and food preparations. *Revista Brasileira de Farmacognosia*, *29*(5), 677–685. https://doi.org/10.1016/J.BJP.2019.03.004

Silva, I., Pinto, R., & Mateus, V. (2019). Preclinical study in vivo for new pharmacological approaches in inflammatory bowel disease: A systematic review of chronic model of TNBS-Induced Colitis. *Journal of Clinical Medicine*, 8(10), 1574. https://doi.org/10.3390/jcm8101574

Silva, L., & Silva, L. (2015). A literature review of inflammation and its relationship with the oral cavity. *Global Journal of Infectious Diseases and Clinical Research*, *2*(1), 1–7. https://doi.org/10.17352/2455-5363.000006

Singh, M. N., Hemant, K. S. Y., Ram, M., & Shivakumar, H. G. (2010). Microencapsulation: A promising technique for controlled drug delivery. *Research in Pharmaceutical Sciences*, *5*(2), 65.

Singh, N., Baby, D., Rajguru, J. P., Patil, P. B., Thakkannavar, S. S., & Pujari, V. B. (2019). Inflammation and Cancer. *Annals of African Medicine*, *18*(3), 121. https://doi.org/10.4103/AAM.AAM_56_18

Smidowicz, A., & Regula, J. (2015). Effect of nutritional status and dietary patterns on human serum C-reactive protein and interleukin-6 concentrations. *Advances in Nutrition*, *6*(6), 738–747. https://doi.org/10.3945/AN.115.009415

Smrdel, P., Bogataj, M., Zega, A., Planinšek, O., & Mrhar, A. (2008). Shape optimization and characterization of polysaccharide beads prepared by ionotropic gelation. *Journal of microencapsulation, 25*(2), 90–105. https://doi.org/10.1080/02652040701776109

Sotnikova, R., Nosalova, V., & Navarova, J. (2013). Efficacy of quercetin derivatives in prevention of ulcerative colitis in rats. *Interdisciplinary Toxicology*, *6*(1), 9. https://doi.org/10.2478/INTOX-2013-0002

Stoll, L., Costa, T. M. H., Jablonski, A., Flôres, S. H., & de Oliveira Rios, A. (2016). Microencapsulation of anthocyanins with different wall materials and its application in active biodegradable films. *Food and Bioprocess Technology*, *9*(1), 172–181. https://doi.org/10.1007/S11947-015-1610-0/FIGURES/2

Sun, D., Huang, S., Cai, S., Cao, J., & Han, P. (2015). Digestion property and synergistic effect on biological activity of purple rice (Oryza sativa L.) anthocyanins subjected to a simulated gastrointestinal digestion in vitro. *Food Research International*, *78*, 114–123. https://doi.org/10.1016/j.foodres.2015.10.029

Sun, X., Du, M., Navarre, D. A., & Zhu, M. J. (2018). Purple potato extract promotes intestinal epithelial differentiation and barrier function by activating AMP-activated protein kinase. *Molecular Nutrition and Food Research*, *62*(4). https://doi.org/10.1002/mnfr.201700536

Suwal, S., Wu, Q., Liu, W., Liu, Q., Sun, H., Liang, M., Gao, J., Zhang, B., Kou, Y., Liu, Z., Wei, Y., Wang, Y., & Zheng, K. (2018). The probiotic effectiveness in preventing experimental colitis is correlated with host gut microbiota. *Frontiers in Microbiology*, *9*(NOV), 2675. https://doi.org/10.3389/FMICB.2018.02675/BIBTEX

Swer, T. L., Mukhim, C., Bashir, K., & Chauhan, K. (2018). Optimization of enzyme aided extraction of anthocyanins from Prunus nepalensis L. *LWT - Food Science and Technology*, *91*, 382–390. https://doi.org/10.1016/j.lwt.2018.01.043

Tadesse Teferra, F. (2019). Direct and Indirect Actions of Inulin as Prebiotic Polysaccharide: A Review. *CPQ Nutrition*, *21* 1–15. https://www.researchgate.net/publication/337415512_Direct_and_Indirect_Actions_of_Inulin_as_Prebiotic_Polysaccharide_A_Review

Talavéra, S., Felgines, C., Texier, O., Besson, C., Lamaison, J. L., & Rémésy, C. (2003). Anthocyanins are efficiently absorbed from the stomach in anesthetized rats. *The Journal of Nutrition*, *133*(12), 4178–4182. https://doi.org/10.1093/JN/133.12.4178

Talbot, S. R., Biernot, S., Bleich, A., Maarten Van Dijk, R., Ernst, L., Häger, C., Oscar, S., Helgers, A., Koegel, B., Koska, I., Kuhla, A., Miljanovic, N., Müller-Graff, F.-T., Schwabe, K., Tolba, R., Vollmar, B., Weegh, N., Wölk, T., Wolf, F., … Zechner, D. (2020). Special Issue: Severity assessment defining body-weight reduction as a humane endpoint: a critical appraisal. *Laboratory Animals*, *54*(1), 99–110. https://doi.org/10.1177/0023677219883319

Tan, J., Han, Y., Han, B., Qi, X., Cai, X., Ge, S., & Xue, H. (2022). Extraction and purification of anthocyanins: A review. *Journal of Agriculture and Food Research*, *8*, 100306. https://doi.org/10.1016/J.JAFR.2022.100306

Tan, J., Li, Y., Hou, D. X., & Wu, S. (2019). The effects and mechanisms of cyanidin-3-glucoside and its phenolic metabolites in maintaining intestinal integrity. *Antioxidants*, *8*(10), 479. https://doi.org/10.3390/ANTIOX8100479

Tarone, A. G., Cazarin, C. B. B., & Marostica Junior, M. R. (2020). Anthocyanins: New techniques and challenges in microencapsulation. *Food Research International*, 133,109092. https://doi.org/10.1016/j.foodres.2020.109092

Tasneem, S., Liu, B., Li, B., Choudhary, M. I., & Wang, W. (2019). Molecular pharmacology of inflammation: Medicinal plants as anti-inflammatory agents. *Pharmacological Research*, 139, 126–140. https://doi.org/10.1016/j.phrs.2018.11.001

Tena, N., & Asuero, A. G. (2022). Up-to-date analysis of the extraction methods for anthocyanins: principles of the techniques, optimization, technical progress, and industrial application. *Antioxidants*, 11(2), https://doi.org/10.3390/antiox11020286

Terzić, J., Grivennikov, S., Karin, E., & Karin, M. (2010). Inflammation and colon cancer. *Gastroenterology*, *138*(6), 2101–2114. https://doi.org/10.1053/j.gastro.2010.01.058

Thantsha, M. S., Mamvura, C. I., & Booyens, J. (2012). Probiotics - What They Are, Their Benefits and Challenges. In *New Advances in the Basic and Clinical Gastroenterology*, 21–50. InTech. https://doi.org/10.5772/32889

Theodoropoulou, A., & Koutroubakis, I. E. (2008). Ischemic colitis: Clinical practice in diagnosis and treatment. *World Journal of Gastroenterology : WJG*, *14*(48), 7302. https://doi.org/10.3748/WJG.14.7302

Thomasset, S., Berry, D. P., Cai, H., West, K., Marczylo, T. H., Marsden, D., Brown, K., Dennison, A., Garcea, G., Miller, A., Hemingway, D., Steward, W. P., & Gescher, A. J. (2009). Pilot study of oral anthocyanins for colorectal cancer chemoprevention. *Cancer Prevention Research (Philadelphia, Pa.)*, *2*(7), 625–633. https://doi.org/10.1158/1940-6207.CAPR-08-0201

Tian, L., Tan, Y., Chen, G., Wang, G., Sun, J., Ou, S., Chen, W., & Bai, W. (2019). Metabolism of anthocyanins and consequent effects on the gut microbiota. *Critical Reviews in Food Science and Nutrition*, *59*(6), 982–991. https://doi.org/10.1080/10408398.2018.1533517

Trelles, J. A., & Rivero, C. W. (2013). Whole cell entrapment techniques. In *Methods in Molecular Biolog*, 1051. Humana Press Inc. https://doi.org/10.1007/978-1-62703-550-7_24/FIGURES/00244

Tsai, D. H., Riediker, M., Berchet, A., Paccaud, F., Waeber, G., Vollenweider, P., & Bochud, M. (2019). Effects of short- and long-term exposures to particulate matter on inflammatory marker levels in the general population. *Environmental Science and Pollution Research*, *26*(19), 19697–19704. https://doi.org/10.1007/s11356-019-05194-y

Tsalamandris, S., Antonopoulos, A. S., Oikonomou, E., Papamikroulis, G. A., Vogiatzi, G., Papaioannou, S., Deftereos, S., & Tousoulis, D. (2019). The role of inflammation in diabetes: Current concepts and future perspectives. *European Cardiology Review*, 14(1), 50–59. https://doi.org/10.15420/ecr.2018.33.1

Turner, M. D., Nedjai, B., Hurst, T., & Pennington, D. J. (2014). Cytokines and chemokines: At the crossroads of cell signalling and inflammatory disease. *Biochimica et Biophysica Acta (BBA) - Molecular Cell Research*, *1843*(11), 2563–2582. https://doi.org/10.1016/J.BBAMCR.2014.05.014

Ukena, S. N., Singh, A., Dringenberg, U., Engelhardt, R., Seidler, U., Hansen, W., Bleich, A., Bruder, D., Franzke, A., Rogler, G., Suerbaum, S., Buer, J., Gunzer, F., & Westendorf, A. M. (2007). Probiotic *Escherichia coli Nissle* 1917 inhibits leaky gut by enhancing mucosal integrity. *PLoS ONE*, *2*(12), 1308. https://doi.org/10.1371/JOURNAL.PONE.0001308

Ungaro, R., Mehandru, S., Allen, P. B., Peyrin-Biroulet, L., & Colombel, J. F. (2017). Ulcerative colitis. *Lancet, 389*(10080), 1756. https://doi.org/10.1016/S0140-6736(16)32126-2

Uribe-Querol, E., & Rosales, C. (2020). Phagocytosis: our current understanding of a universal biological process. *Frontiers in Immunology*, *11*, 1066. https://doi.org/10.3389/FIMMU.2020.01066/BIBTEX

Valdez, J. C., & Bolling, B. W. (2019). Anthocyanins and intestinal barrier function: a review. *Journal of Food Bioactives*, *5*, 18–30. https://doi.org/10.31665/jfb.2019.5175

Varela, M. L., Mogildea, M., Moreno, I., & Lopes, A. (2018). Acute Inflammation and Metabolism. *Inflammation 2018 41:4*, *41*(4), 1115–1127. https://doi.org/10.1007/S10753-018-0739-1

Venancio, V. P., Cipriano, P. A., Kim, H., Antunes, L. M. G., Talcott, S. T., & Mertens-Talcott, S. U. (2017). Cocoplum (Chrysobalanus icaco L.) anthocyanins exert anti-inflammatory activity in human colon cancer and non-malignant colon cells. *Food & Function*, *8*(1), 307–314. https://doi.org/10.1039/C6FO01498D

Verediano, T. A., Stampini Duarte Martino, H., Dias Paes, M. C., & Tako, E. (2021). Effects of anthocyanin on intestinal health: A systematic review. In *Nutrients*, 13(4), 1331. https://doi.org/10.3390/nu13041331

Vergara, C., Pino, M. T., Zamora, O., Parada, J., Pérez, R., Uribe, M., & Kalazich, J. (2020). Microencapsulation of anthocyanin extracted from purple flesh cultivated potatoes by spray drying and its effects on in vitro gastrointestinal digestion. *Molecules*, https://doi.org/10.3390/molecules25030722

Viernstein, H., Raffalt, J., & Polheim, D. (2005). Stabilisation of probiotic microorganisms. *Applications of Cell Immobilisation Biotechnology*, 439–453. https://doi.org/10.1007/1-4020-3363-x_25

Vinolo, M. A. R., Rodrigues, H. G., Hatanaka, E., Sato, F. T., Sampaio, S. C., & Curi, R. (2011). Suppressive effect of short-chain fatty acids on production of proinflammatory mediators by neutrophils. *Journal of Nutritional Biochemistry*, *22*(9), 849–855. https://doi.org/10.1016/J.JNUTBIO.2010.07.009

Wagenaar, C. A., van de Put, M., Bisschops, M., Walrabenstein, W., de Jonge, C. S., Herrema, H., & van Schaardenburg, D. (2021). The effect of dietary interventions on chronic inflammatory diseases in relation to the microbiome: A systematic review. In *Nutrients*, MDPI. https://doi.org/10.3390/nu13093208

Wallace, J. L., Ianaro, A., Flannigan, K. L., & Cirino, G. (2015). Gaseous mediators in resolution of inflammation. *Seminars in Immunology*, *27*(3), 227–233. https://doi.org/10.1016/J.SMIM.2015.05.004

Wallace, T. C., & Giusti, M. M. (2015). Anthocyanins. *Advances in Nutrition*, *6*(5), 620. https://doi.org/10.3945/AN.115.009233

Wang, B., Wu, L., Chen, J., Dong, L., Chen, C., Wen, Z., Hu, J., Fleming, I., & Wang, D. W. (2021). Metabolism pathways of arachidonic acids: mechanisms and potential therapeutic targets. *Signal Transduction and Targeted Therapy,* *6*(1), 1–30. https://doi.org/10.1038/s41392-020-00443-w

Wang, M.-Y., Wang, Z.-X., Huang, L.-J., Yang, R.-X., Zou, Z.-Y., Ge, W.-S., Ren, T.-Y., & Fan, J.-G. (2022). Premorbid Steatohepatitis Increases the Seriousness of Dextran Sulfate Sodium-induced Ulcerative Colitis in Mice. *Journal of Clinical and Translational Hepatology*, *000*, 0–0. https://doi.org/10.14218/jcth.2021.00315

Ware, J. H., Wan, X. S., Newberne, P., & Kennedy, A. R. (1999). Bowman-Birk inhibitor concentrate reduces colon inflammation in mice with dextran sulfate sodium-induced ulcerative colitis. *Digestive Diseases and Sciences*, *44*(5), 986–990. https://doi.org/10.1023/A:1026616832119

Wei, J., Zhang, G., Zhang, X., Xu, D., Gao, J., & Fan, J. (2017). Anthocyanins delay ageing-related degenerative changes in the liver. *Plant Foods for Human Nutrition*, *72*(4), 425–431. https://doi.org/10.1007/S11130-017-0644-Z

Wessel, F., Winderlich, M., Holm, M., Frye, M., Rivera-Galdos, R., Vockel, M., Linnepe, R., Ipe, U., Stadtmann, A., Zarbock, A., Nottebaum, A. F., & Vestweber, D. (2014). Leukocyte extravasation and vascular permeability are each controlled in vivo by different tyrosine residues of VE-cadherin. *Nature Immunology*, *15*(3), 223–230. https://doi.org/10.1038/NI.2824

Wilkowska, A., Ambroziak, W., Czyzowska, A., & Adamiec, J. (2016). Effect of microencapsulation by spray drying and freeze drying technique on the antioxidant properties of blueberry (*Vaccinium myrtillus*) juice polyphenolic compounds. *Polish Journal of Food and Nutrition Sciences*, *66*(1), 11–16. https://doi.org/10.1515/PJFNS-2015-0015

Williams, T. J., & Peck, M. J. (1977). Role of prostaglandin-mediated vasodilatation in inflammation. *Nature, 270*(5637), 530–532. https://doi.org/10.1038/270530a0

Wroblewski, L. E., Peek, R. M., & Coburn, L. A. (2016). The role of the microbiome in gastrointestinal cancer. *Gastroenterology Clinics of North America*, *45*(3), 543–556. https://doi.org/10.1016/J.GTC.2016.04.010

Wu, C. W., & Yu, J. (2012). General introduction. In *From Inflammation to Cancer: Advances in Diagnosis and Therapy for Gastrointestinal and Hepatological Diseases* (pp. 3–14). World Scientific Publishing Co. https://doi.org/10.1142/9789814343602_0001

Xiong, D., Yu, L. X., Yan, X., Guo, C., & Xiong, Y. (2012). Effects of root and stem extracts of asparagus cochinchinensis on biochemical indicators related to aging in the brain and liver of mice. *The American journal of chinese medicine*, *39*(4), 719–726. https://doi.org/10.1142/S0192415X11009159

Xu, X., Lin, S., Yang, Y., Gong, X., Tong, J., Li, K., & Li, Y. (2020). Histological and ultrastructural changes of the colon in dextran sodium sulfate-induced mouse colitis. *Experimental and Therapeutic Medicine*, *20*(3), 1987. https://doi.org/10.3892/ETM.2020.8946

Yamashita, C., Chung, M. M. S., dos Santos, C., Mayer, C. R. M., Moraes, I. C. F., & Branco, I. G. (2017). Microencapsulation of an anthocyanin-rich blackberry (Rubus spp.) by-product extract by freeze-drying. *LWT - Food Science and Technology*, *84*, 256–262. https://doi.org/10.1016/j.lwt.2017.05.063

Yan, Y., Kolachala, V., Dalmasso, G., Nguyen, H., Laroui, H., Sitaraman, S. V., & Merlin, D. (2009). Temporal and spatial analysis of clinical and molecular parameters in dextran sodium sulfate induced colitis. *PLoS ONE*, https://doi.org/10.1371/journal.pone.0006073

Yu, Y., & Lv, Y. (2019). Degradation kinetic of anthocyanins from rose (Rosa rugosa) as prepared by microencapsulation in freeze-drying and spray-drying. *Https://Doi.Org/10.1080/10942912.2019.1701011*, *22*(1), 2009–2021. https://doi.org/10.1080/10942912.2019.1701011

Zavros, Y., & Merchant, J. L. (2005). Modulating the cytokine response to treat Helicobacter gastritis. *Biochemical Pharmacology*, *69*(3), 365–371. https://doi.org/10.1016/J.BCP.2004.07.043

Zhan, X., Peng, W., Wang, Z., Liu, X., Dai, W., Mei, Q., & Hu, X. (2022). Polysaccharides from garlic protect against liver injury in dss-induced inflammatory bowel disease of mice via suppressing pyroptosis and oxidative damage. *Oxidative Medicine and Cellular Longevity*, *2022*, 2042163. https://doi.org/10.1155/2022/2042163

Zhang, J. M., & An, J. (2007). Cytokines, inflammation and pain. *International Anesthesiology Clinics*, *45*(2), 27. https://doi.org/10.1097/AIA.0B013E318034194E

Zhang, P. C. (2012). The effects of cooked common beans on dss-induced colitis in mice. http://atrium.lib.uoguelph.ca/xmlui/handle/10214/3981

Zhang, Y., Zhao, X., Zhu, Y., Ma, J., Ma, H., & Zhang, H. (2018). Probiotic mixture protects dextran sulfate sodium-induced colitis by altering tight junction protein expressions and increasing tregs. *Mediators of Inflammation*, *2018*(Apr). https://doi.org/10.1155/2018/9416391

Zhao, B., Xia, B., Li, X., Zhang, L., Liu, X., Shi, R., Kou, R., Liu, Z., & Liu, X. (2020). Sesamol supplementation attenuates DSS-induced colitis via mediating gut barrier integrity, inflammatory responses, and reshaping gut microbiome. *Journal of Agricultural and Food Chemistry*, *68*(39), 10697–10708. https://doi.org/10.1021/ACS.JAFC.0C04370/SUPPL_FILE/JF0C04370_SI_002.PDF

Zhao, H., Wu, L., Yan, G., Chen, Y., Zhou, M., Wu, Y., & Li, Y. (2021). Inflammation and tumor progression: signaling pathways and targeted intervention. *Signal Transduction and Targeted Therapy*, *6*(1), 263. https://doi.org/10.1038/s41392-021-00658-5

Zhao, J., Hong, T., Dong, M., Meng, Y., & Mu, J. (2013). Protective effect of myricetin in dextran sulphate sodium-induced murine ulcerative colitis. *Molecular Medicine Reports*, *7*(2), 565–570. https://doi.org/10.3892/MMR.2012.1225/HTML

Zhao, L., Zhang, Y., Liu, G., Hao, S., Wang, C., & Wang, Y. (2018). Black rice anthocyanin-rich extract and rosmarinic acid, alone and in combination, protect against DSS-induced colitis in mice. *Food & Function*, *9*(5), 2796–2808. https://doi.org/10.1039/C7FO01490B

Zheng, D., Liwinski, T., & Elinav, E. (2020). Interaction between microbiota and immunity in health and disease. *Cell Research*, *30*(6), 492–506. https://doi.org/10.1038/S41422-020-0332-7

Zhou, G., Chen, L., Sun, Q., Mo, Q. G., Sun, W. C., & Wang, Y. W. (2019). Maqui berry exhibited therapeutic effects against DSS-induced ulcerative colitis in C57BL/6 mice. *Food & Function*, *10*(10), 6655–6665. https://doi.org/10.1039/C9FO00663J

Zhou, J. S., Shu, Q., Rutherfurd, K. J., Prasad, J., Gopal, P. K., & Gill, H. S. (2000). Acute oral toxicity and bacterial translocation studies on potentially probiotic strains of lactic acid bacteria. *Food and Chemical Toxicology*, *38*(2–3), 153–161. https://doi.org/10.1016/S0278-6915(99)00154-4

Zuo, T., Yue, Y., Wang, X., Li, H., & Yan, S. (2021). Luteolin relieved dss-induced colitis in mice via HMGB1-TLR-NF-κB signaling pathway. *Inflammation*, *44*(2), 570–579. https://doi.org/10.1007/S10753-020-01354-2/FIGURES/9

## APPENDIX A: COLON HISTOPATHOLOGICAL SCORING

| Score | Leukocyte infiltrate | Crypt damage | Ulceration | Edema | Crypt hyperplasia |
|---|---|---|---|---|---|
| 0 | **none** (including lymphoid aggregates often seen in healthy colon) | **none** (may be rare patch "empty" or vacuoles in healthy) | **none** (intact epithelium, wary of histological artefacts) | **none** (mucularis mucosa tight to mucos and muscle | **none** (crypt heights generally uniform but may differ at different areas) |
| 1 | occasional patchy cells (limited to base of crypt lamina propria in IL-10ko, ± submucosal in DSS) | patchy crypt loss, spaces appear between crypts | small, focal ulcers (<3 total and <15 crypt widths) | present and obvious, (may be patchy, typically with cells) | 1 or 2 patches visible at low power, < 75% higher than the average flanking crypts & boundary clear |
| 2 | significant presence of cells in lamina propria, limited to focal areas | 1 or 2 long stretches lacking crypts, loss of goblet cells, some shortening of crypts | frequent small ulcers (>3 < 5 crypt widths, or 1 or 2 > 15 crypt widths) | | 1 or 2 patches ~75% higher than flanking crypts |
| 3 | infiltrate present in submucosa in focal areas | single long stretch, < 15 crypt widths | multiple large stretches lacking surface epithelium, not necessarily >50% length | | >2 patches or ≥75% higher than flanking crypts, striking at low power |
| 4 | large numbers in submucosa, lamina propria and surrounding blood vessels, covering ~50% of colon length or involves proximal colon | multiple large stretches lacking crypts though < 50% colon length, typically obscured by infiltration or involves proximal (colon is "mushy") | | | |
| 5 | occupying ≥50% of colon length and/or transmural inflammation or abundant crypt abscesses (colon is mushy) | | | | |